SiPM applications for low-light detection in particle and astroparticle physics

The Bonaudi-Chiavassa School **June 17th to June 21th, 2024**

Luigi Rignanese rignanes@bo.infn.it

INFN

OUTLINE

- Introduction on Single-photon detectors
- SPAD working principles
- SiPM technologies
- Features and performance
- Electronics
- Radiation damage
- Applications: Cherenkov and LAr scintillator

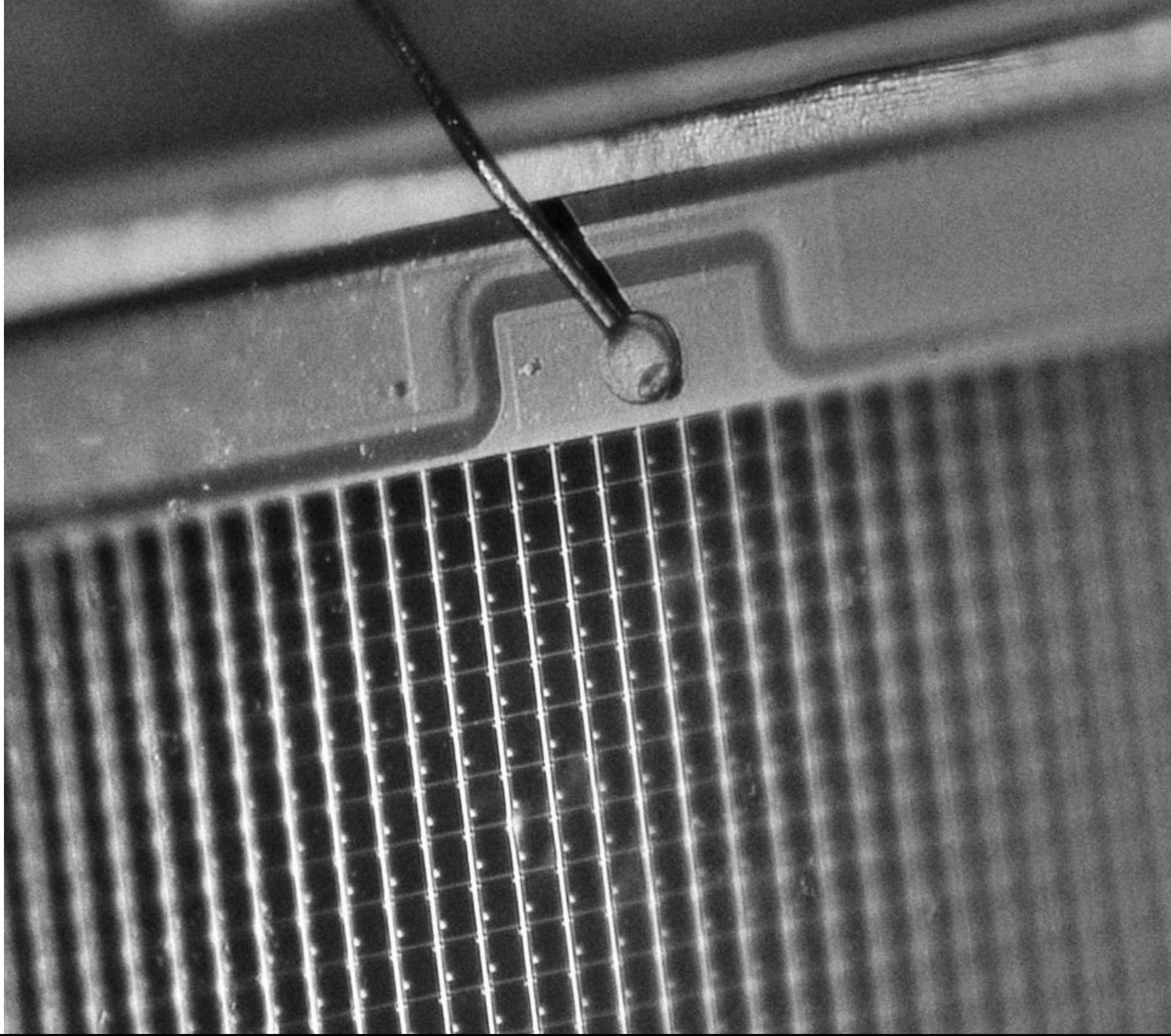

Single photon-detectors

SPDs: Generate a **measurable** electrical **signal** from a single-photon interaction → **PHOTODETECTION**

Energy carried by a single visible photon:
1.65 **eV to 3.10 eV** ≈ **2.375 eV**
SPDs must be able to convert this energy in electrons (**quantum efficiency**)

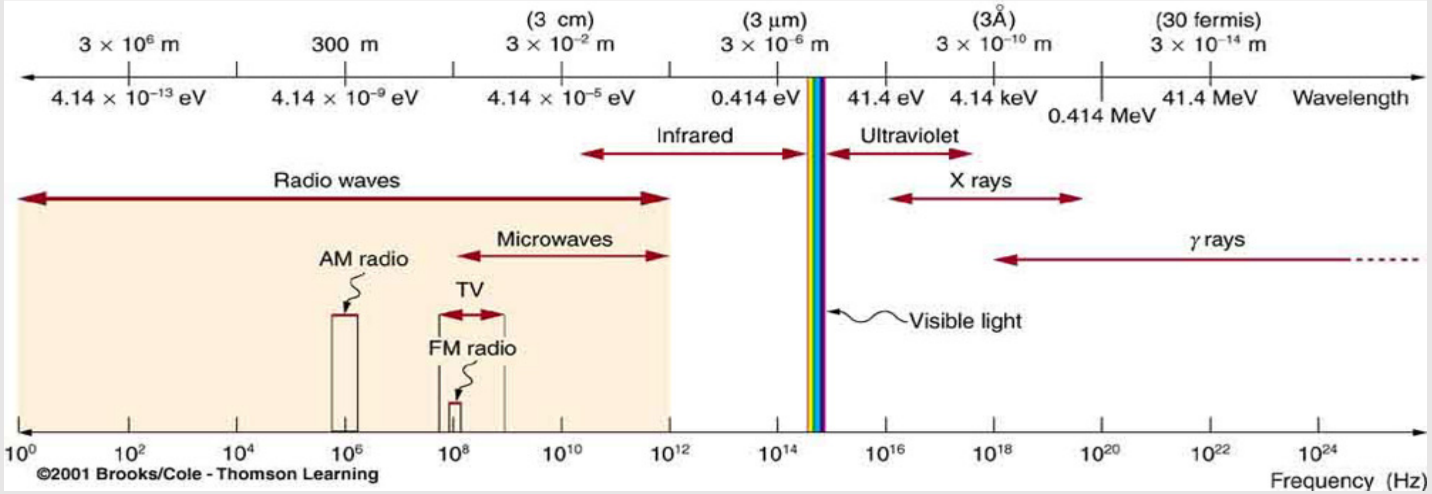

A significant physical **amplification** process is needed in the photodetector to produce the **voltage pulse** to be measured.

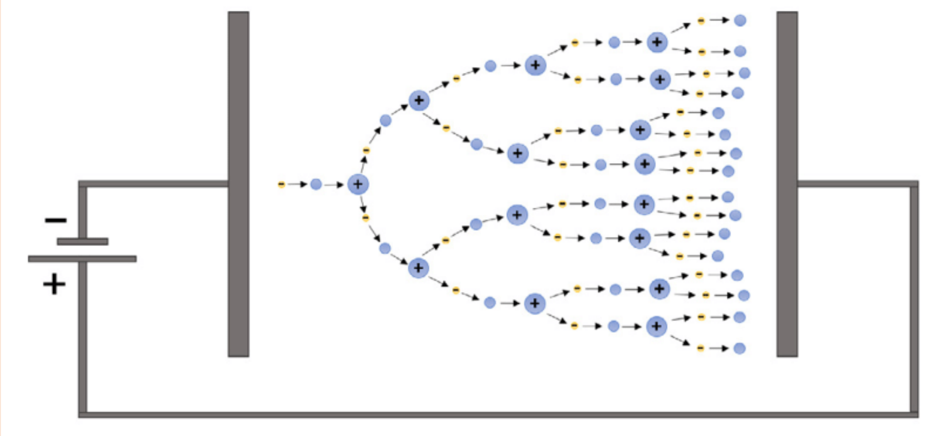

Single photon-detectors types

5 classes of SPDs:
1. Vacuum based
2. Gas filled
3. Cryogenic superconducting
4. Hybrid solutions
5. Solid state

Photomultipliers PMTs

5 classes of SPDs:

1. **Vacuum based**
2. Gas filled
3. Cryogenic superconducting
4. Hybrid solutions
5. Solid state

Photomultiplier tubes (**PMTs**), invented in 1936, are vacuum tubes and were the primary choice for **single-photon** counting with **low-noise** performance.

They can be of **different shapes** and dimensions to be adapted to several applications and need **high bias voltages** (0.5 kV- 2 kV)

Imaging capabilities with Multi-anode PMTs (MAPMTs)

They are bulky and the vacuum construction makes them hard to operate in harsh environments.

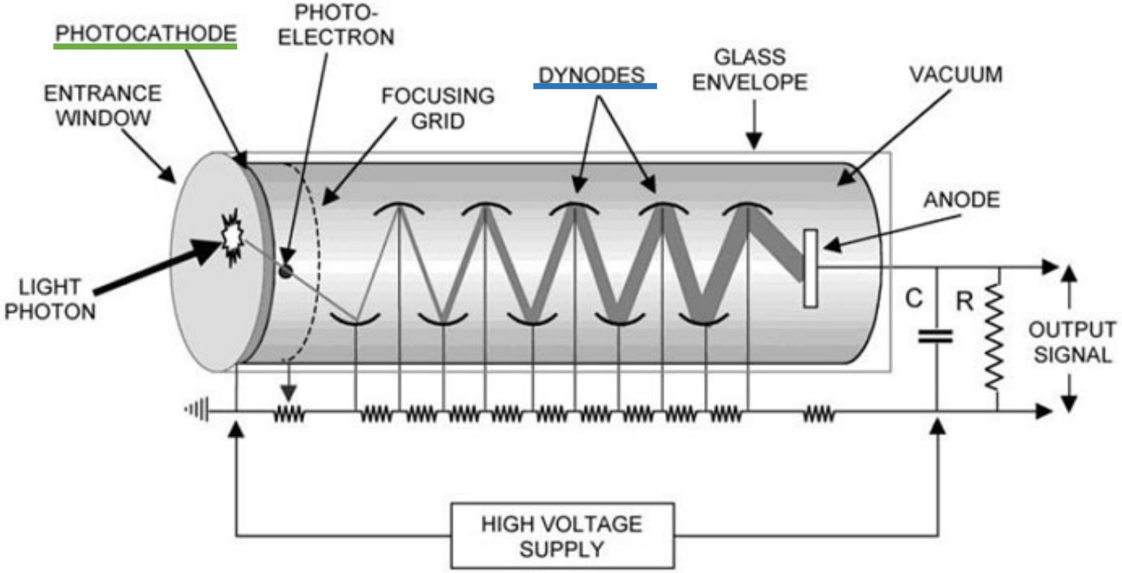

PMTs: photocathodes

5 classes of SPDs:

1. **Vacuum based**
2. Gas filled
3. Cryogenic superconducting
4. Hybrid solutions
5. Solid state

Photocathode = sensitive surface made of thin layer of multiple alkali-metals antimonide.
Photoelectrons are generated through the photoelectric effect.
QE ≈ 43 % [1]
QE = N_e/N_p
N_e= number of photoelectrons
N_p= number of absorbed photons

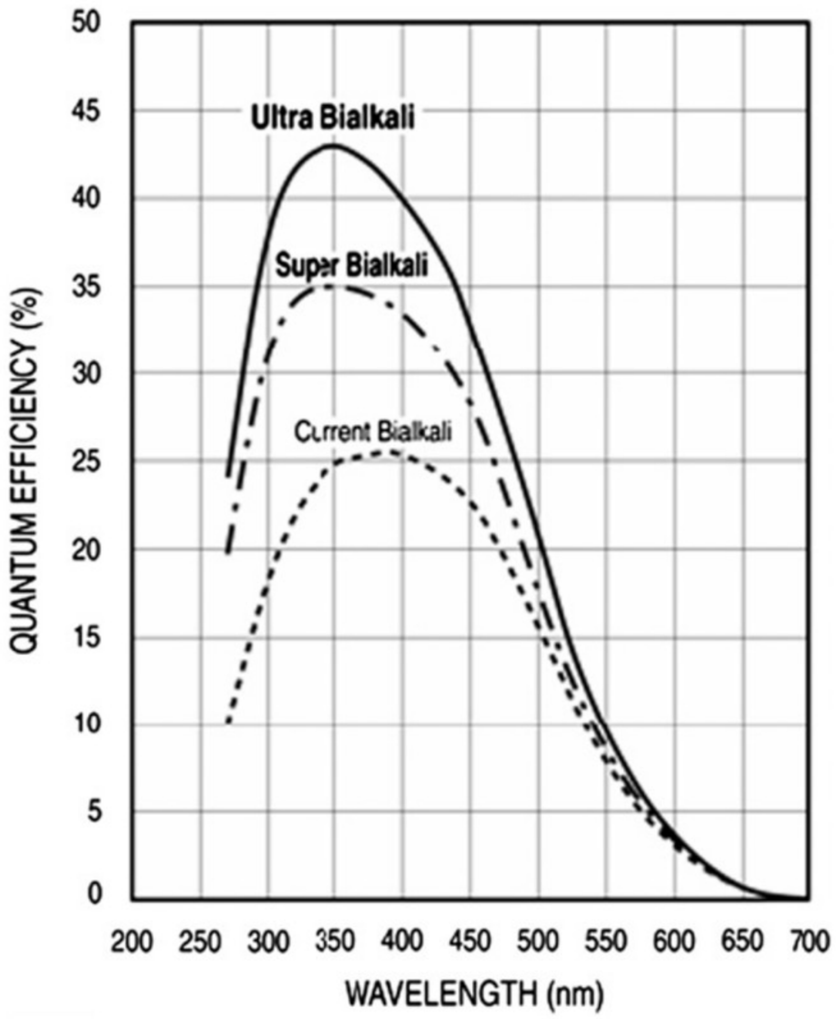

[1] Kimitsugu Nakamura et al, Latest bialkali photocathode with ultra high sensitivity

PMTs: dynodes

5 classes of SPDs:

1. **Vacuum based**
2. Gas filled
3. Cryogenic superconducting
4. Hybrid solutions
5. Solid state

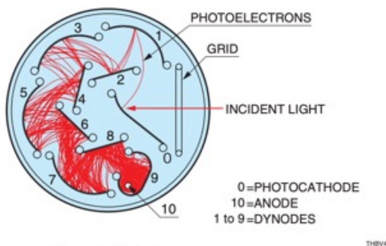

Figure 2-3: Circular-cage type

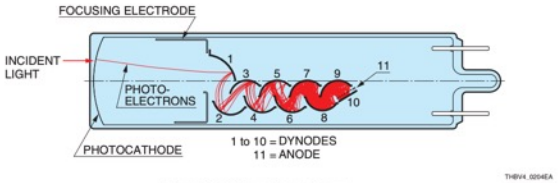

Figure 2-4: Linear-focused type

Dynodes = multiplication electrodes made of metallic plates placed at an increasing voltage potential.
Secondary electrons are generated through the photoelectric effect.

$G = a^n \cdot V^{kn}$
a = constant
V = bias voltage
k = 0.8 depends on the material of the dynode
n = number of dynodes

The resulting **signal** is a **current pulse** that can be converted in a **voltage** pulse by a **load resistor**.

T.T.S. (Transit Time Spread) or jitter > hundred ps. Depends on the trajectories of secondary electrons.

Trajectories of secondary electrons are sensitive to **magnetic fields**!

Different **shapes** for high gains, timing, compactness.

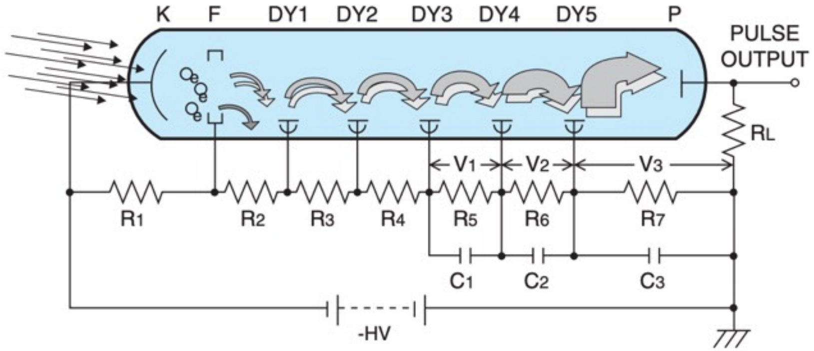

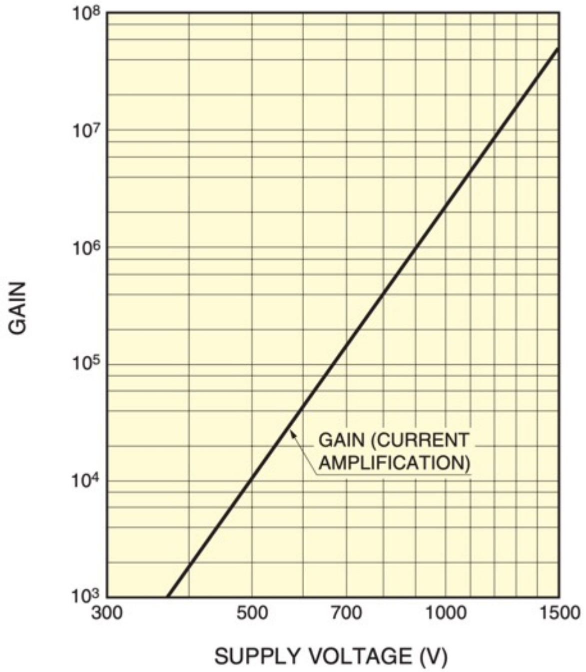

[1] Kimitsugu Nakamura et al, Latest bialkali photocathode with ultra high sensitivity
[2] Hamamatsu PMT handbook

PMTs applications

5 classes of SPDs:
1. **Vacuum based**
2. Gas filled
3. Cryogenic superconducting
4. Hybrid solutions
5. Solid state

RICH1 and **RICH2** upgrades of **LHCB** experiment at **CERN** use **MAPMTs**

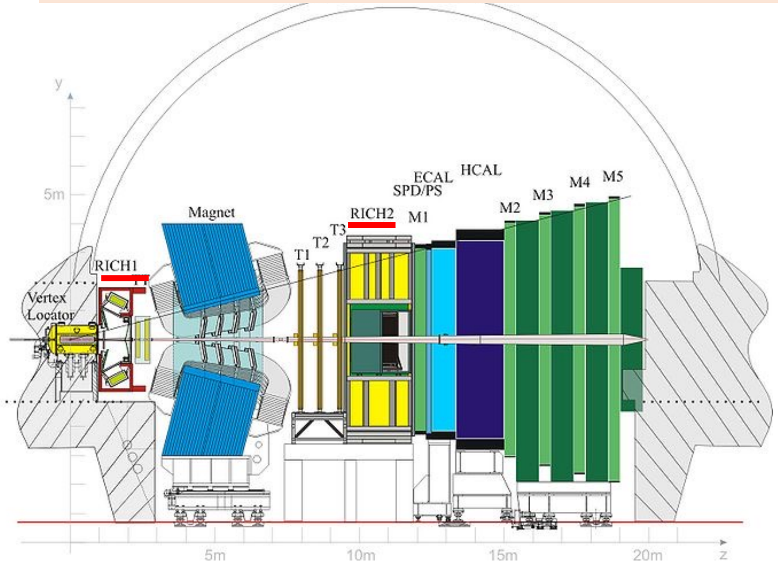

PID between pions, kaons and protons, at **LHCb** is provided by two Ring Imaging Cherenkov systems, **RICH 1** and **RICH 2**. **momentum range 2-100 GeV/c**

The RICHs located in the fringe field of the LHCb dipole magnet **2.5 mT** in some regions occupied by the **RICH 1** photodetectors.

2 types of 8 × 8 pixel Hamamatsu **MaPMT** with two different pixel sizes:
RICH 1 - central region of **RICH 2** - **R13742** with a **2.8 × 2.8 mm²** pixel size
outer part of **RICH 2** - **R13743** type with a 5.6 × 5.6 mm² pixel size covers.
200 ps time resolution

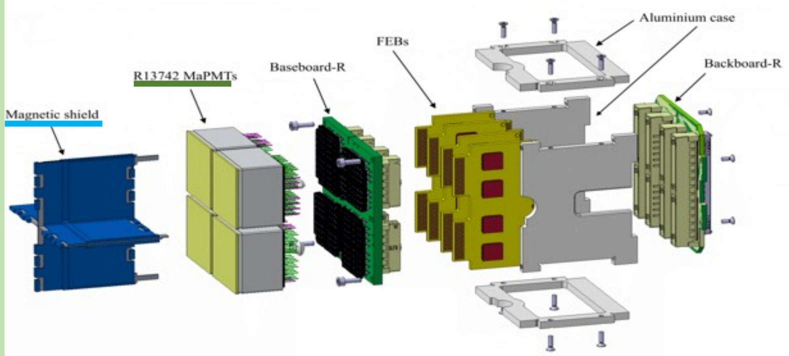

"Quality assurance for the LHCb RICH upgrade Photon-Detection chain
The Upgrade of the LHCb RICH detector

PMTs applications

5 classes of SPDs:
1. **Vacuum based**
2. Gas filled
3. Cryogenic superconducting
4. Hybrid solutions
5. Solid state

The XENONnT Dark Matter Experiment

DARK MATTER experiments: Xenon nT
Improvements in NUV region and low radiation background

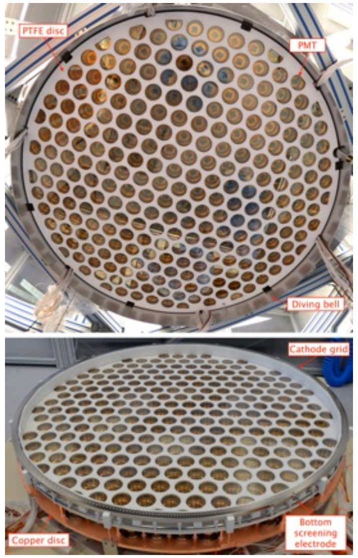

The **TPC** filled by **5.9 t** active **Lxe** (**166 K**) target for the **direct detection of DM**. **Wimps** interaction with LXe nuclei produces scintillation light (46 γ/keV @ 178 nm).
253 (TOP) and 241 (BOTTOM) Hamamatsu R11410-21 low-background cryogenic PMTs developed jointly by Hamamatsu and the XENON collaboration.
PMTs selection almost 10% of PMTs failing during operation. 5% a high after-pulsing rate, and < 5% light leak.
1.5 kV bias to **avoid instabilities** such as transient flashes.
A typical dark count rate of ~40 Hz was measured at LXe temperature for all PMTs.

Property	Unit	Result	
		Mean	Spread
Quantum efficiency	%	34.0	2.8
Gain at 1.5 kV	10^6	8.4	2.3
HV for gain of 5×10^6	kV	1.41	0.04
SPE resolution (median)	%	25.1	1.5
Peak-to-valley ratio (median)	-	4.3	0.4
Transit time spread	ns	9.2	0.5

PMTs applications

5 classes of SPDs:
1. **Vacuum based**
2. Gas filled
3. Cryogenic superconducting
4. Hybrid solutions
5. Solid state

The KM3NeT multi-PMT optical module

Neutrino physics: KM3NeT

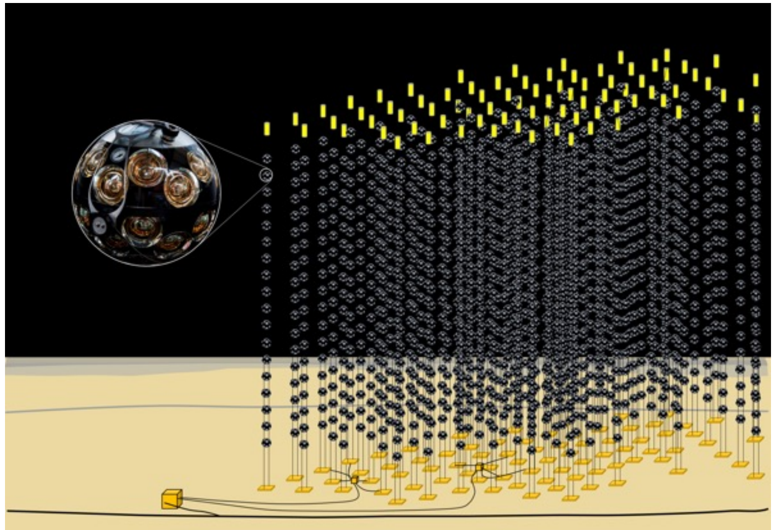

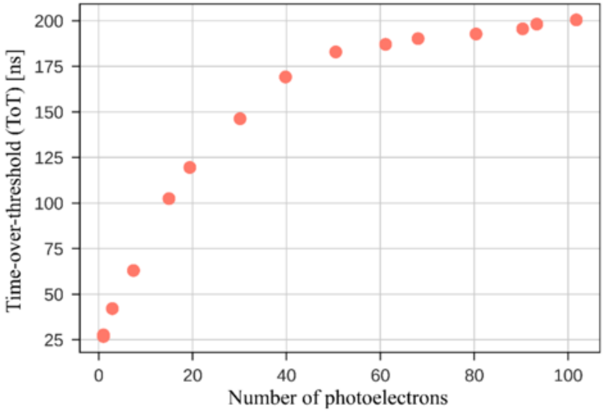

KM3NeT is a research infrastructure housing the next generation **neutrino telescopes**. **15240** optical modules **3000 m underwater** to detect **light** from **charged particles** originating from **collisions** of the **neutrinos** and the Earth. Hamamatsu R14374, with **improved transit time spread**. The PMTs have a convex **bialkali photocathode**, with a diameter of **80 mm**, and a 10-stage dynode structure. To **minimise** the effect of **ageing** in the projected **lifetime** of **15 y** of the detectors , a relatively **low nominal gain of 3 × 10^6** has been chosen.

Photocathode diameter	>72 mm
Nominal Voltage for gain 3×10^6	900÷1300 V
Quantum Efficiency at 470 nm	> 18%
Quantum Efficiency at 404 nm	> 25%
Peak-to-Valley ratio	> 2.0
Transit Time Spread (FWHM)	< 5 ns
Dark count rate (0.3 spe threshold, at 20 °C)	2000 cps max

PMTs applications

5 classes of SPDs:
1. **Vacuum based**
2. Gas filled
3. Cryogenic superconducting
4. Hybrid solutions
5. Solid state

Gain	< 10^8 (10^6 typ)
DCR	≈ O(10) kHz @ RT
Quantum efficiency	45%
Dimensions	20-200 mm
Construction	"artisanal" commercial pricey
Bias voltage	≈ O(1) kV
Working temp	RT (typ) but LN
Difficulties* *in part solved in several experiments	Magnetic field Bulky Vacuum

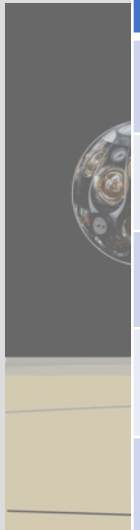

The KM3NeT multi-PMT optical module

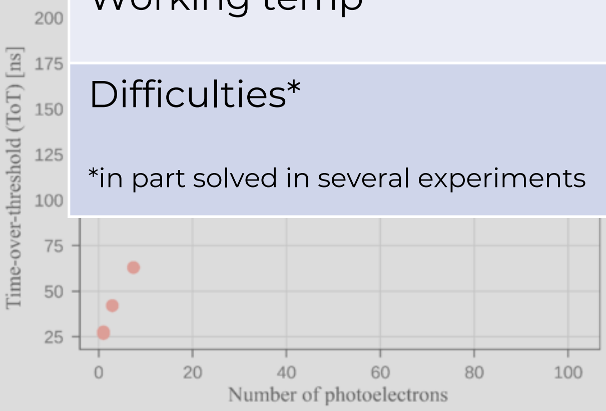

…ch infrastructure housing the …utrino telescopes.
…ules **3000 m underwater** to … **harged particles** originating …he **neutrinos** and the Earth.
…4, with **improved transit time** …have a convex **bialkali** …h a diameter of **80 mm**, and a …ructure. To **minimise** the effect …ojected **lifetime** of **15 y** of the …ely **low nominal gain of 3 × 10^6**

Photocathode diameter	>72 mm
Nominal Voltage for gain 3 × 10^6	900÷1300 V
Quantum Efficiency at 470 nm	> 18%
Quantum Efficiency at 404 nm	> 25%
Peak-to-Valley ratio	> 2.0
Transit Time Spread (FWHM)	< 5 ns
Dark count rate (0.3 spe threshold, at 20 °C)	2000 cps max

Photosensitive Gaseous Detectors (PGD)

5 classes of SPDs:
1. Vacuum based
2. **Gas filled**
3. Cryogenic superconducting
4. Hybrid solutions
5. Solid state

Photosensitive Gaseous Detectors (PGDs) are **like PMTs** but operates with a **gas-filled chamber** instead of a vacuum.
Photons are **converted** in photoelectrons by a **gas (TMAE, TEA)** or a **solid photocathode** (**CsI**)
Photoelectrons are drifted towards the anode wire where multiplication occurs due to Townsend discharge (**avalanche multiplication**).

How to collect photoelectrons?
Multiwire proportional chambers (**MWPCs**)
Electrons are drifted to the wires while
Such detector can reach single-photon detection capability in the ultraviolet spectrum (**CsI QE** ~ **25% @ 175 nm**) with gain up to **10^5**.

CsI RICHdetectors in high energy physics experiments

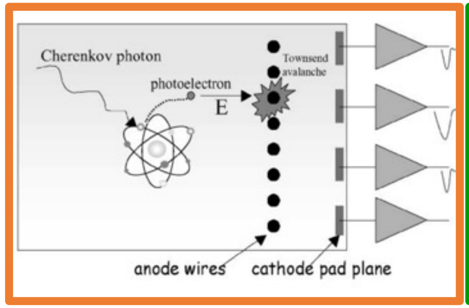

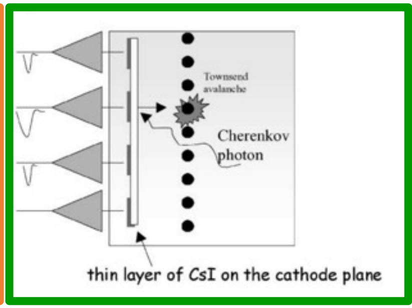

ALICE

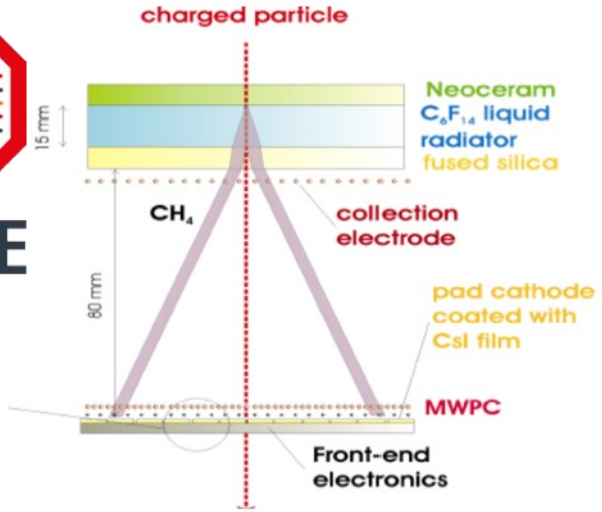

ALICE HMPID operating with a voltage of **2 kV** and flushed with **CH_4**.

Photosensitive Gaseous Detectors (PGD)

5 classes of SPDs:
1. Vacuum
2. **Gas fille**
3. Cryoger superco
4. Hybrid s
5. Solid sta

Photosensitive Gaseous Detectors (PGDs) are

Problems:

- **Avalanche** initiates **close** to the **wire** O(mm) from the **photocathode** leads to **secondary avalanches** mediated by **photons** and **ions limiting** the **gain** and its capability for single-photon detection.
- **Ions back-flow** impacts the **lifetime** of the **solid photocathode**.
- **Secondary avalanches affect signal timing** and the ability to **localize** photons by increasing the charge induced on the readout elements
- **Ageing** of the **wire** due to polymerization of organic components of the gas
- **High ionization** events such as neutrons or gamma detection to the creation of a local charge density exceeding the Raether limit (10^7 electron–ion pairs) leading to the formation of a streamer, and eventually to a **discharge**.

ALICE HMPID operating with a voltage of **2 kV** and flushed with $\mathbf{CH_4}$.

Micro Pattern Gaseous Detector technology MPGD

5 classes of SPDs:
1. Vacuum based
2. **Gas filled**
3. Cryogenic superconducting
4. Hybrid solutions
5. Solid state

Mitigation of the problems by adding **intermediate structures** called **micropattern electron multiplier geometries**:

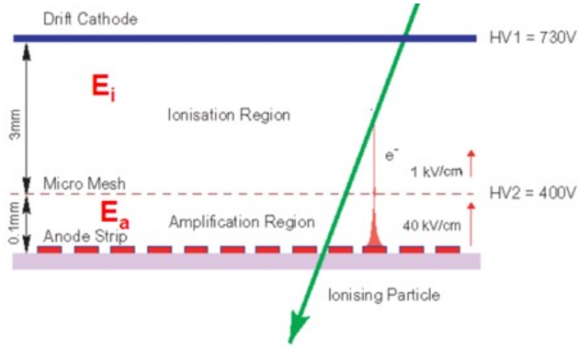

- **Micromegas** (MICRO MEsh GAseous Structure) **ion confination** by the mesh reduces backflow [Y. Giomataris-G. Charpack et al., Nucl. Instr. and Meth. A376(1996)29]
- **GEM (**Gas Electron Multuplier) O(50) μm thick **kapton foil**, **copper** clad on each side and **perforated** by an high surface-density of biconical channels. **Potential difference** between the two **copper sides**, **holes** acting as **multiplication** channels [F. Sauli, CERN, ~1997]

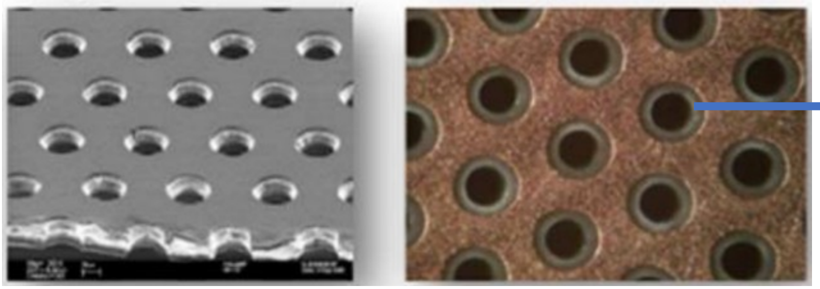

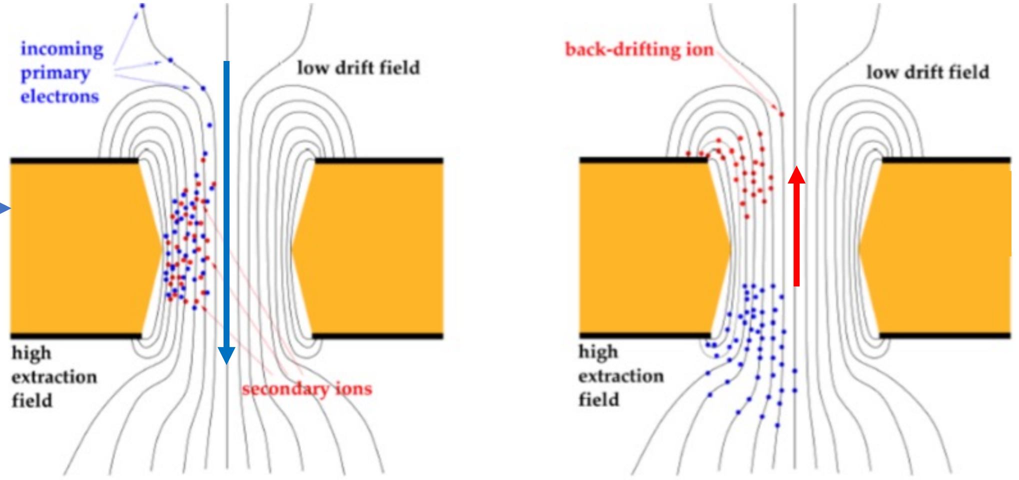

INFN

Micro Pattern Gaseous Detector technology MPGD

5 classes of SPDs:
1. Vacuum based
2. **Gas filled**
3. Cryogenic superconducting
4. Hybrid solutions
5. Solid state

COMPASS RICH-1 uses two THick GEM (THGEM) stages followed by a MICROMEGAS multiplication stage and anode pads to build a **600 × 600 mm²** single-photon detector. Filled with a 50:50 mixture of Ar and CH_4, it reaches single-photon detection capability with gain of **≈ 10^5** and **backflow** of ions to the photocathode surface lower than or equal to **3%.**

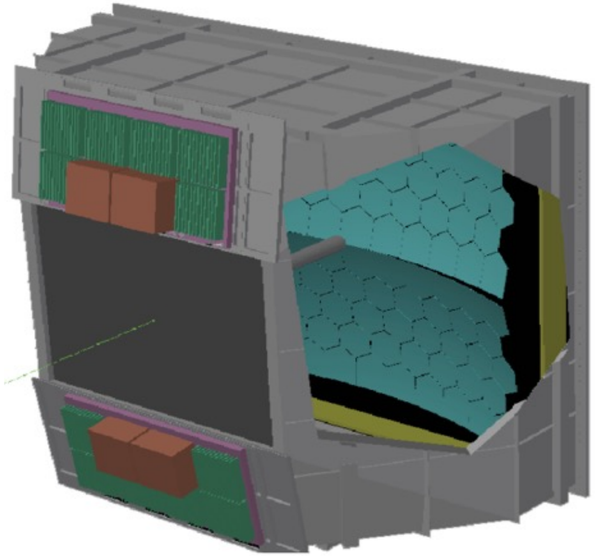

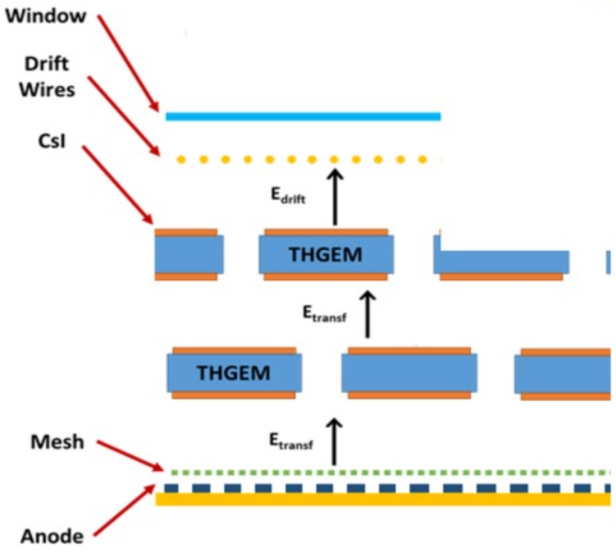

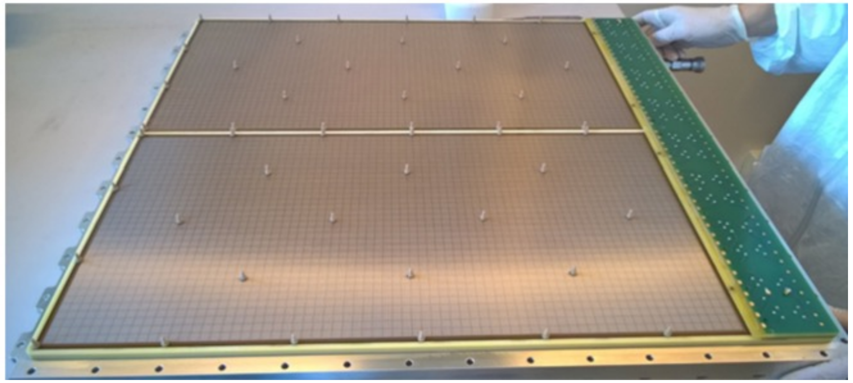

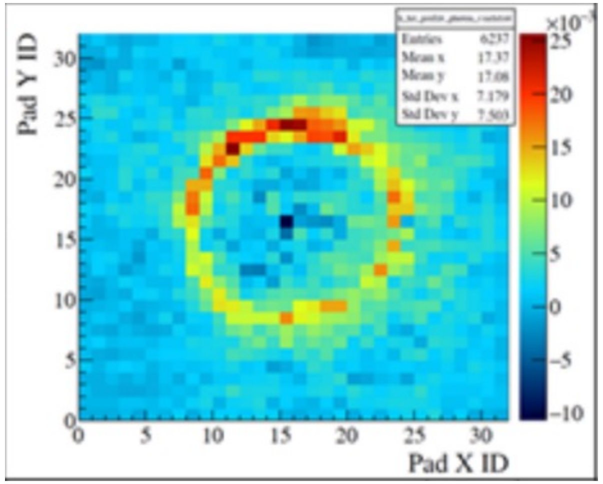

The Hybrid MPGD-based photon detectors of COMPASS RICH-1

Micro Pattern Gaseous Detector technology MPGD

5 classes of SPDs:

1. Vacuum based
2. **Gas filled**
3. Cryogenic superconducting
4. Hybrid solutions
5. Solid state

COM
stag
stag
sing
of A
capa
to th
3%.

Gain	10^5 limited by ion backflow and discharges
Quantum efficiency	25% UV
Dimensions	m^2
Construction	totally custom not commercial
Bias voltage	≈ O(3) kV
Working temp	RT
Difficulties	Not able to detect visible photons with high QE and long term stability

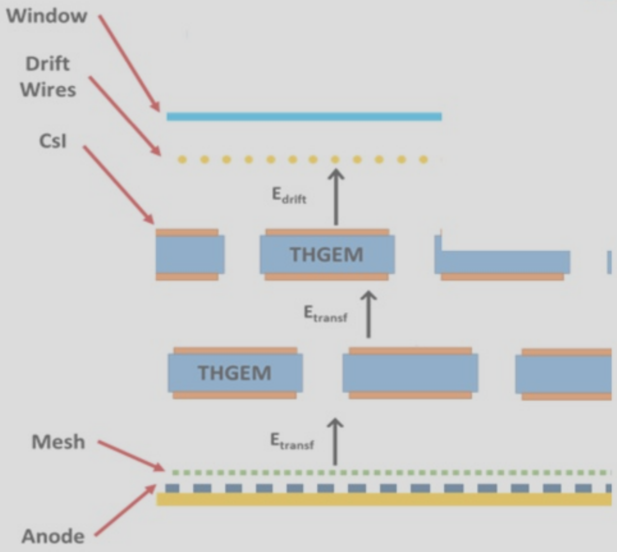

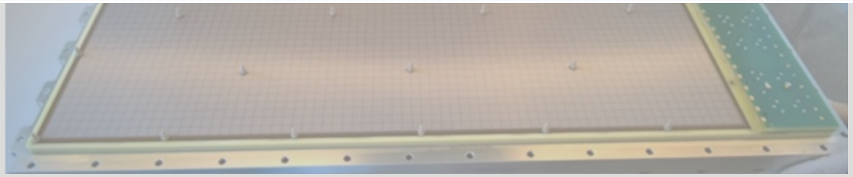

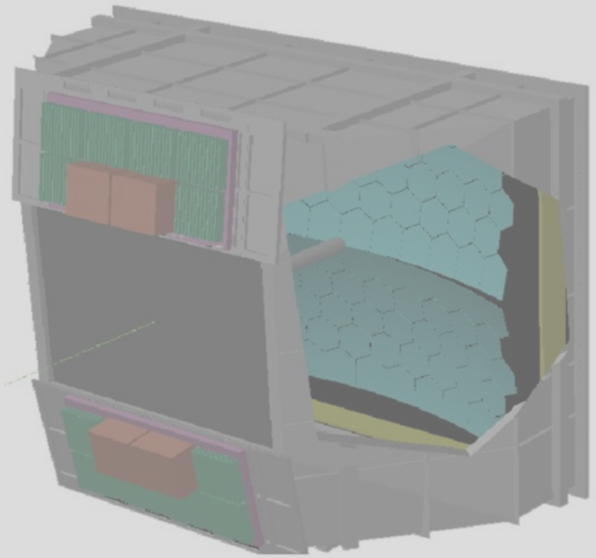

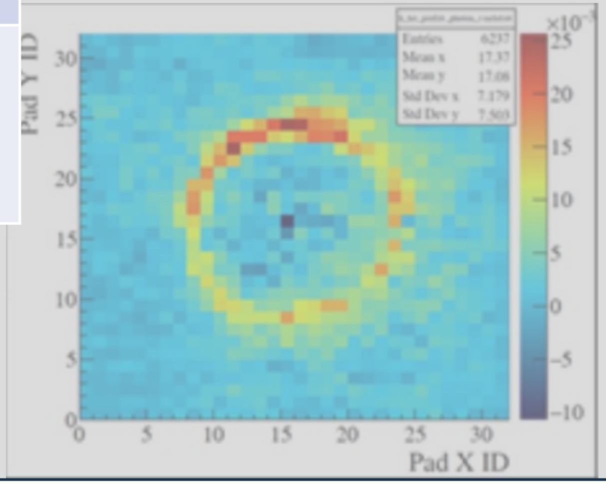

INFN

Superconducting nanowires (SNSPD)

5 classes of SPDs:
1. Vacuum based
2. Gas filled
3. **Cryogenic superconducting**
4. Hybrid solutions
5. Solid state

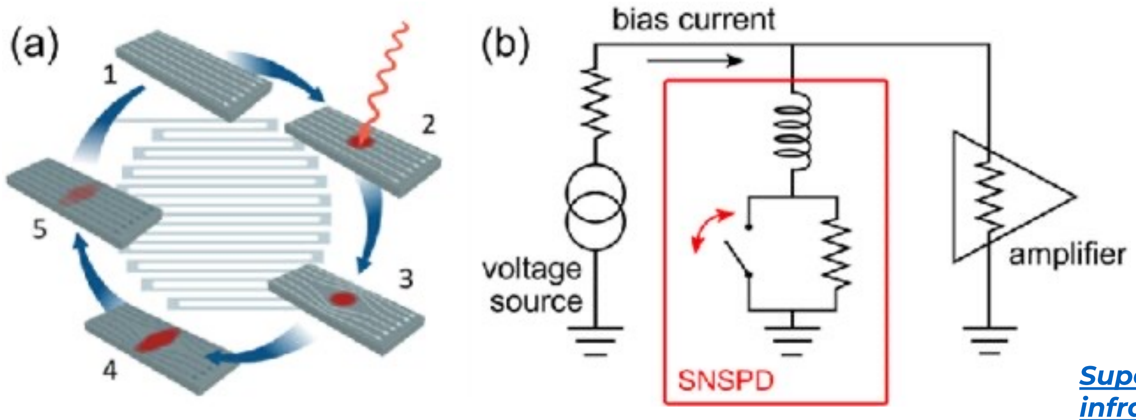

[Superconducting single-photon detectors in the mid-infrared for physical chemistry and spectroscopy]

Nanowires made of **superconducting** (SC) **materials** below their SC current and **biased** below the critical current.

Single-photon is **absorbed** by a nanowire (**photoconversion**), it **disrupts** multiple **Cooper** pairs, which are responsible for **SC**.
Small **resistance** leads an **increase** in local **current** density **above** the **critical SC** current in adjacent nanowires **generates secondary hot spots**, leading to the **breakdown** of SC (**multiplication**) and the formation of a resistive barrier. The increased **resistance** results in a measurable **voltage drop**.
Quantum efficiency can be tuned to different wavelenghts and can reach **90%** with very **fast response** time O(10 ps.
Most **limiting** factor is the low **temperature** (**few K**) which limits their applicability in **current** nuclear and astrophysics **experiments**.

Superconducting nanowires (SNSPD)

5 classes of SPDs:

1. Vacuum based
2. Gas filled
3. **Cryogenic superconducting**
4. Hybrid solutions
5. Solid state

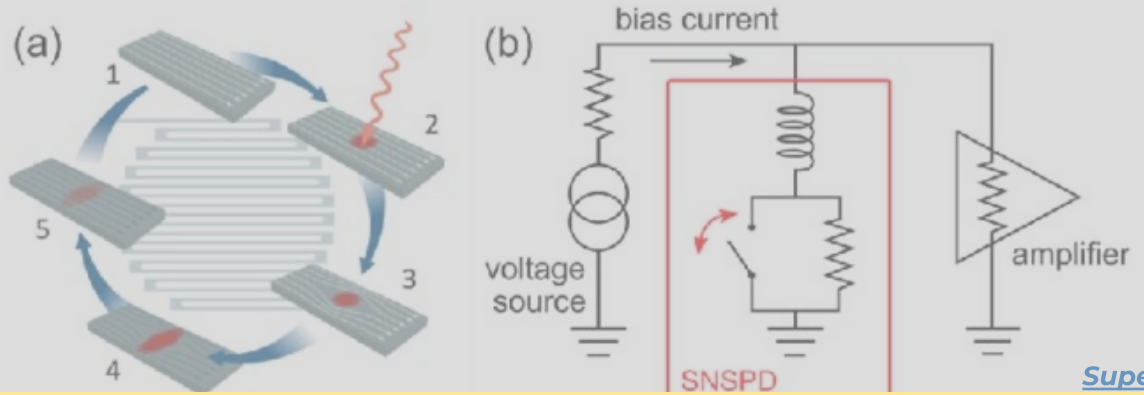

Superconducting single-photon detectors in the mid-
oscopy

More on this in the Thursday class on **Cryogenic Detectors** by Marco Vignati

Nanowires made of **superconducting** (SC) **materials** below their SC current and **biased** below the critical current.

Single-photon is **absorbed** by a nanowire (**photoconversion**), it **disrupts** multiple **Cooper** pairs, which are responsible for **SC**.
Small **resistance** leads an **increase** in local **current** density **above** the **critical SC** current in adjacent nanowires **generates secondary hot spots**, leading to the **breakdown** of SC (**multiplication**) and the formation of a resistive barrier. The increased **resistance** results in a measurable **voltage drop**.
Quantum efficiency can be tuned to different wavelenghts and can reach **90%** with very **fast response** time O(10 ps).
Most **limiting** factor is the low **temperature** (**few K**) which limits their applicability in **current** nuclear and astrophysics **experiments**.

Luigi Rignanese rignanes@bo.infn.it

HYBRID SPD (HPDs and HAPD)

Devices combine principles from vacuum and solid-state detectors into a single unit.

5 classes of SPDs:

1. Vacuum based
2. Gas filled
3. Cryogenic superconducting
4. **Hybrid solutions**
5. Solid state

- Hybrid Photon-Detectors (**HPDs**) developed for the **RICH1** of the LHCb experiment. **Photoelectron** conversion by a bi-alkali **photocathode** accelerated and focused in a vacuum tube by three high voltages (≈ **20 kV**) onto the anode consisting of 300 μm thick **silicon pixel sensor**. Single-photon detection with a quantum efficiency ≈**30%** at 270 nm with a spatial resolution of 2.5 x 2.5 mm^2.

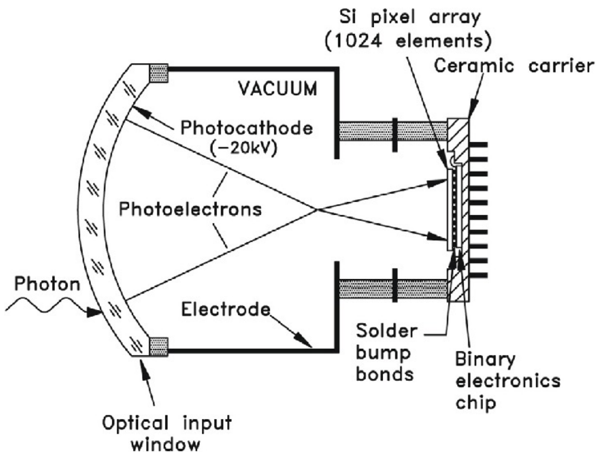

- **BELLE-II** Hybrid Avalanche PhotoDetector (**HAPD**). **photoelectron** conversion by a super bi-alkali cathode accelerated in a vacuum tube biased at 8 kV towards 144 **APD** with a spatial resolution of 4.9 x 4.9 mm^2 each. The total gain is **7 x 10⁴** and is the combination of the **acceleration** of the photoelectrons and the amplification in the **avalanche photodiode**.

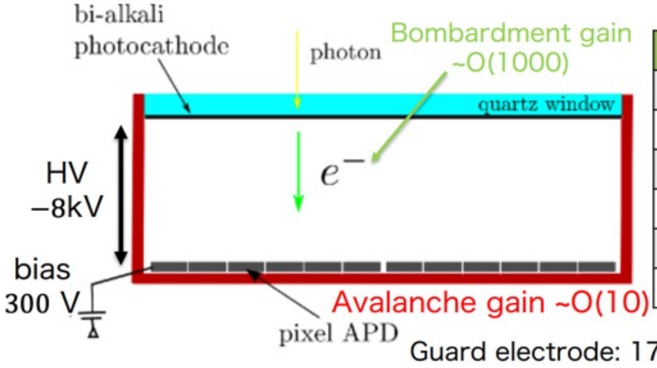

Developed by Hamamatsu Photonics

	HAPD
Size	73×73×28 mm^3
# of channels	12×12 = 144 ch
Channel size	4.9×4.9 mm^2
Effective area	65%
Peak QE	~30%
Total Gain	~70000

HYBRID SPD (HPDs and HAPD)

Devices combine principles from vacuum and solid-state detectors into a single unit.

5 classes of SPDs:

1. Vacuum based
2. Gas filled
3. Cryogenic superconducting
4. **Hybrid solutions**
5. Solid state

- Hybrid Photon-Detectors (**HPDs**) developed for the **RICH1** of the LHCb experiment. **Photoelectron** conversion by a bi-alkali **photocathode** accelerated and focused in a vacuum tube by three high voltages (≈ **20 kV**) onto the anode consisting of 300 μm thick **silicon pixel sensor**. Single-photon detection with a quantum efficiency ≈**30%** at 270 nm with a spatial resolution of 2.5 x 2.5 mm2 [23].

HPDs already substituted with MAPMT.
Bulky and vacuum construction

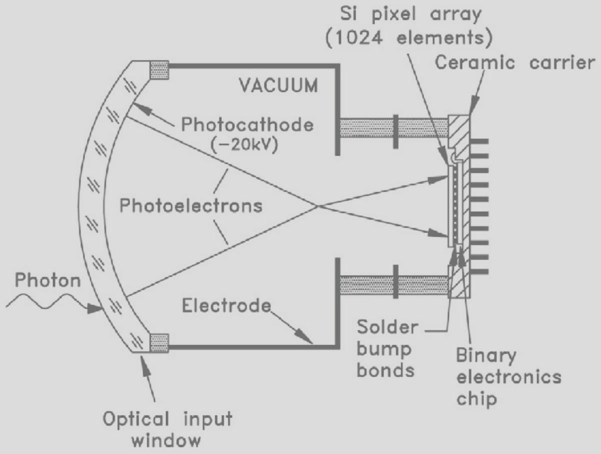

- **BELLE-II** Hybrid Avalanche PhotoDetector (**HAPD**). **photoelectron** conversion by a super bi-alkali cathode accelerated in a vacuum tube biased at 8 kV towards 144 **APD** with a spatial resolution of 4.9 x 4.9 mm^2 each. The total gain is **7 x 10^4** and is the combination of the **acceleration** of the photoelectrons and the amplification in the **avalanche photodiode**.

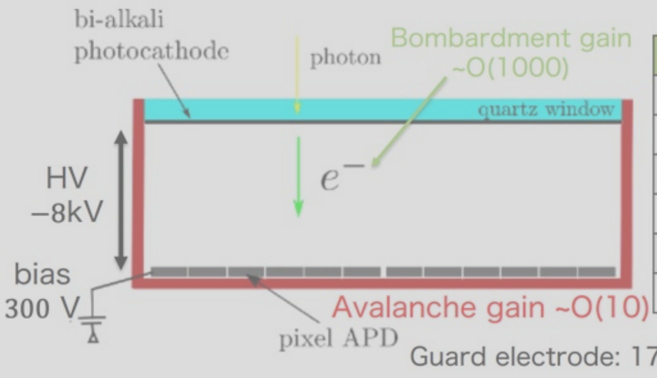

Developed by Hamamatsu Photonics

	HAPD
Size	73×73×28 mm^3
# of channels	12×12 = 144 ch
Channel size	4.9×4.9 mm^2
Effective area	65%
Peak QE	~30%
Total Gain	~70000

INFN

Silicon Photomultipliers (SiPMs)

5 classes of SPDs:
1. Vacuum based
2. Gas filled
3. Cryogenic superconducting
4. Hybrid solutions
5. **Solid state**

SiPMs are **solid state** detectors made of an array of **Single Photon Avalanche Photodiodes** (**SPADs**) connected in parallel typically to a single readout channel. Each SPAD is a square with **10-100 um edge** length.
SiPMs produce a **large electric signal** upon the detection of a **single photon** with **high quantum efficiency**. The signal is **fast** enough to achieve very good **timing performance**.
Dimensions: **mm²** (single devices) several **cm²** (arrays) up to few **m²**

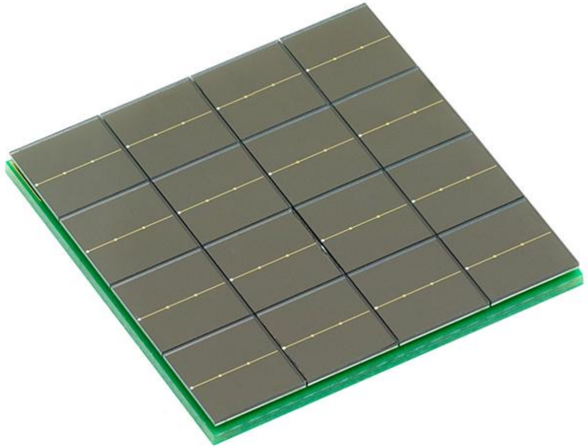

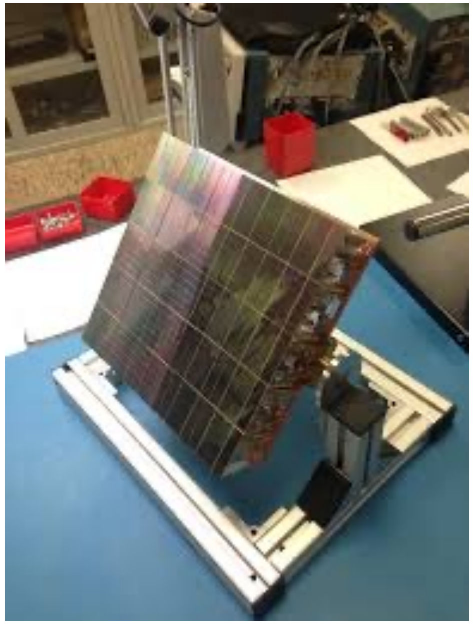

Silicon Photomultipliers (SiPMs)

5 classes of SPDs:
1. Vacuum based
2. Gas filled
3. Cryogenic superconducting
4. Hybrid solutions
5. **Solid state**

SiPMs are **solid state** detectors made of an array of **Single Photon Avalanche Photodiodes** (**SPADs**) connected in parallel typically to a single readout channel. Each SPAD is a square with **10-100 um edge** length.
SiPMs produce a **large electric signal** upon the detection of a **single photon** with **high quantum efficiency**. The signal is **fast** enough to achieve very good **timing performance**.

Among the advantages of this technology:
- Operate at **low voltage** and **low temp**
- **Compact**
- **Robust**
- **Insensitive to magnetic fields**
- **Cheap**
- **Commercially available**
- **Customizable**

Several **producers** SiPMs **around** the **world**, reflecting the **growing interest** and applications of this technology in various fields. Notable manufacturers include Hamamatsu Photonics, SensL Technologies (Part of ON Semiconductor), and Broadcom Inc. that acquired KETEK GmbH in 2021. It is worth noting that other realities are involved in the R&D and small-scale production of SiPMs, typically targeting research applications, like Fondazione Bruno Kessler.

SiPM sensors first commercially available in 2006

Singe **P**hoton **A**valanche **P**hotodiode (**SPAD**)

Pioneering work on avalanche photodiode operated in linear and Geiger mode in the **1960s** in **RCA** (same company of the first commercialized PMT) **USA** and in the **1970s** in **Japan**. **Performance** were **low** but **Single Photons** were seen!

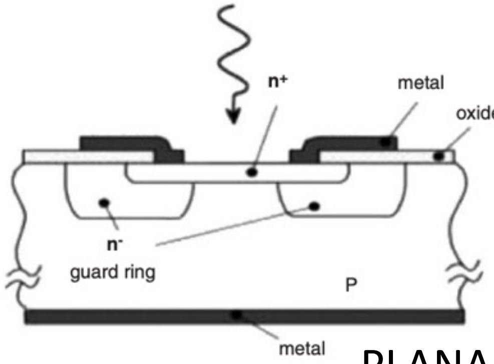

PLANAR

R. H. Haitz J. Appl. Phys., Vol. 36, No. 10 (**1965**) 3123

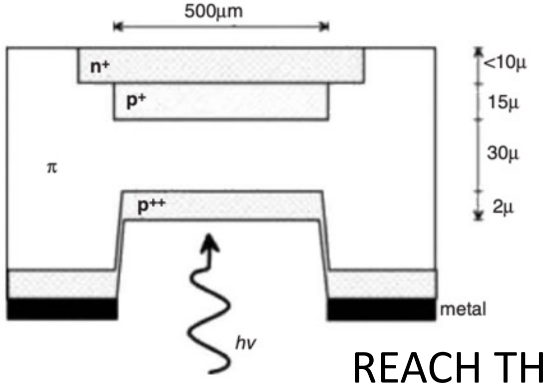

REACH THROUGH

J.R. McIntire IEEE Trans. Elec. Dev. ED-13 (**1966**) 164

1987 the Solid State PhotoMultiplier (**SSPM**). This is an **APD** with very high **donor concentration** which creates an impurity band **50 meV** below the conducting band. Later this device was modified to be less sensitive to **infrared light** and is now called **Visible Light Photon Counter** (VLPC). The small band gap forces an operation at very low temperatures of **few degree Kelvin**. **Fermilab Tevatron**

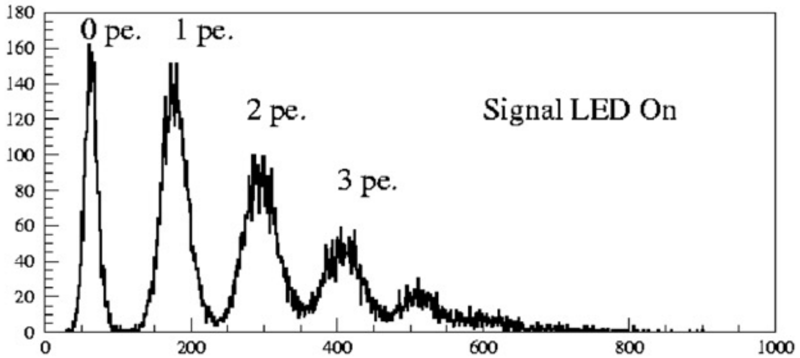

A. Bross, et al. Nucl. Instr. And Meth. A, 477 (**2002**)

SPAD working principle: the photoconversion

In a **photodiodes**, the **photoconversion** happens in the **p-n junction**. A region in the device is free of mobile charge carriers called **depletion region**. When light strikes the diode, it may be absorbed, creating electron-hole pairs (**photoelectrons)**.
By applying a reverse bias voltage (Vbias) to the photodiode, an electric field across the depletion region is created. This causes electrons to be accelerated towards the cathode while the holes towards the anode, resulting in a current flow.

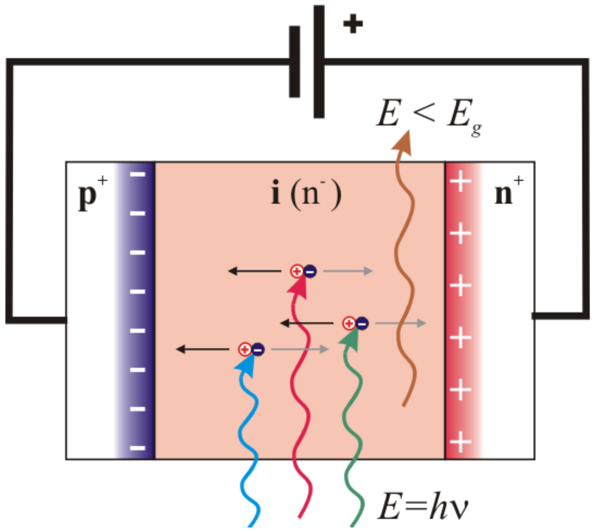

This is not enough to detect single photons because of noise in the electronics that acquire the electric signal.
Remember the mean energy of a visible photon is only 2.4 eV!

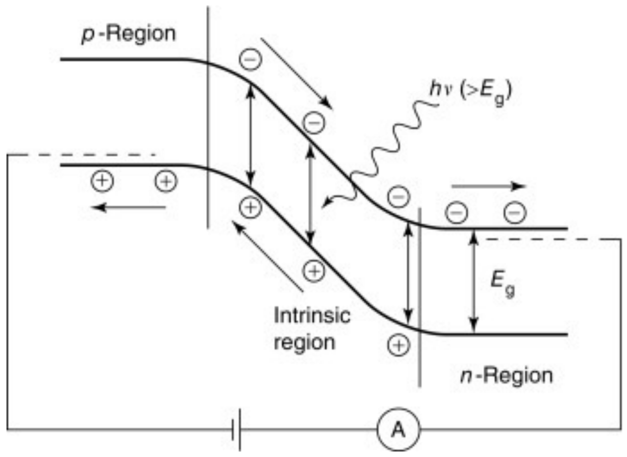

https://www.sciencedirect.com/topics/physics-and-astronomy/photodiode

SPAD working principle: the multiplication

3 regions correspond to three behaviors (3 different devices)

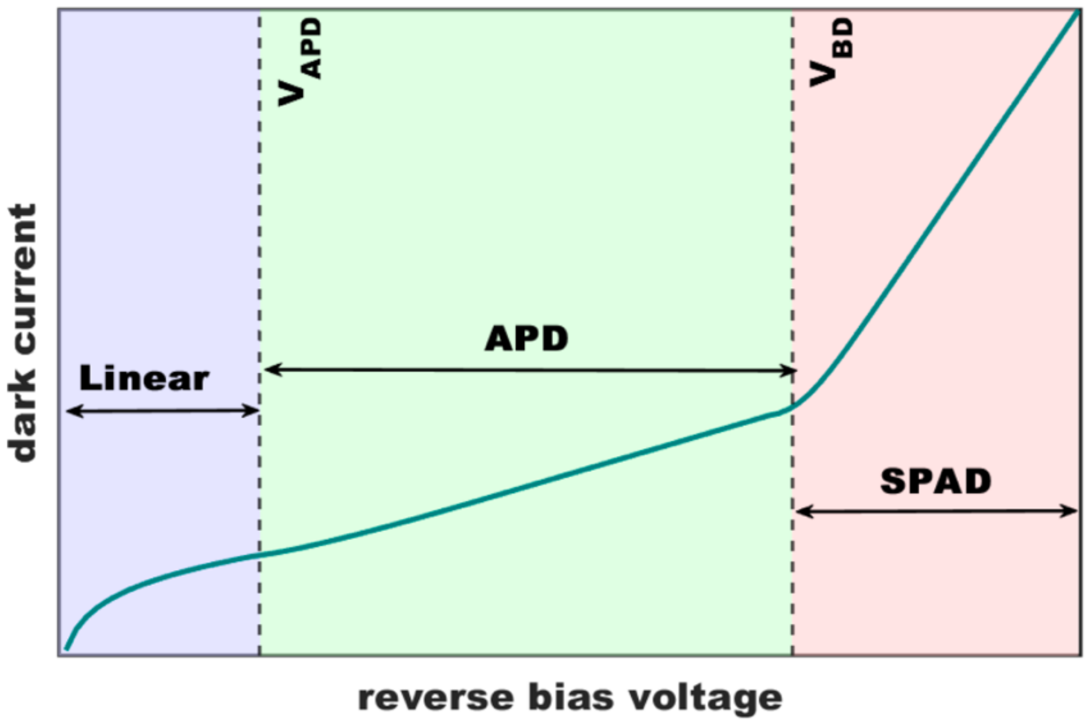

SPAD working principle: the multiplication

3 regions correspond to three behaviors (3 different devices)

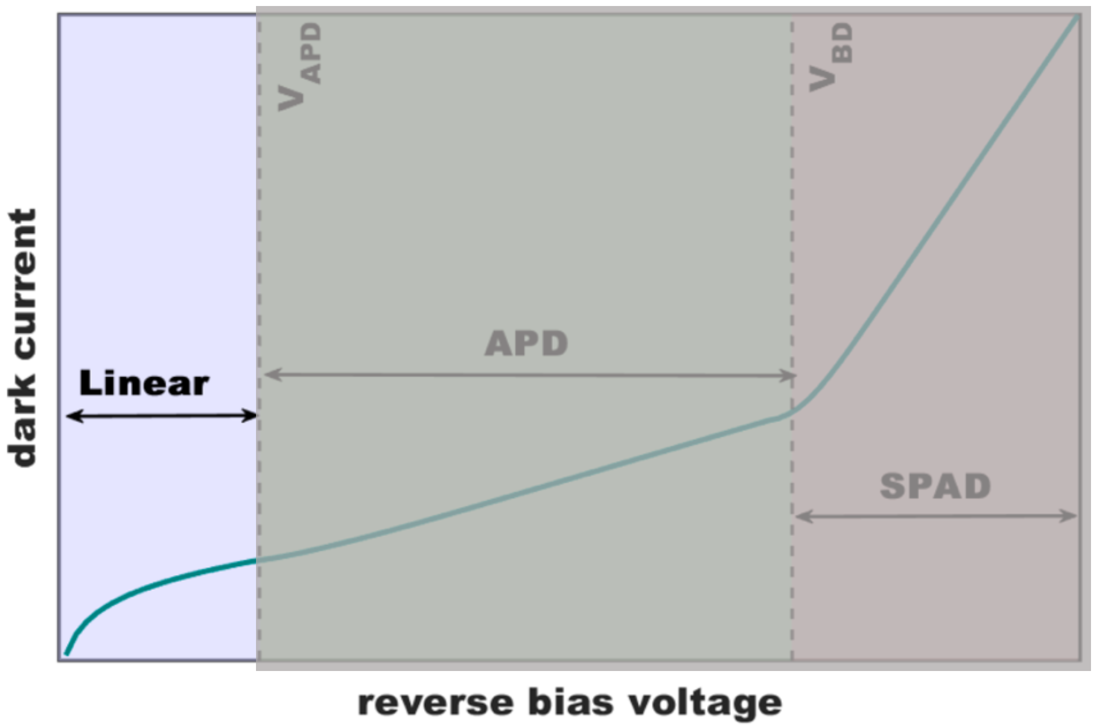

unity-gain: the **electrodes** simply **collect** the **charge generated** by photons absorbed in the **depleted region** of the **p-n junction**. **Increase in the bias volage, increase the depletion width.**

SPAD working principle: the multiplication

3 regions correspond to three behaviors (3 different devices)

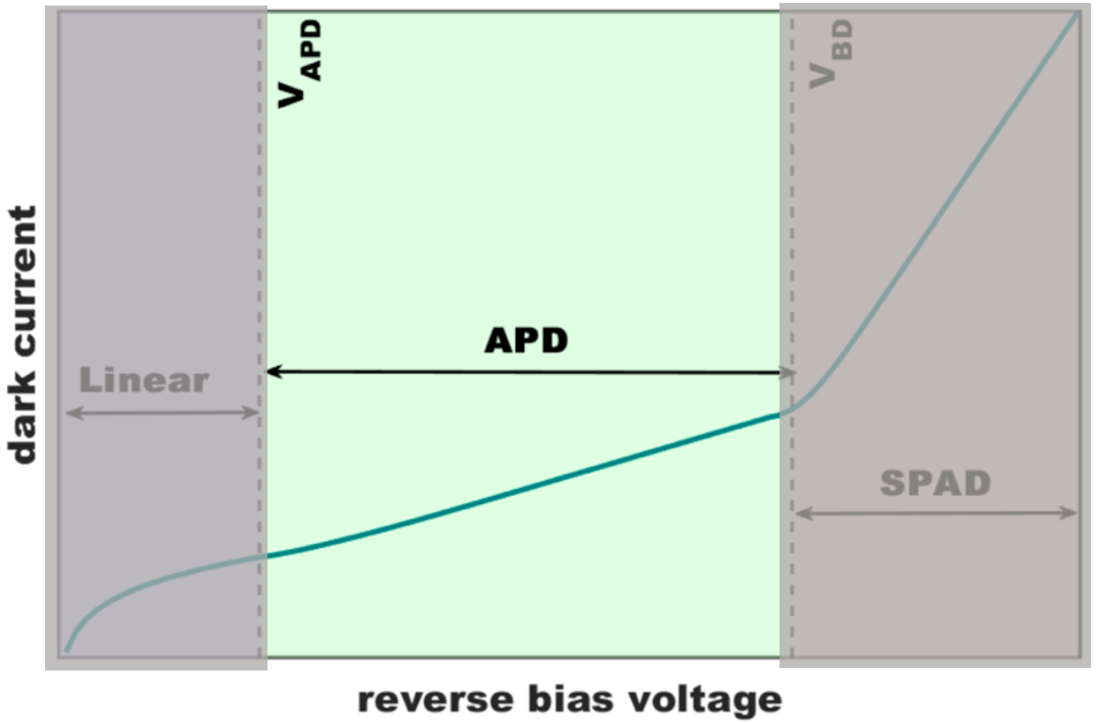

Carrier multiplication: **electrons accelerated** to have sufficient kinetic energy to **create secondary charge pairs** through **impact ionization**.
Stable gain (≈ 10^3) and linear response
Only electrons generate additional electron-hole pairs: the **avalanche is unidirectional and inherently self-quenched**

SPAD working principle: the multiplication

3 regions correspond to three behaviors (3 different devices)

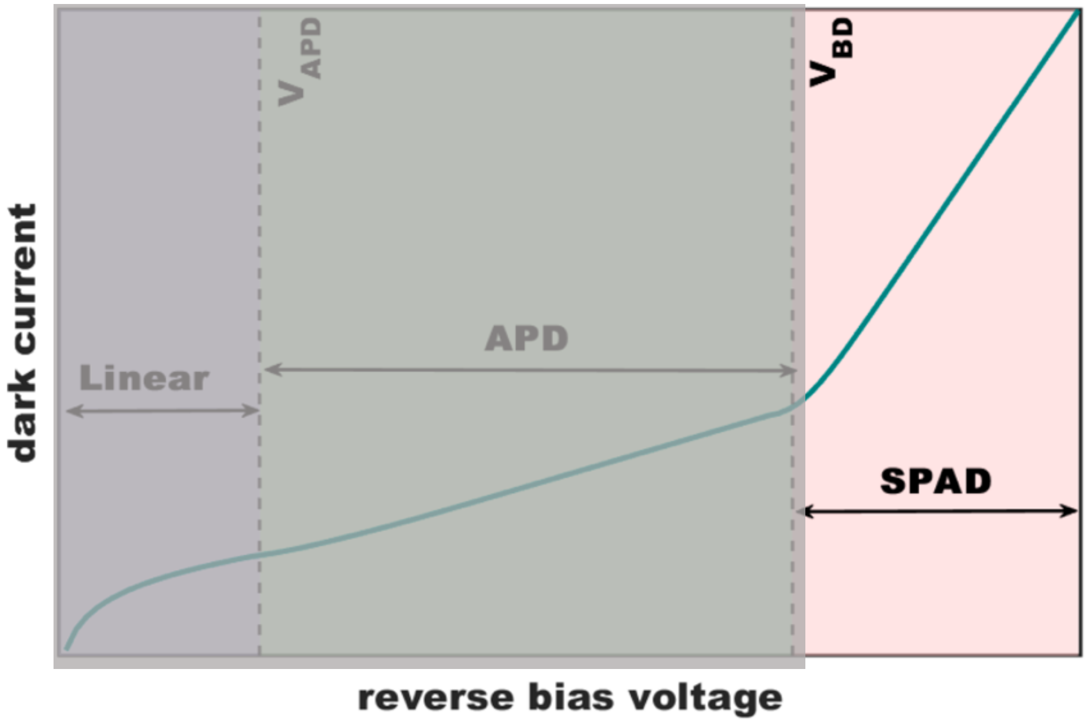

Bias voltage above the **breakdown voltage** (V_{BD}) = **electric field** across the **junction** reaches a critical level (**E ≥ 10^5 V/cm^2**) **Geiger discharge** regime.
Secondary charges have the energy to create further ionization, triggering a **diverging avalanche process**, causing **discharge of the depletion region**. This results **in a sub nanoseconds but macroscopic current spike (≈1 mA).** The **gain** reaches **10^6** and the photodiode can detect single-photons, for this reason it is called **SPAD**. In analogy with **Geiger counters**, the resulting electric signal (current) is **not proportional to the amount of energy (number of photons) detected**.
It is worth noting that in this regime, even holes can create secondary charges.

SPAD: quenching mechanism

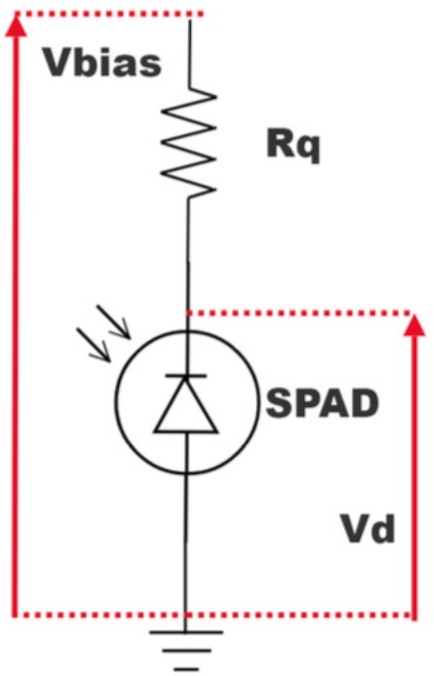

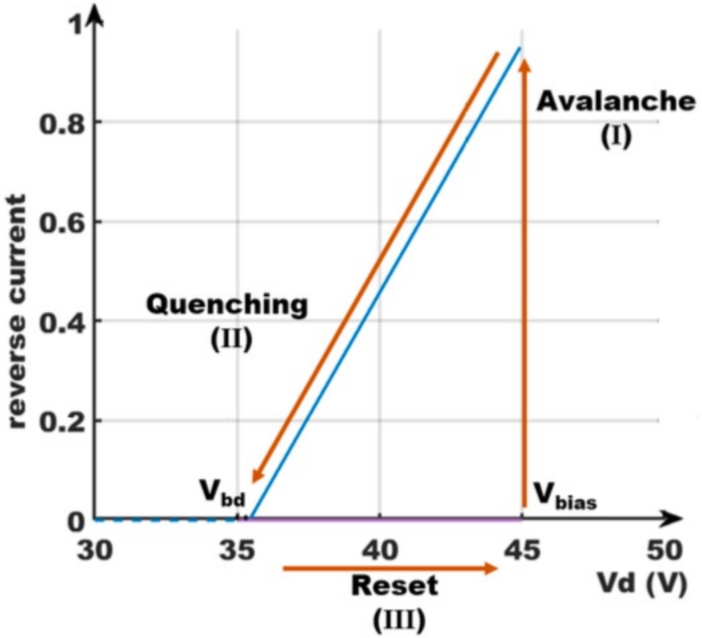

Once triggered, the avalanche is perpetual and the SPAD is insensitive to light (**light switch**).
Quenching means lowering the bias voltage closer to V_{BD} where the electric field is too low to sustain the avalanche.
The silmpliest implementation is by connencting in series to the SPAD a quenching resistor (Rq).
The avalanche current flowing through Rq produces a voltage drop at the SPAD that stops the avalanche.
Typical values of Rq O(500) kΩ
Rq can be implemented by an external component, but it is usually embedded in the devices.

SPAD: quenching mechanism

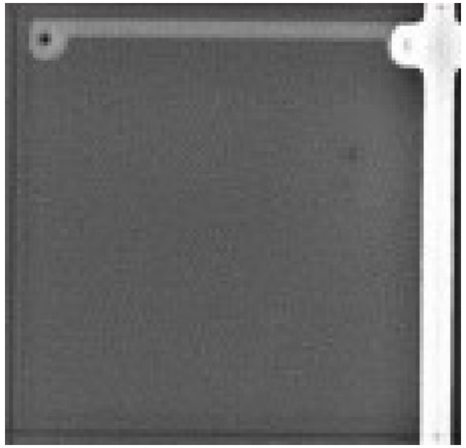

Embedded Rq can be made in:

- Poly Silicon (high T coeff, difficult process)
- Thin Metal film (low T coeff, simpler process, semitransparent to light)
- Bulk resistor (first type of Rq, easy to produce but not a lot of devices)
- Silicon Resistor (FBK, reduced T dependance, small and easy to implement)

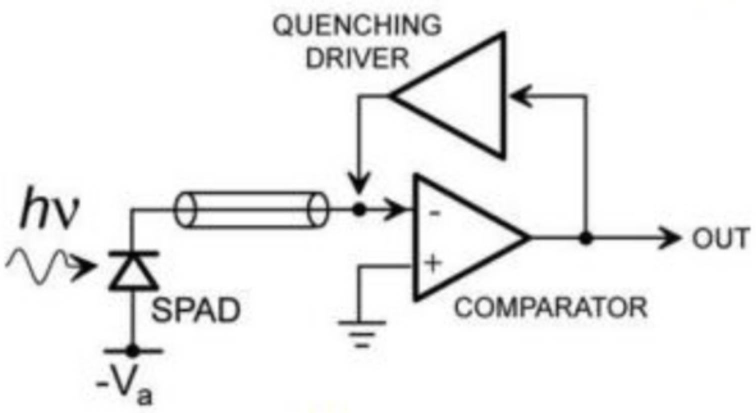

Active quenching. External/internal active quenching circuit. Comparator senses the signal and through a driver (transistors) stop the avalanche resulting in a more complex but generally faster and more stable quenching mechanism.

SPAD: junction and photodetection probability

$$PDP(\lambda, V_{oV}) = Tr(\lambda) * QE(\lambda) * P_t(\lambda, V_{oV})$$

$\boldsymbol{Tr(\lambda)}$ optical window **transmission** (1/R) Limiting factors for short wavelengths: - ARC Transmittance

$QE(\lambda, T)$ carrier Photo-generation probability for a photon to generate a carrier (in the active region) that reaches the high field region

$P_t(\lambda, V_{oV})$ avalanche triggering probability probability for a carrier traversing the high-field to generate the avalanche

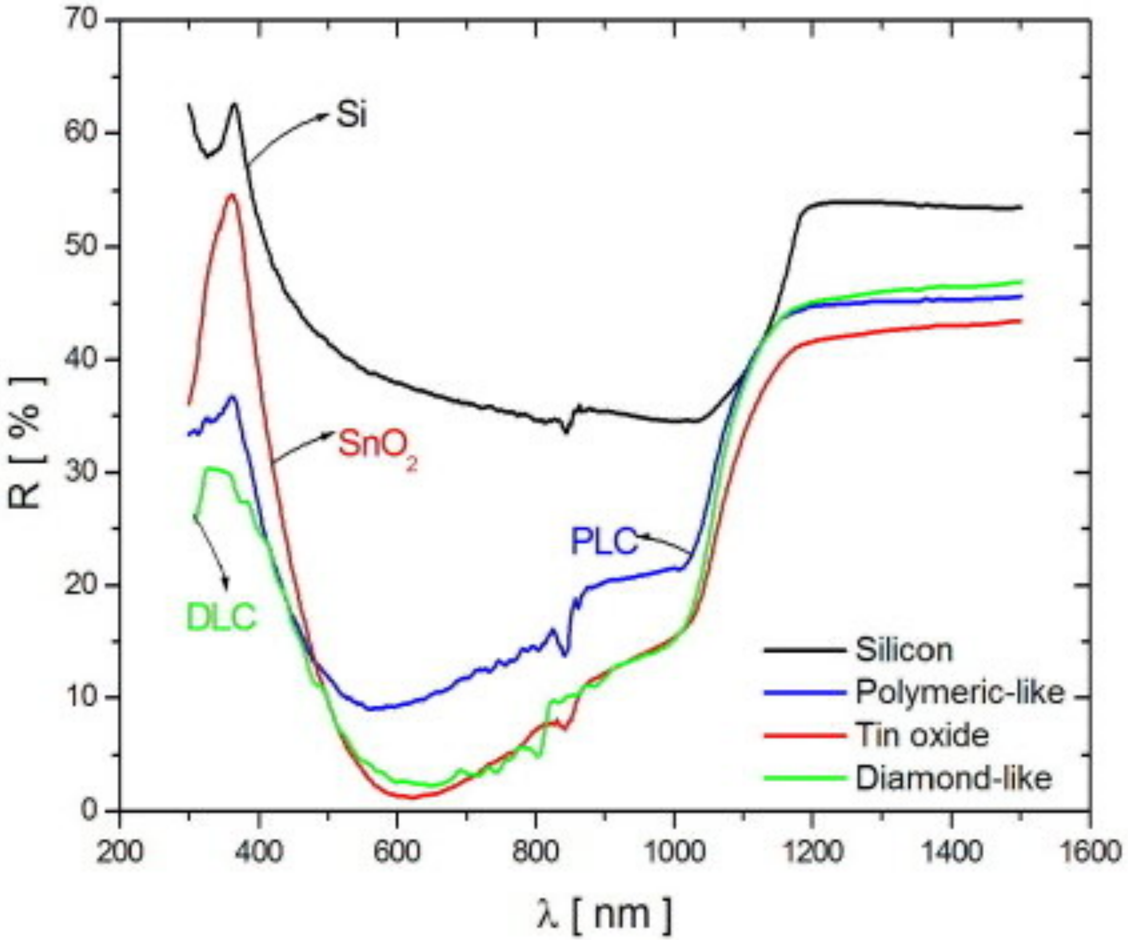

SPAD: junction and photodetection probability

$$PDP(\lambda, T, V_{oV}) = Tr(\lambda) * QE(\lambda, T) * P_t(\lambda, V_{oV})$$

$\boldsymbol{Tr(\lambda)}$ optical window **transmission** (1/R) Limiting factors for short wavelengths: - ARC Transmittance

$\boldsymbol{QE(\lambda, T)}$ carrier **Photo-generation probability** for a photon to generate a carrier (in the active region) that reaches the high field region

$P_t(\lambda, V_{oV})$ avalanche triggering probability probability for a carrier traversing the high-field to generate the avalanche

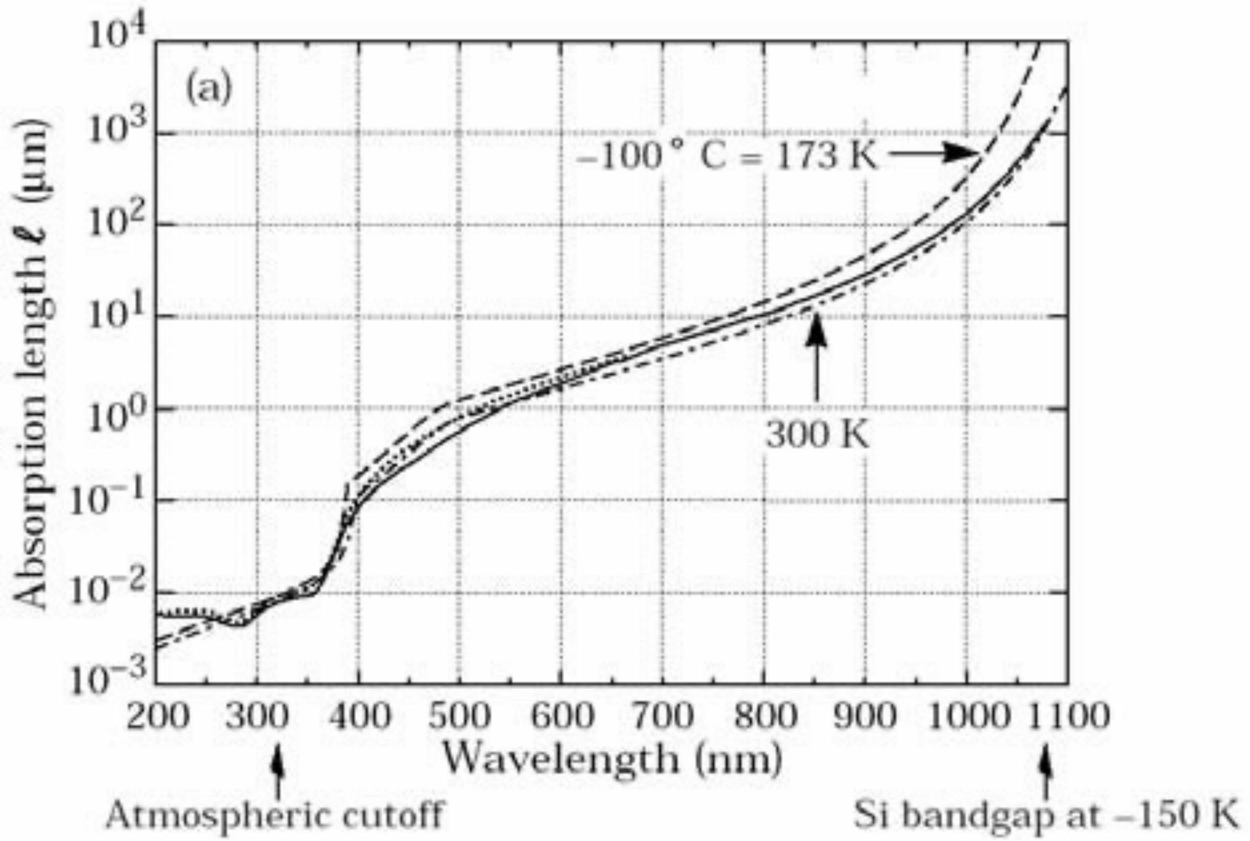

Hakeem Oluseyi **Characterization and deployment of large-format fully depleted back-illuminated p-channel CCDs for precision astronomy**

SPAD: junction and photodetection probability

$$PDP(\lambda, T, V_{oV}) = Tr(\lambda) * QE(\lambda, T) * P_t(\lambda, V_{oV})$$

$\boldsymbol{Tr(\lambda)}$ optical window **transmission** (1/R) Limiting factors for short wavelengths: - ARC Transmittance

$\boldsymbol{QE(\lambda, T)}$ carrier Photo-generation probability for a photon to generate a carrier (in the active region) that reaches the high field region

$\boldsymbol{P_t(\lambda, V_{oV})}$ **avalanche triggering probability probability** for a carrier traversing the high-field to generate the avalanche

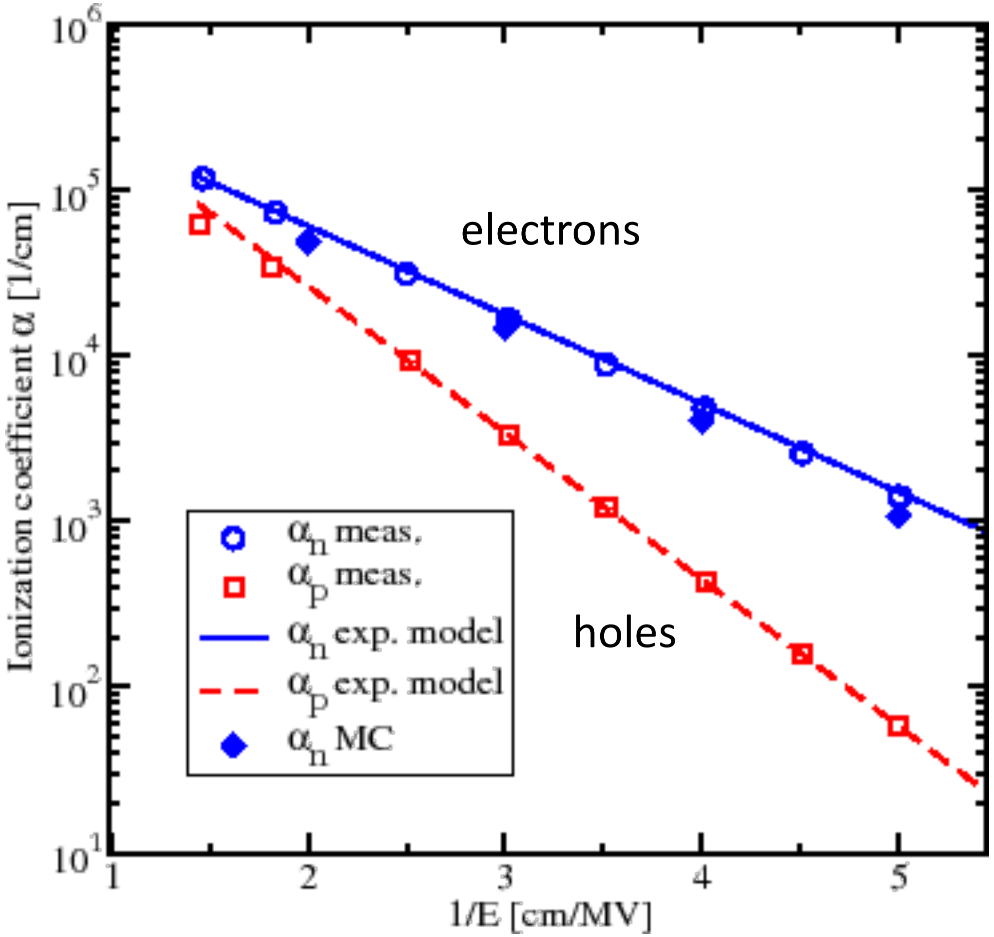

https://www.iue.tuwien.ac.at/phd/triebl/node20.html

SPAD: junction and photodetection probability

$$PDP(\lambda, T, V_{OV}) = Tr(\lambda) * QE(\lambda, T) * P_t(\lambda, V_{OV})$$

$\boldsymbol{Tr(\lambda)}$ optical window **transmission** (1/R) Limiting factors for short wavelengths: - ARC Transmittance

$\boldsymbol{QE(\lambda, T)}$ carrier **Photo-generation probability** for a photon to generate a carrier (in the active region) that reaches the high field region

$\boldsymbol{P_t(\lambda, V_{OV})}$ **avalanche triggering probability probability** for a carrier traversing the **high-field** to generate the avalanche

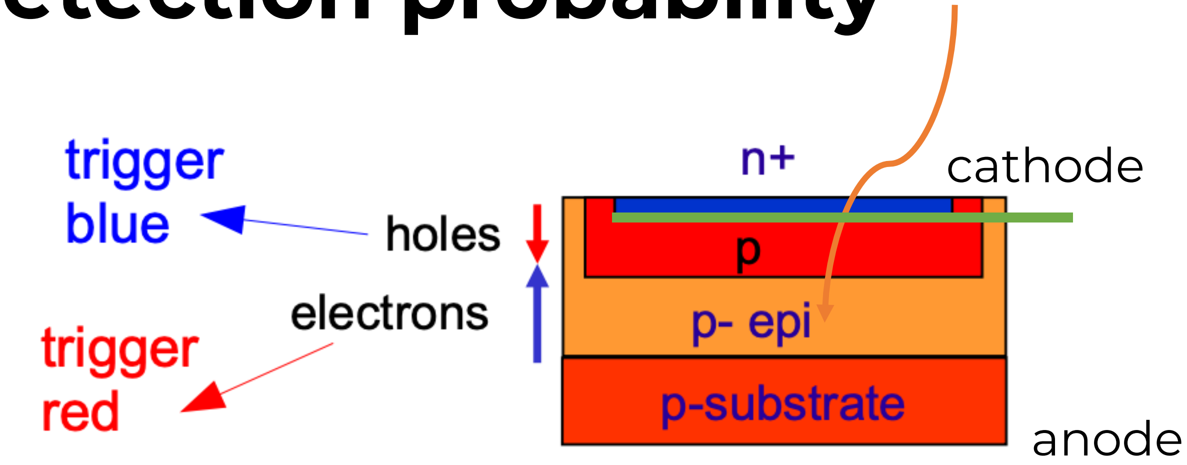

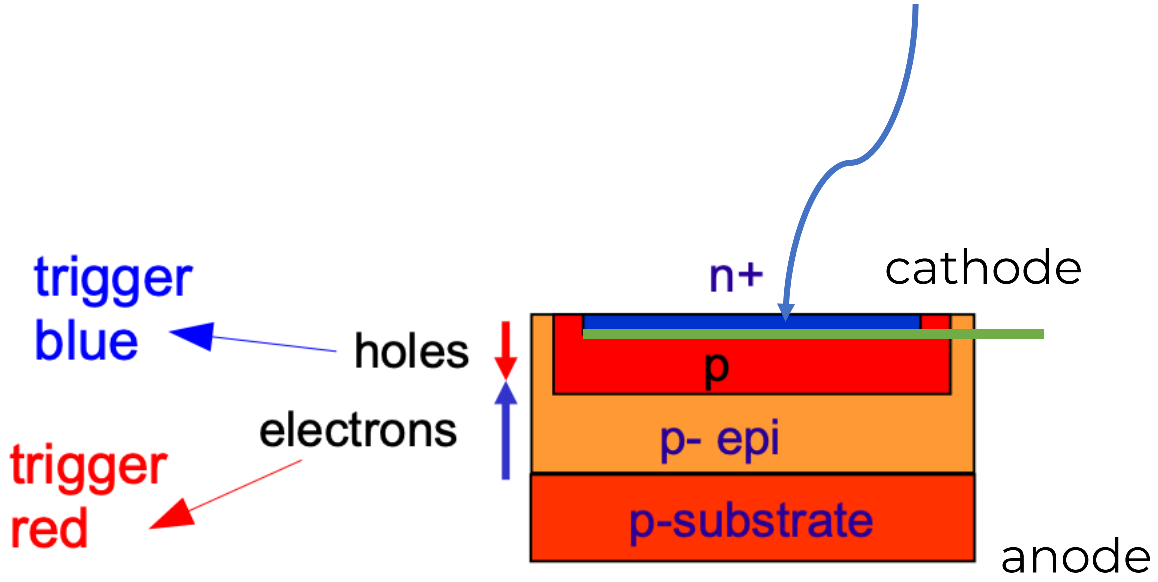

SPAD: junction and photodetection probability

$$PDP(\lambda, T, V_{oV}) = Tr(\lambda) * QE(\lambda, T) * P_t(\lambda, V_{oV})$$

$Tr(\lambda)$ optical window **transmission** (1/R) Limiting factors for short wavelengths: - ARC Transmittance

$QE(\lambda, T)$ carrier **Photo-generation probability** for a photon to generate a carrier (in the active region) that reaches the high field region

$P_t(\lambda, V_{oV})$ **avalanche triggering probability probability** for a carrier traversing the high-field to generate the avalanche

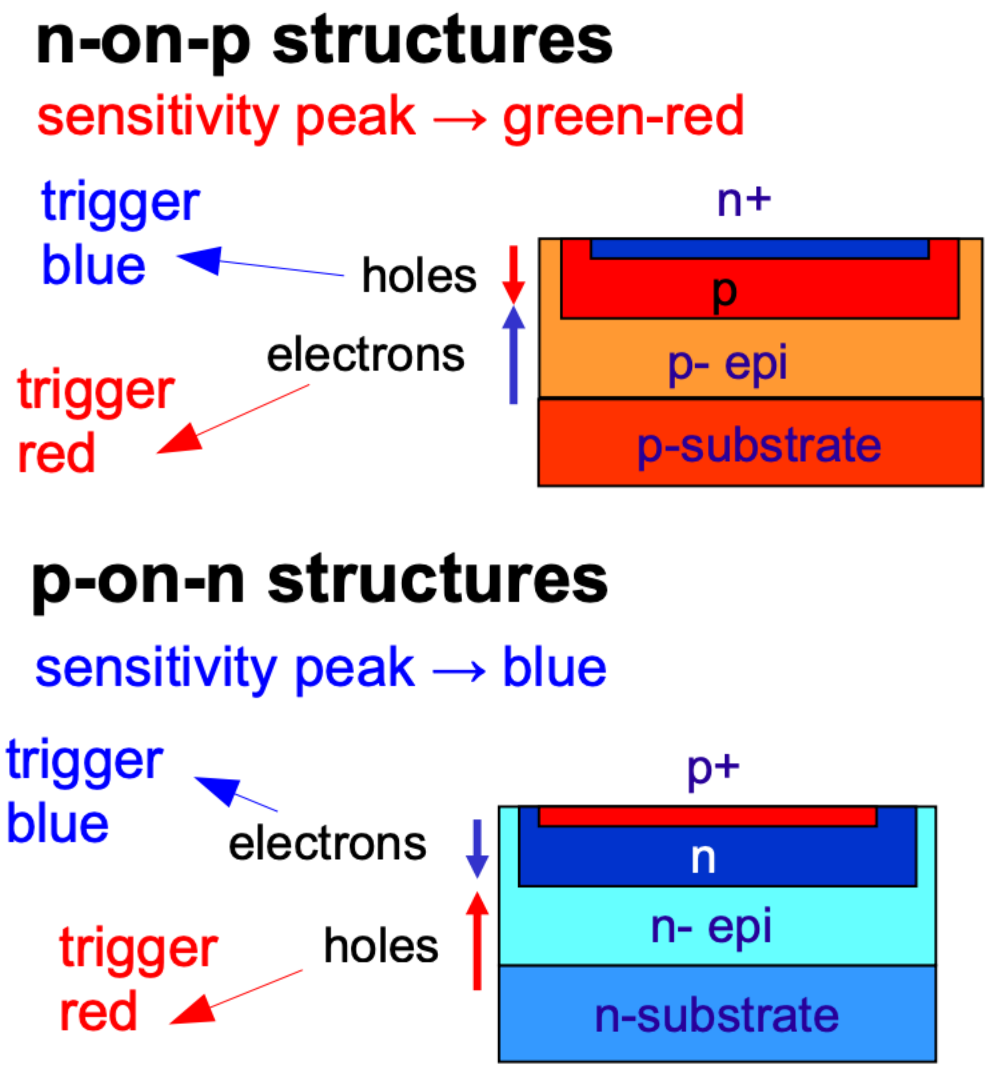

SPAD: junction and photodetection probability

$$PDP(\lambda, T, V_{oV}) = Tr(\lambda) * QE(\lambda, T) * P_t(\lambda, V_{oV})$$

$Tr(\lambda)$ optical window **transmission** (1/R) Limiting factors for short wavelengths: - ARC Transmittance

$QE(\lambda, T)$ carrier **Photo-generation probability** for a photon to generate a carrier (in the active region) that reaches the high field region

$P_t(\lambda, V_{oV})$ **avalanche triggering probability probability** for a carrier traversing the high-field to generate the avalanche

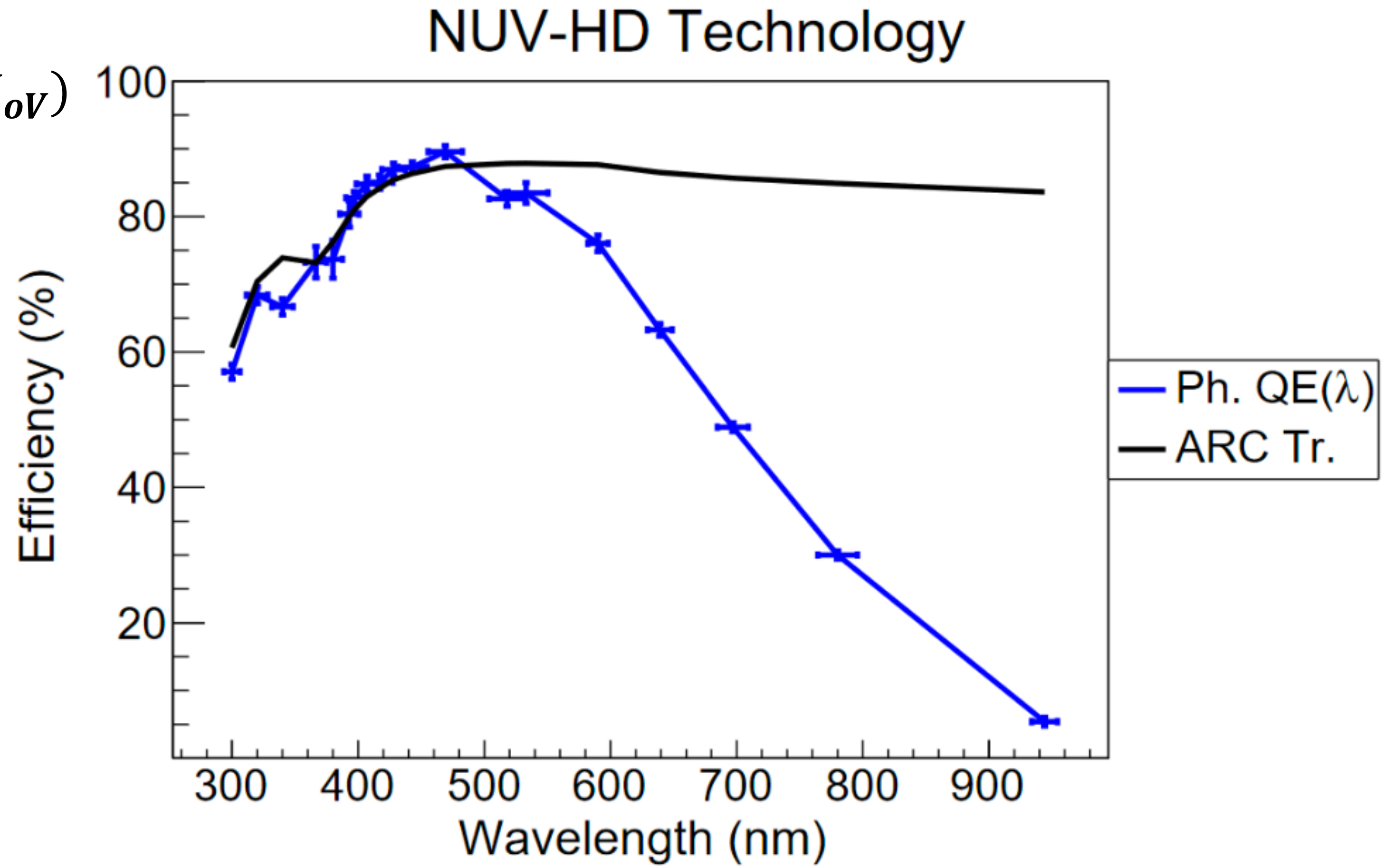

Zappalà, G. Study of the photo-detection efficiency of fbk high- density silicon photomultipliers

SPAD fabrication

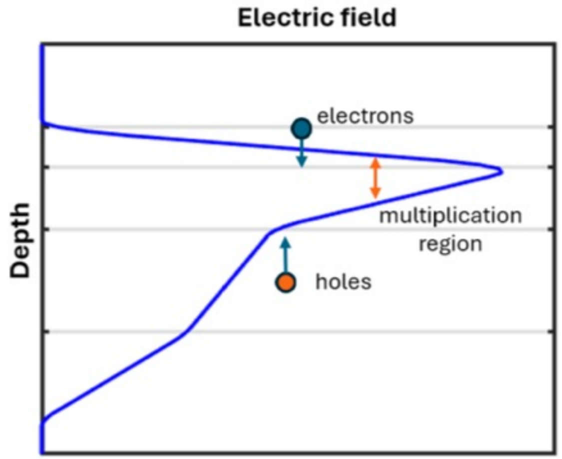

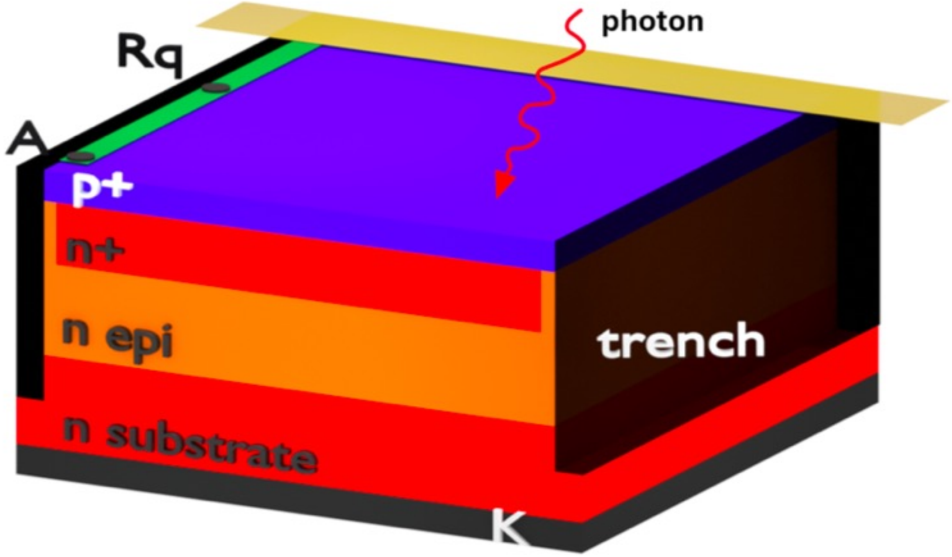

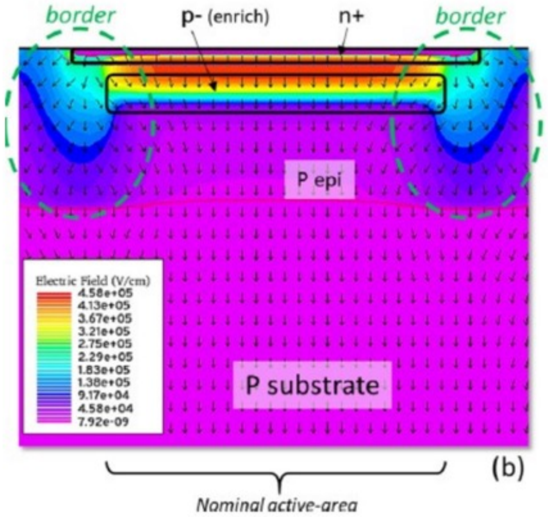

- A **shallow very thin** (~ 100 nm) p+ layer characterized by a high number of acceptors.
- A **n+ implant** that creates the **junction** with the **p+ layer**.
- A **low doping n** epitaxial layer.
- A final **n substrate** with low **resistivity** that acts as contact for the **cathode** (K)

Electric field **visualization** with **TCAD** simulation
minimize microplasma creation by having uniform electric field close to the border.

Acerbi F. Understanding and simulating SiPMs

Luigi Rignanese rignanes@bo.infn.it

SPAD: electrical model

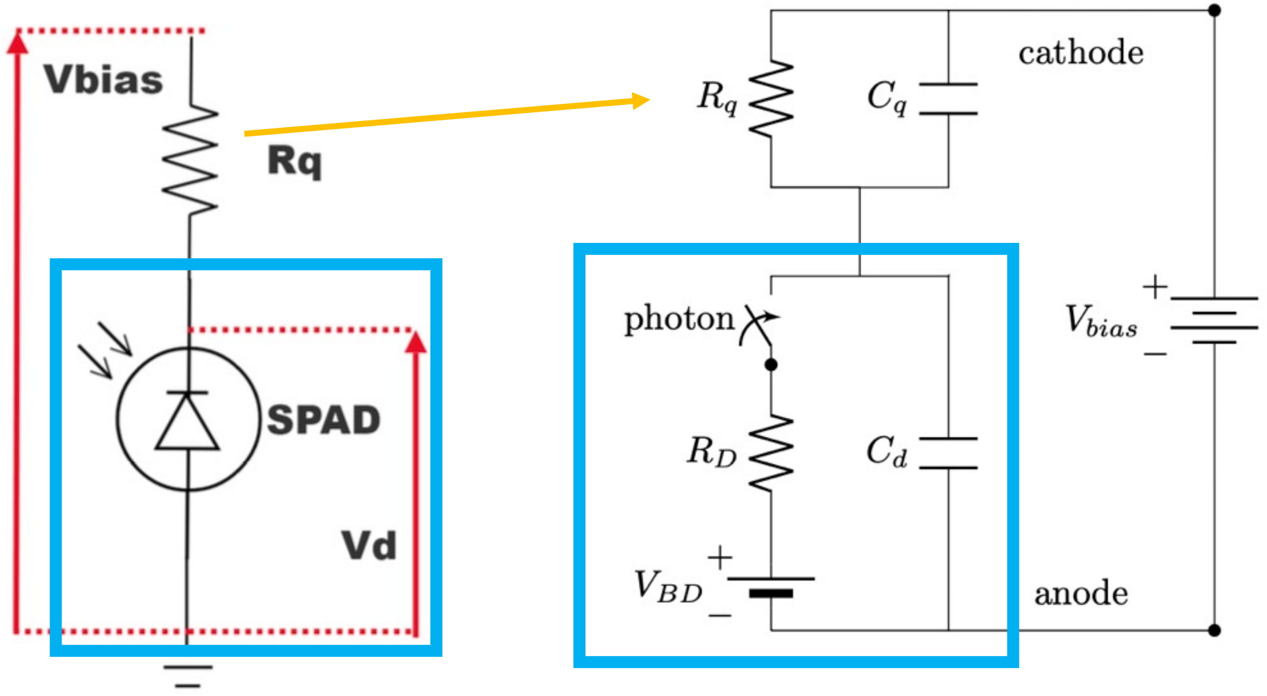

$$C_D = \frac{\epsilon_0 \epsilon_{Si} A}{W_D}$$

$$W_D = \sqrt{\frac{2\epsilon_r \epsilon_{Si}}{q} \left(\frac{1}{N}\right) \left(V_{bi} - V_{bias} - \frac{2kT}{q}\right)}$$

$$C_D = A \sqrt{\frac{N q \epsilon_0 \epsilon_{Si}}{2}} \left(V_{bi} - V_{bias} - \frac{2kT}{q}\right)^{-\frac{1}{2}}$$

A = area of the SPAD
W_D = depletion region width
N = dopant density
V_{bi} = contact potential
ε_0 and ε_{Si} are the dielectric constant

SPAD: electrical model

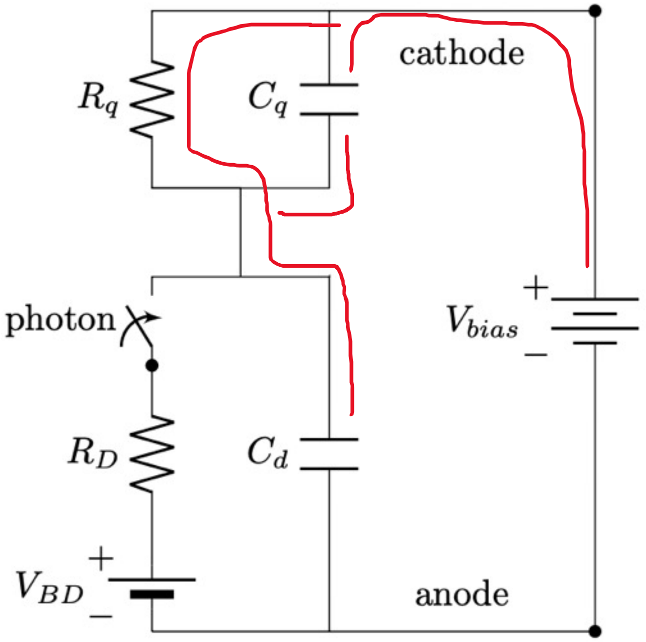

- Before photon detection: the switch is open, C_D is charged up to the V_{bias} and C_q is discharged

SPAD: electrical model

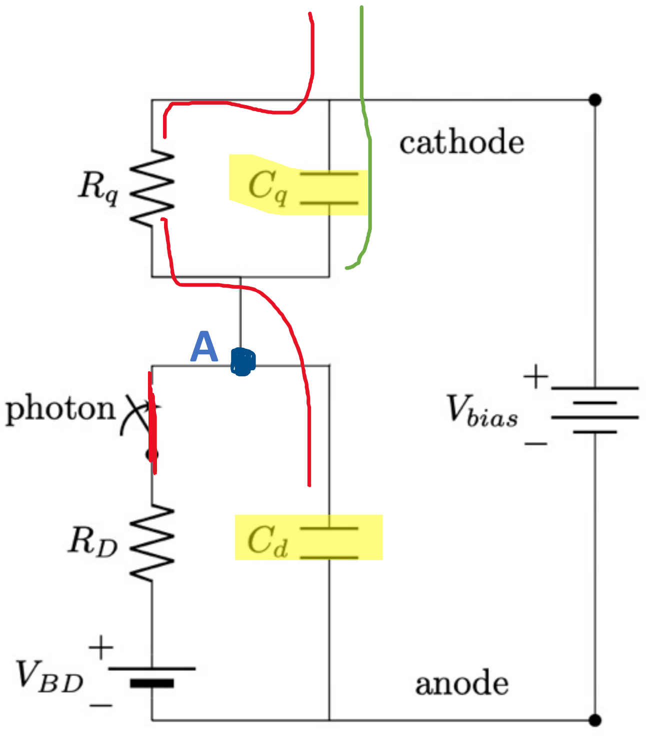

- Photon detection: the switch closes.
  A point is at V_{BD} initiating a **current** that discharges C_D through R_D with an initial value of ($V_{OV} = V_{bias} - V_{BD}$):

$$I_D = V_{OV} / (R_D + R_Q)$$

- The voltage drop in A induces a voltage change across C_q, generating another, **faster current spike**
- The cumulative charge generated during the avalanche is the summation of the two capacitances multiplied by V_{OV}, and the gain (**G**) is defined as the total charge divided by the elementary charge:

$$G = \frac{V_{OV}(C_D + C_q)}{q}$$

SPAD: electrical model

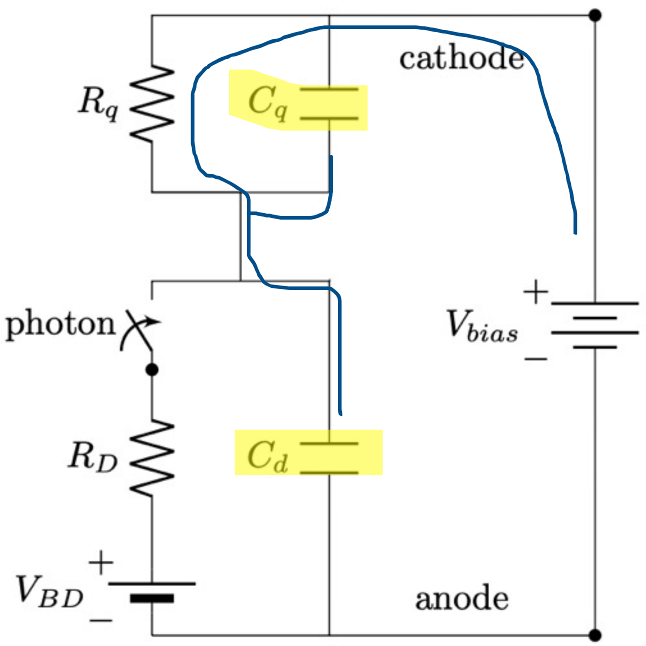

- Once the avalanche is quenched: switch open
  C_D is recharged/Cq discharged through R_q

SPAD: electrical signal

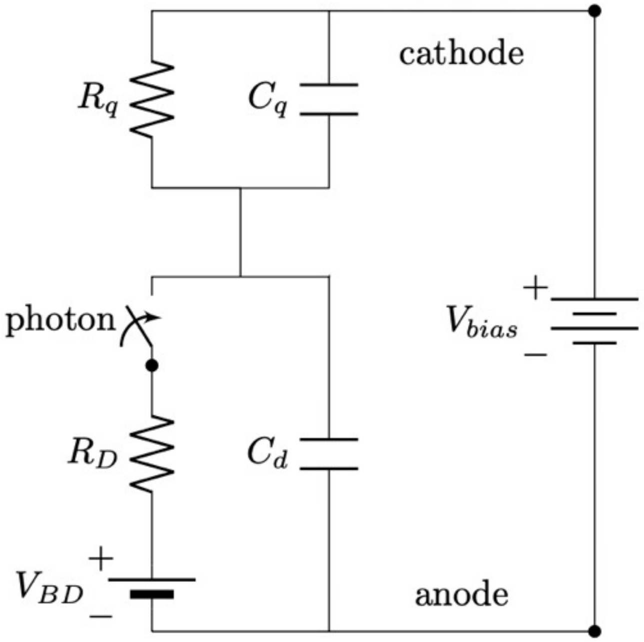

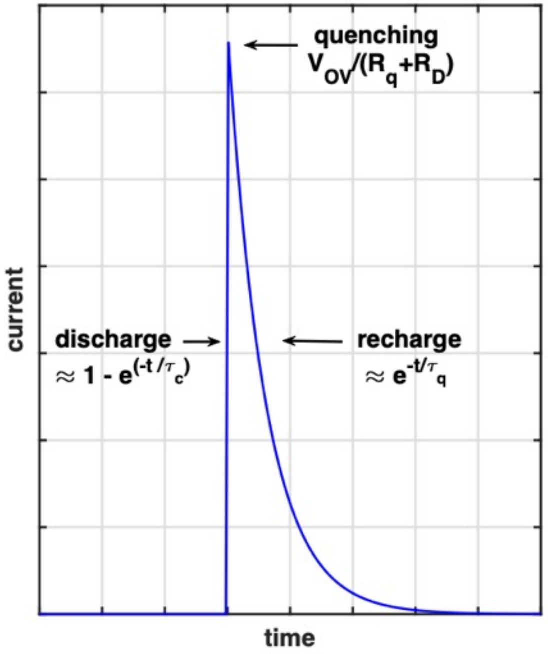

2 time constant characterize the signal shape:

1. $\tau_c \approx (\mathbf{C_D} + C_q)(R_d \parallel R_q)$
2. $\tau_q \approx R_q x(C_q + \mathbf{C_D})$

Typical values of $R_D \sim 1$ kΩ and $R_q \sim 500$ kΩ, the rise time is extremely rapid O(100) ps, whereas the decay time is slower O(100) ns.

Both values are related to $\mathbf{C_D}$.

Smaller SPADs are typically faster but have less gain than SPADs with larger areas (at the same V_{OV}).

Depending on the required timing performance, especially in low-light measurements, larger SPADs are advantageous due to their elevated gain.

SPAD: Pros and limitations

SPADs have high **QE** (up to **80%**) and can be tuned to different wavelength

SPADs have very **high gain** (up to **10^7**) with moderate overvoltage

BUT:

SPADs can’t count photons = binary devices

Large area SPAD has large C_D = very long time constants

Large area SPAD has large C_D = generate a lot of charge that is hard to quench

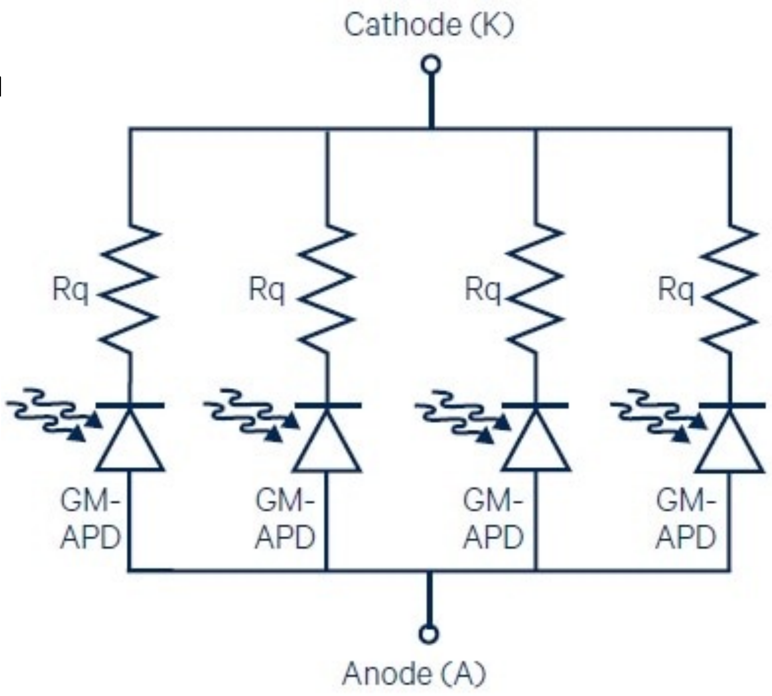

SOLUTION first proposed in the late ’80s by **Golovin** and **Sadygov** (russian Patent) Avalanche Micro-channel/pixel Photo Diodes (AMPD) with integrated bulk quenching resistor.
Divide the active area in **smaller SPADs** each one with its **R_q** and connect them in **parallel**.

Smaller C_D, cells are isolated by the **Rq**, **single readout**

SiPM-MPPC

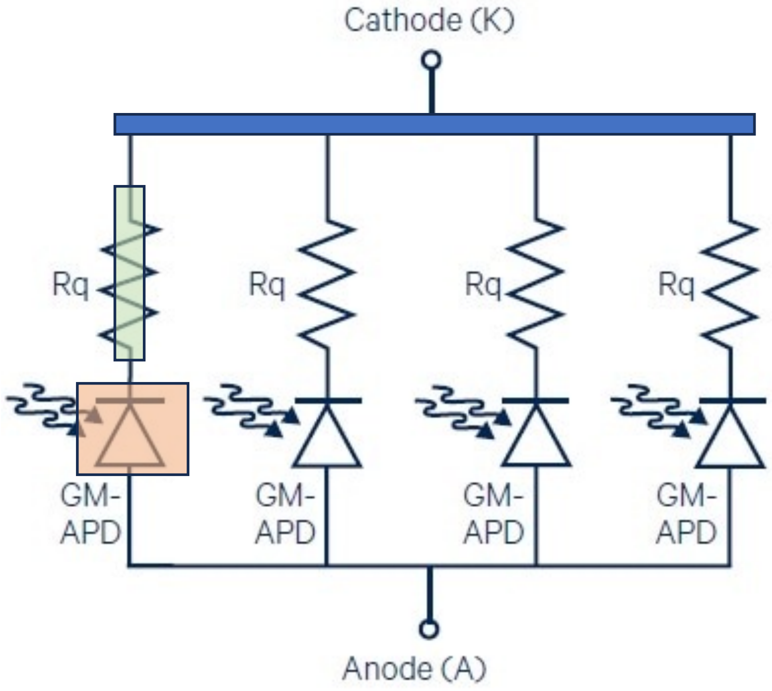

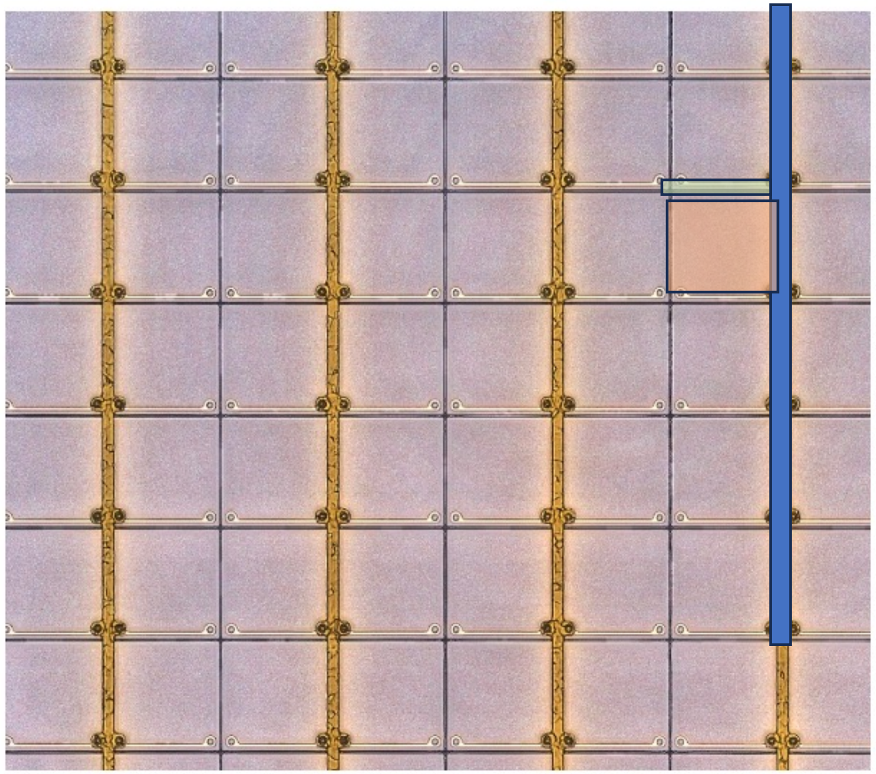

Broadcom AFBR-S4N33C013 3 x 3 mm^2 SiPM.
Each a SPAD with a pitch of 30 x 30 μm^2

SiPM-MPPC

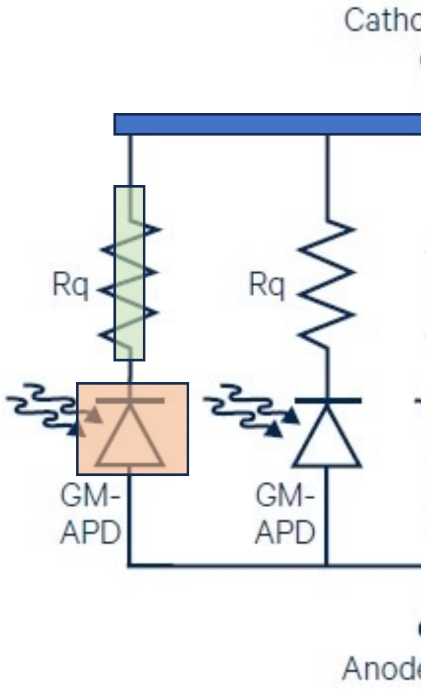

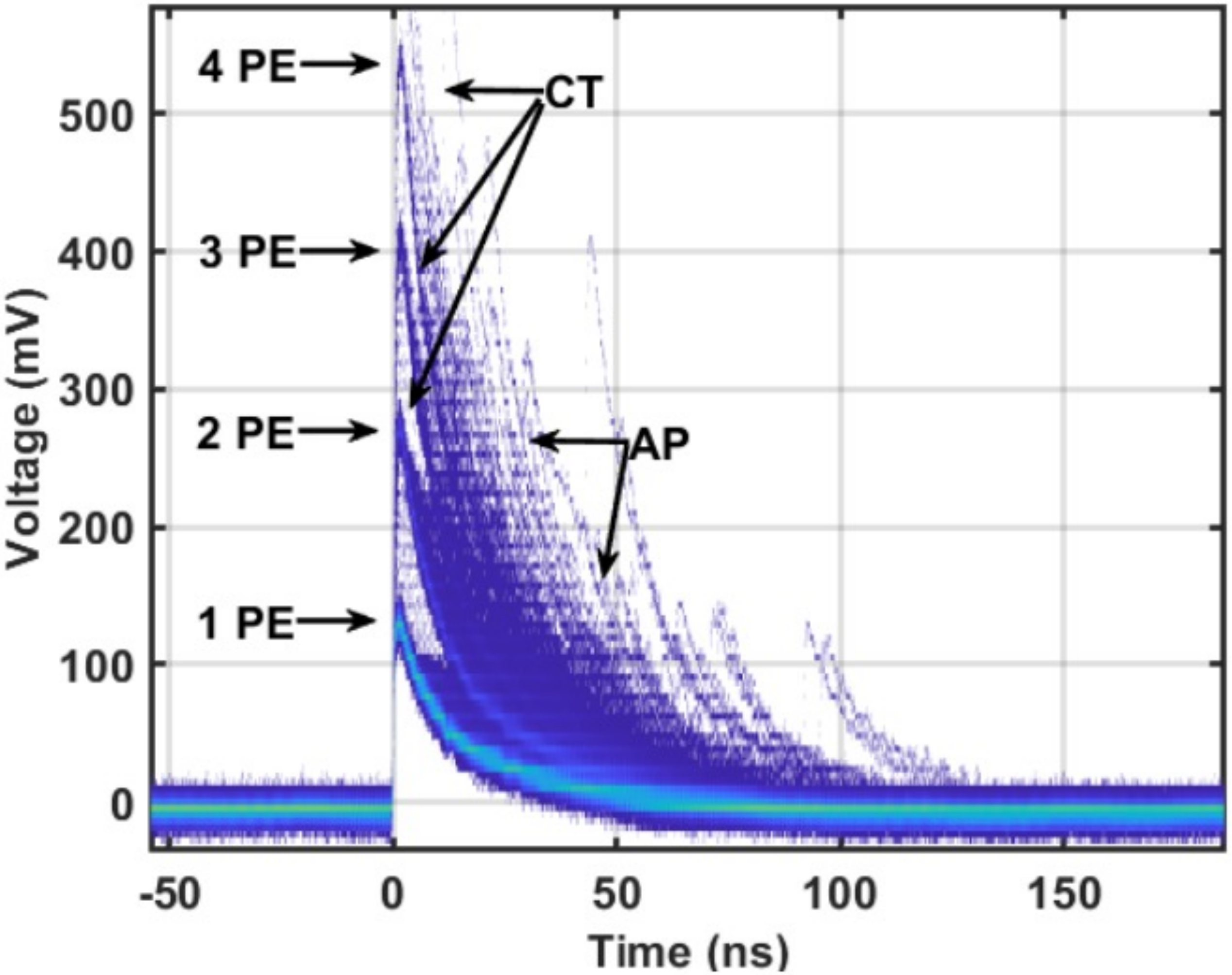

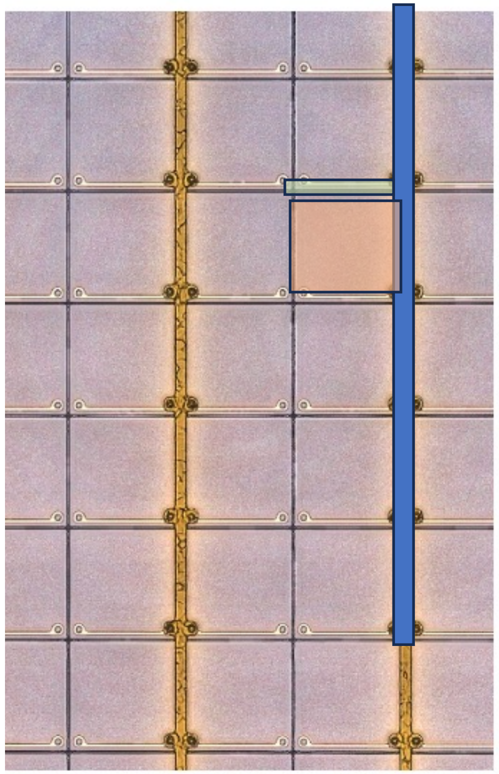

-N33C013 3 x 3 mm^2 SiPM.
pitch of 30 x 30 μm^2

INFN

SiPM

- **Photo Detection Efficiency** (extend the concept od PDP for a matrix of SPADs)
- **Gain**
- **Noise sources**
  - **Primary noise**
  - **Correlated noise**
- **IV curve and breakdown voltage** (Current-Voltage curve and BD extraction)
- **Signal Shape** (electric model and how passive cells impact on signal shape, amplitude measurement)
- **Electronics** (charge, voltage and current amplifier)
- **Timing** (avalanche propagation and electronic noise for time measurement)

SiPM

- **Photo Detection Efficiency** (extend the concept od PDP for a matrix of SPADs)
- **Gain**
- **Noise sources**
  - **Primary noise**
  - **Correlated noise**
- **IV curve and breakdown voltage** (Current-Voltage curve and BD extraction)
- **Signal Shape** (electric model and how passive cells impact on signal shape, amplitude measurement)
- **Electronics** (charge, voltage and current amplifier)
- **Timing** (avalanche propagation and electronic noise for time measurement)

Photo Detection Efficiency PDE

Extension of the **PDP** considering the **dead area** in between **SPADs**
Fill Factor: fraction of **active area** wrt the area of the SiPM. **Dead area** are **trenches**, **quenching resistors** and **metallic structures** on top of the device.

$$PDE(\lambda, V_{oV}) = PDP(\lambda, V_{oV}) * FF$$

$Tr(\lambda)$

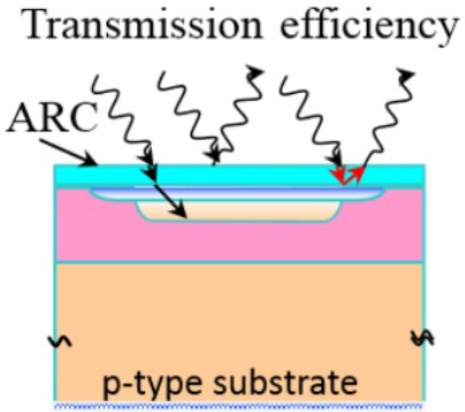

$QE(\lambda)$

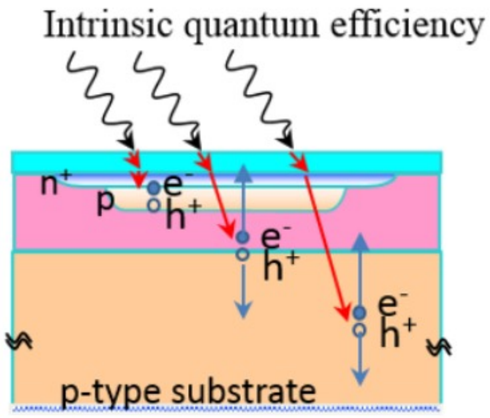

$P_t(\lambda, V_{oV})$

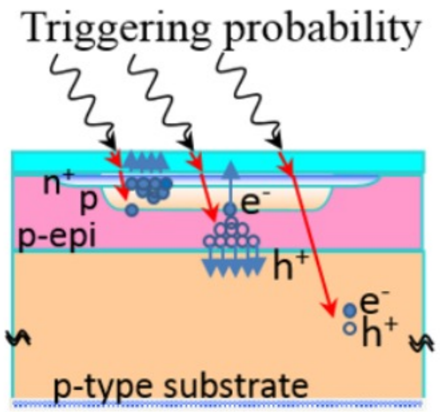

FF

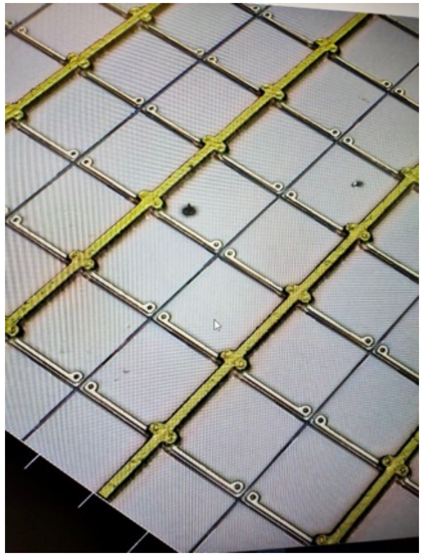

Photo Detection Efficiency PDE

PDE tuning

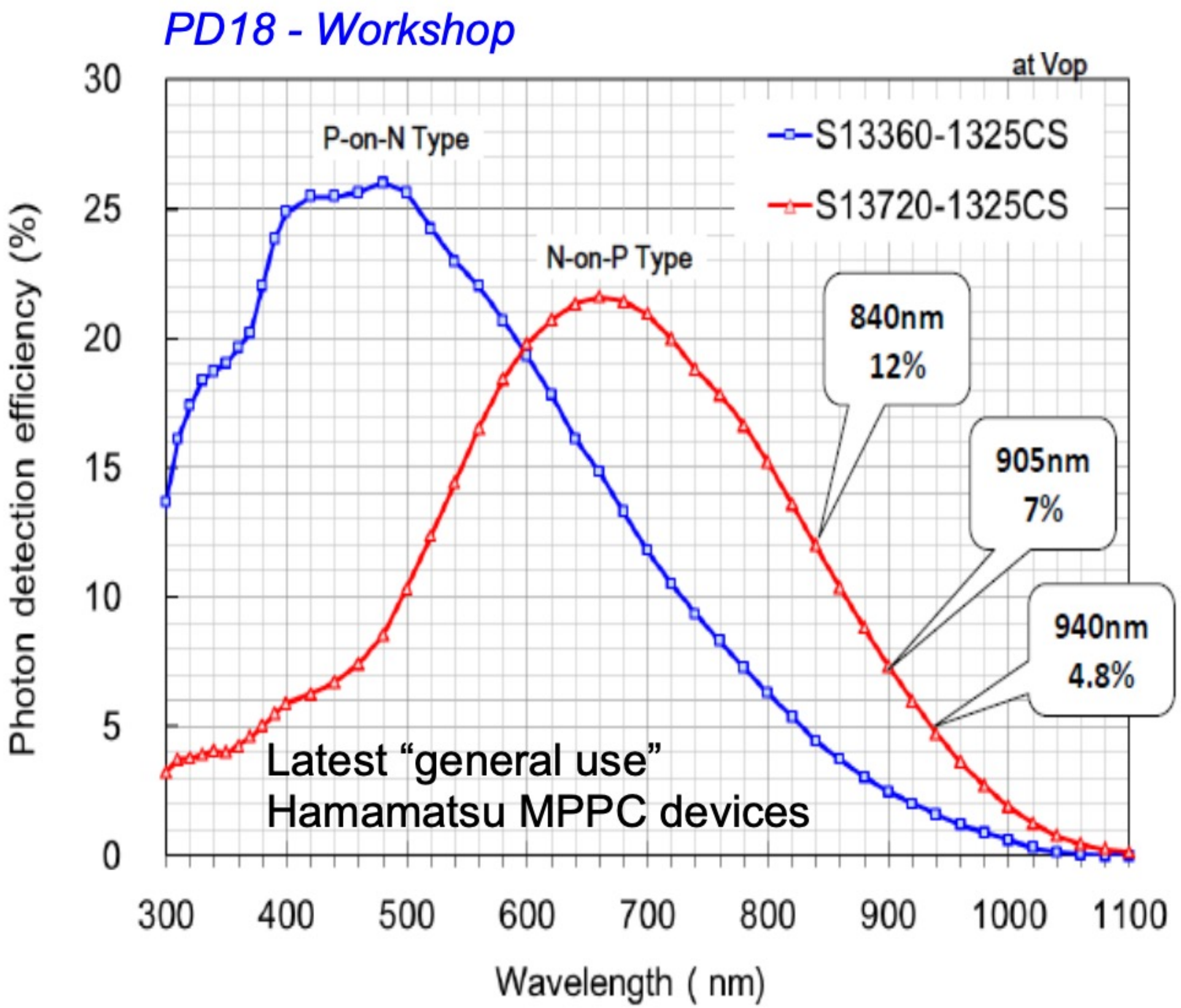

PDE at different VOV

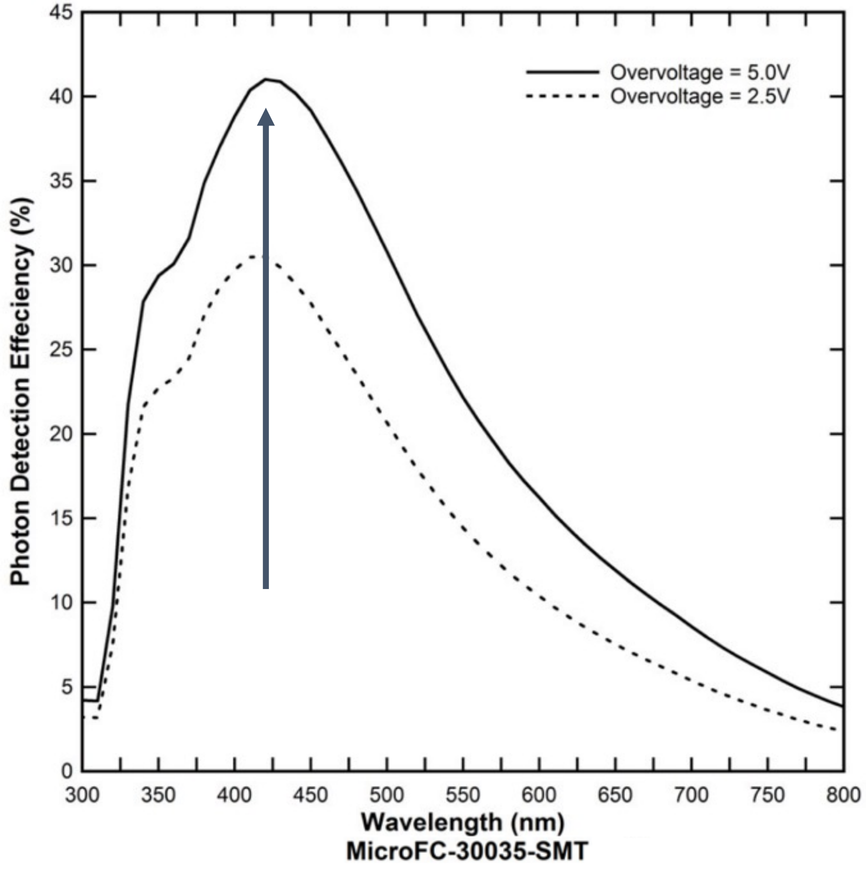

PDE

FF is strictly **proportional** to the **SPAD** dimension and the **PDE** changes accordingly

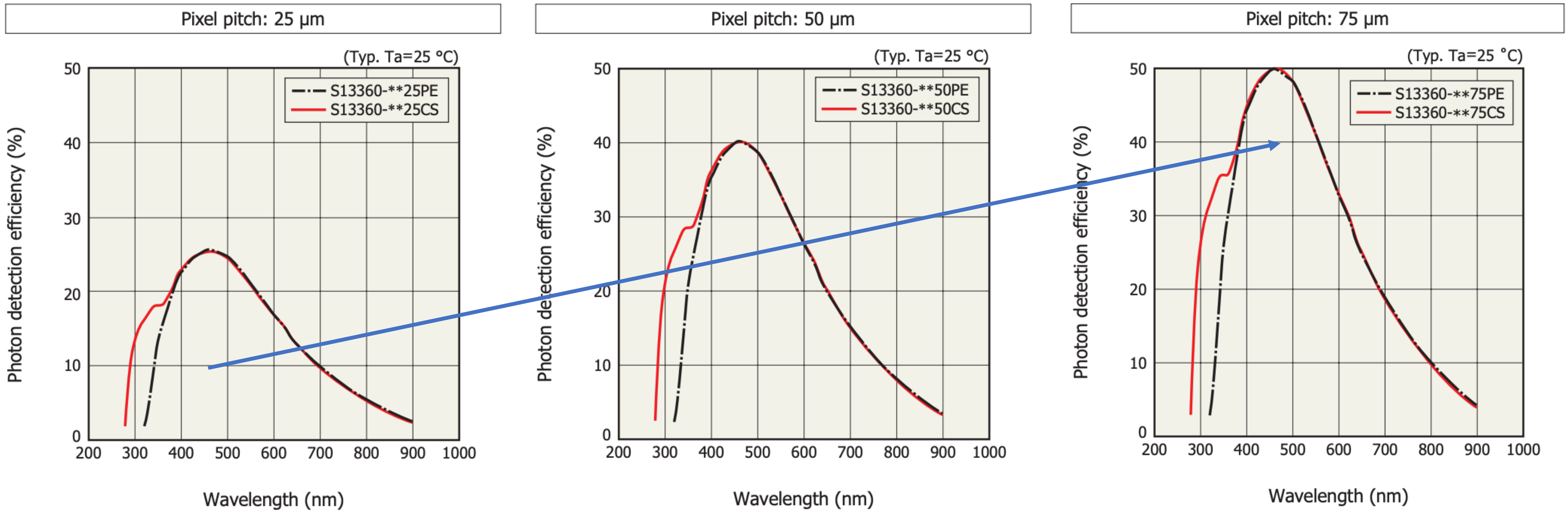

PDE improvements

Trenches between cells are **needed** to **optical** and **electric isolation**. **Improvements** in this field means **deep** and **narrow** trenches.

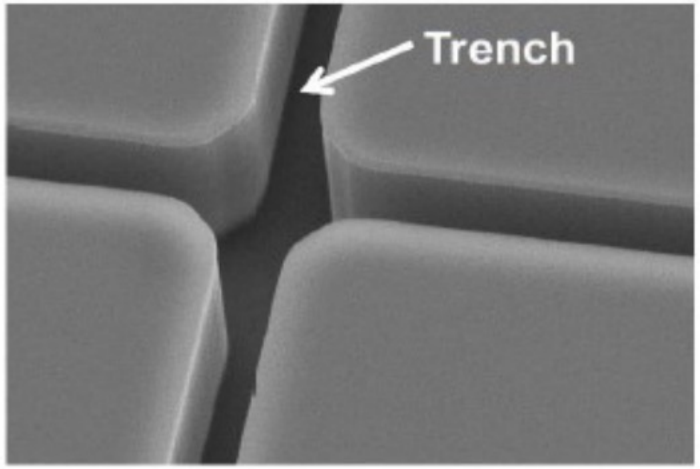

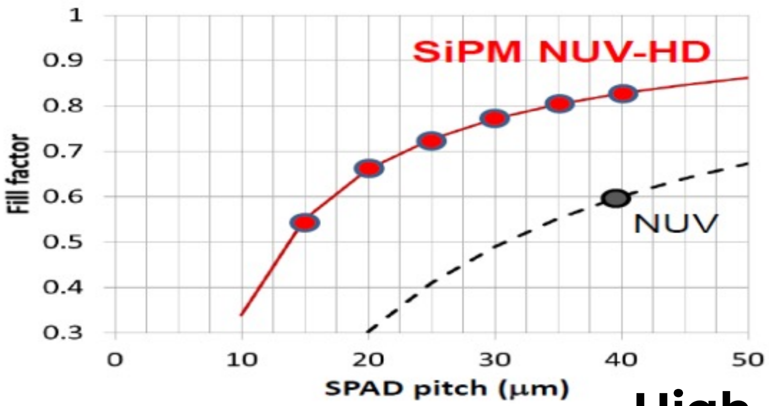

High Density FBK tecnology

Operating the SiPMs at **higher overvoltage improves** the **PDE** but need **very uniform electric** field across the device (latest improvements)…**pay attention to noise**!

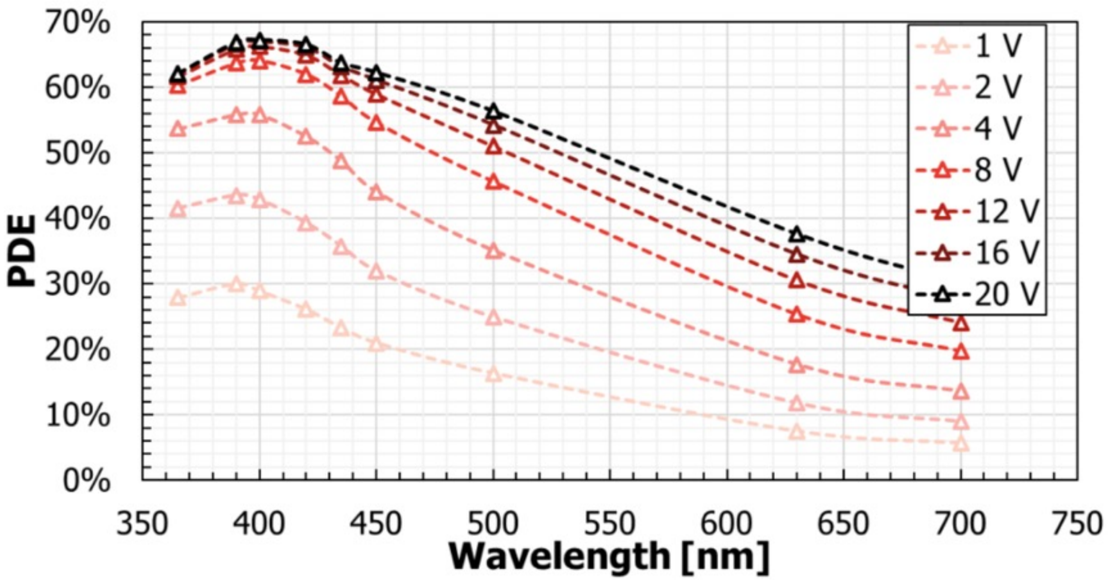

HD Metal filled threnches FBK tecnology

https://iopscience.iop.org/article/10.1088/1748-0221/18/05/P05040

PDE of commercial SiPMs

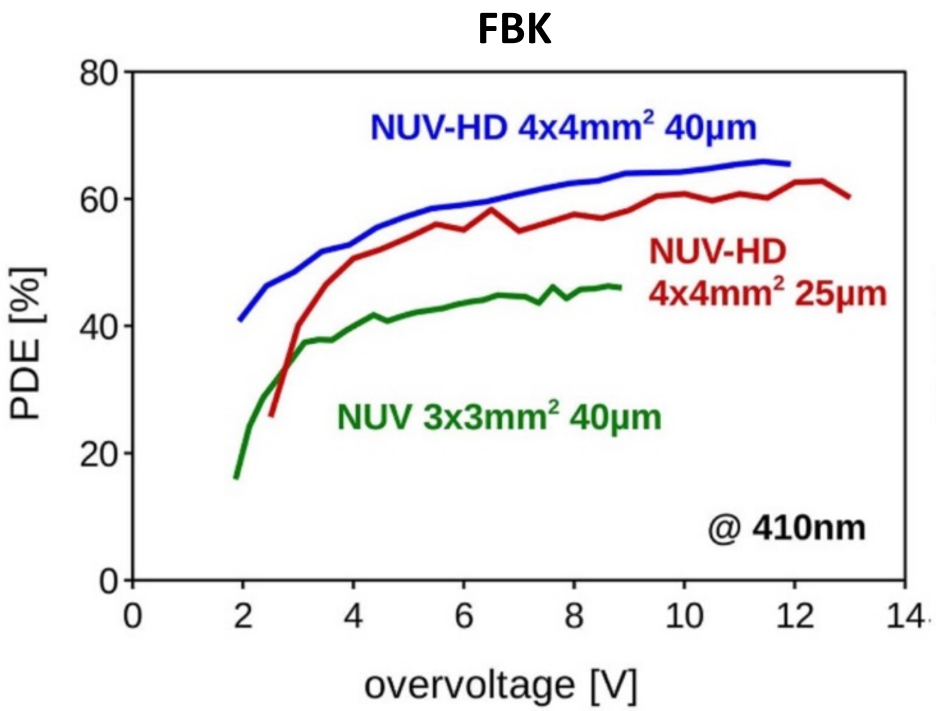

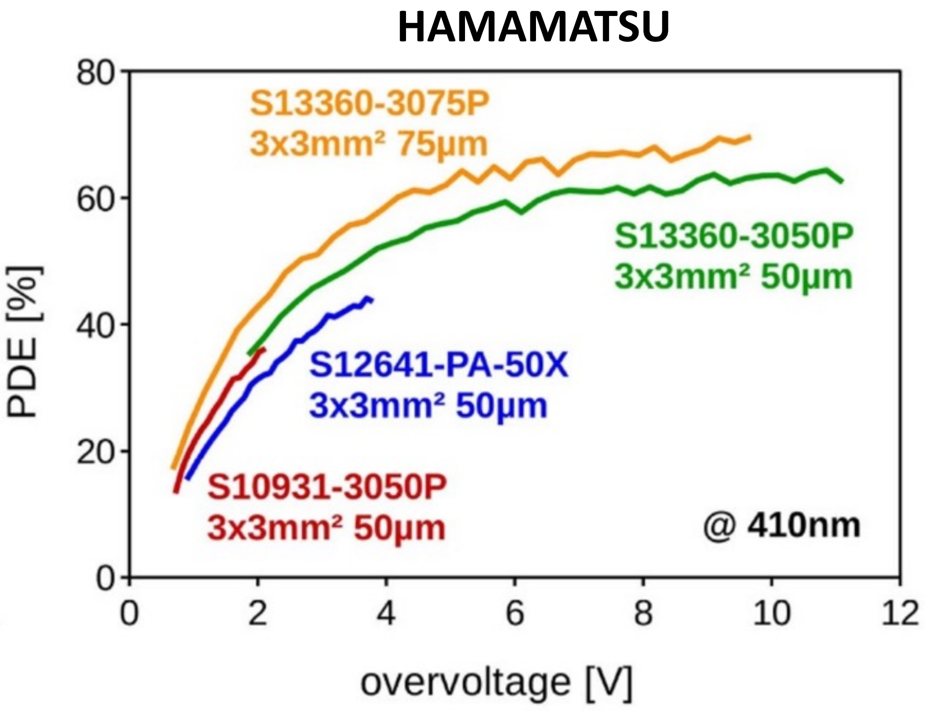

Increase over the years of almost 50% thanks to better trenches and electric field uniformity.

The silicon photomultiplier: fundamentals and applications of a modern solid-state photon detector

Importance of PDE for SPDs

It is obvious that when measuring a small number of photons, PDE plays a fundamental role in maximizing the amount of signal.

Big SPADs should be preferred and the right technology to match the wavelength of the detected light.

Measuring PDE

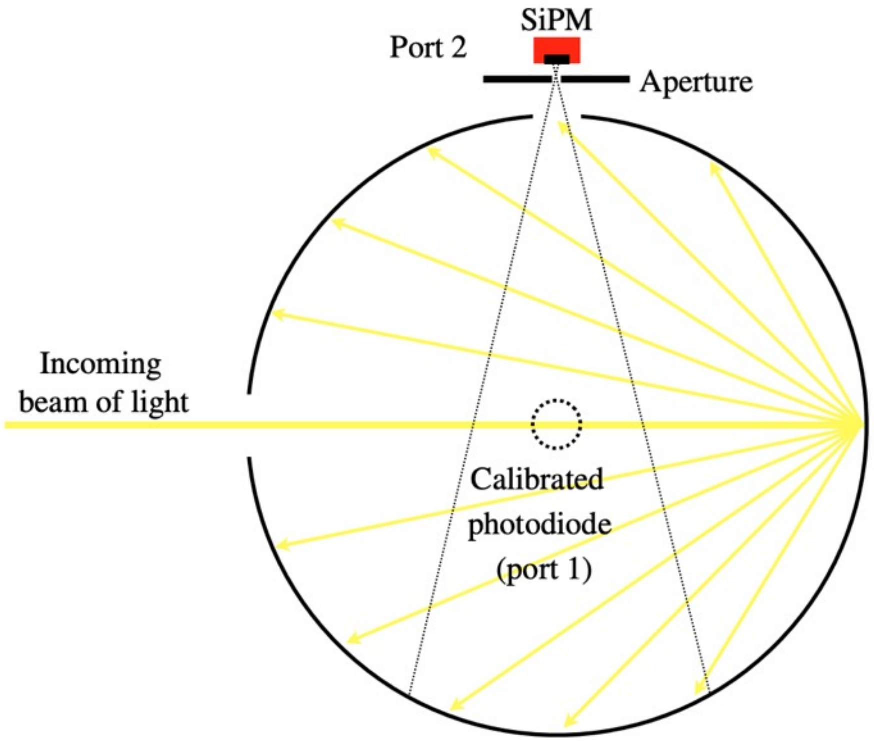

PDE=N_{pe}/N_{ph}

Integrating sphere to distribute an incoming beam of light between the SiPM and a calibrated photodiode used to determine the absolute amount of light which reaches the SiPM.

1. Estimate the light arriving in port 2 by the ratio P1/P2 using the calibrated PD.
2. **N_{ph}** is the photodiode current divided by hνAα, where ν is the photon frequency, A is the area and α is the photodiode responsivity (given by the producer).
3. **N_{pe}** can be measured using two different methods:
    1. The **DC current** method relies on the difference between the actual current and the dark current all divided by the gain G
    2. The **pulse counting** methods relies on the difference between the counting rate subtracted by the dark count rate

Characterisation studies of silicon photomultipliers

GAIN

Gain is defined by the **charge** developed in one cell (**SPAD**) by a primary charge carrier (**photoelectron**).
Same definition as for the **SPAD**

$$G = \frac{Q}{q} = \frac{(C_D + C_q)(V_{bias} - V_{BD})}{q} = \frac{(C_D + C_q)V_{OV}}{q}$$

G increases linearly with V_{bias} at given V_{BD}. It can be measured as the distance between two consecutive peaks in the SPE spectrum

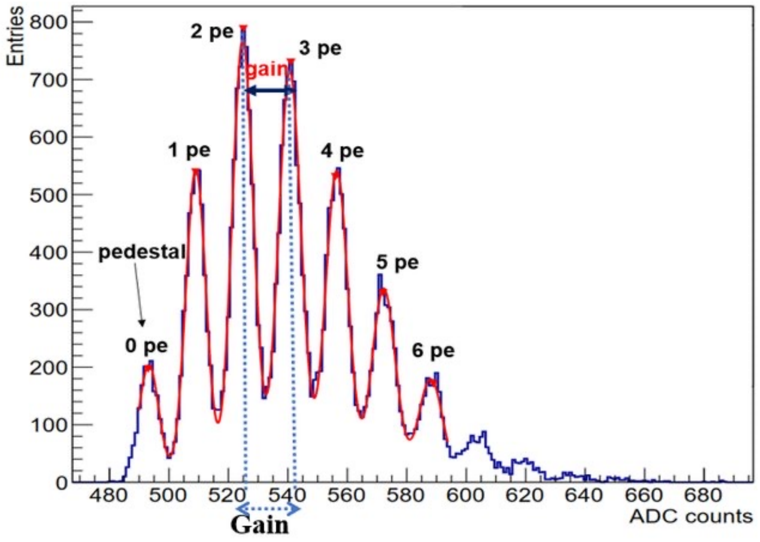

Operation and Calibration of a Highly Granular Hadron Calorimeter with SiPM-on-Tile Read-out

The slope of the fit of G vs V_{OV} gives the total cell capacity (this value is typically indicated in the datasheet)

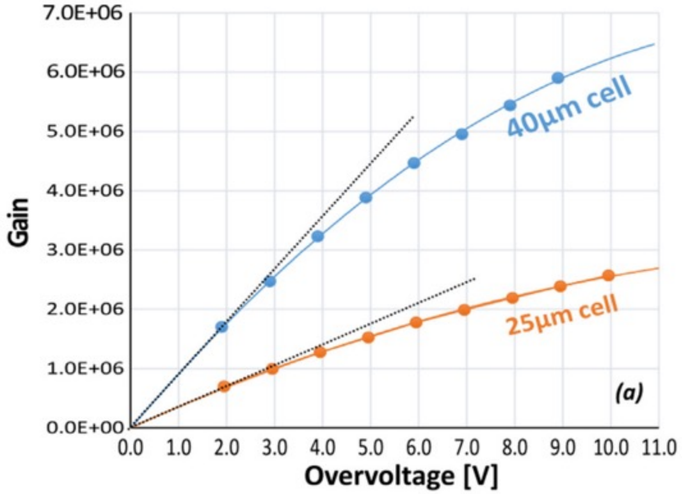

Divergences from linearity due to change in C_D for some devices.

Acerbi F. Understanding and simulating SiPMs

G variations (gaussian peaks) in a SiPM are mainly dependent on C_D and V_{BD} uniformity

$$\frac{\partial G}{G} = \frac{\partial V_{BD}}{V_{BD}} \oplus \frac{\partial C_{Dq}}{C_{Dq}} \oplus \frac{\partial V_{baseine}}{V_{baseline}}$$

Electronic noise

Electric field uniformity across the SiPM
Doping densities

Importance of GAIN for SPDs

Gain plays an important role in detecting single photons. It allows to "see" SPE signal above the electronic noise and makes counting PEs easier

SiPM noise

Primary noise: Dark Count Rate (DCR)
The number of pulses registered by the SiPM in the absence of light. Due to free charge carrier, generated in the depletion layer, that has diffused into the high-field region and triggered a Geiger discharge

Two main sources

- **Generation/Recombination SRH noise**

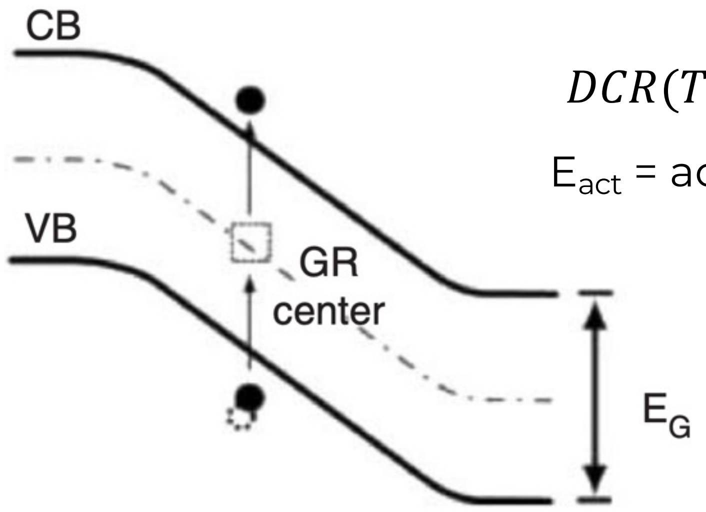

$$DCR(T) \sim e^{-E_{act}/K_B T}$$

E_{act} = activation energy << E_G

It has a strong dependance on T, the electric field and the density and relative energy of the traps, created by impurities and lattice defects .
Its effect is decreased by lowering the operative temperature and by using good quality low defects epitaxial layer

Electron transfers from the valence to the conduction band via a state (or trap) within the band gap

Geiger-mode avalanche photodiodes, history, properties and problems

SiPM noise

Primary noise: Dark Count Rate (DCR)
The number of pulses registered by the SiPM in the absence of light. Due to free charge carrier, generated in the depletion layer, that has diffused into the high-field region and triggered a Geiger discharge

Two main sources

- **Band-to-band Tunneling noise**

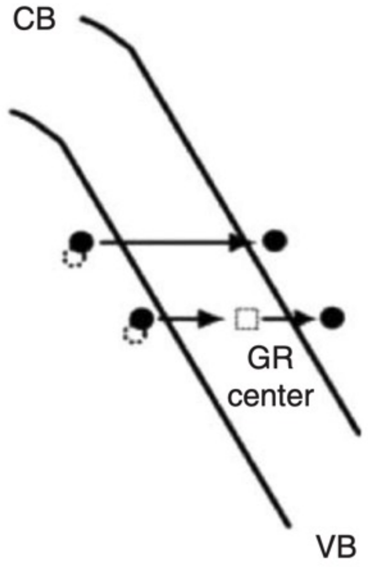

Rate is sensitive to the strength of the electric field and is only weakly inversely dependent on temperature.
It dominates at low temperatures (<200 K) and can be mitigated by properly engineering the electric field

direct tunneling (top)
field-assisted generation (bottom) of primary free carriers

[Geiger-mode avalanche photodiodes, history, properties and problems](#)

SiPM noise

Primary noise: Dark Count Rate (DCR)
The number of pulses registered by the SiPM in the absence of light. Due to free charge carrier, generated in the depletion layer, that has diffused into the high-field region and triggered a Geiger discharge

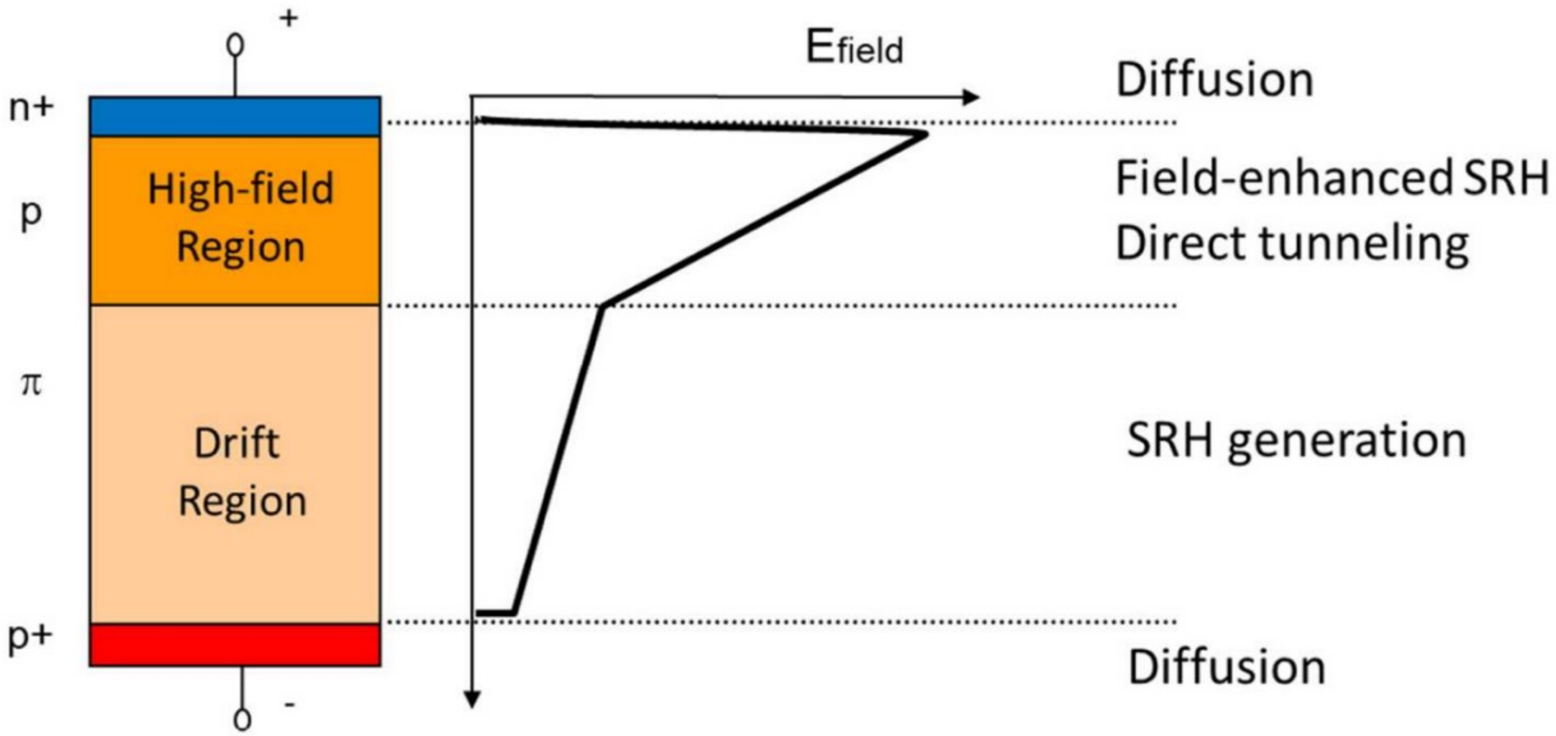

[Overview on the main parameters and technology of modern Silicon Photomultipliers]

SiPM noise

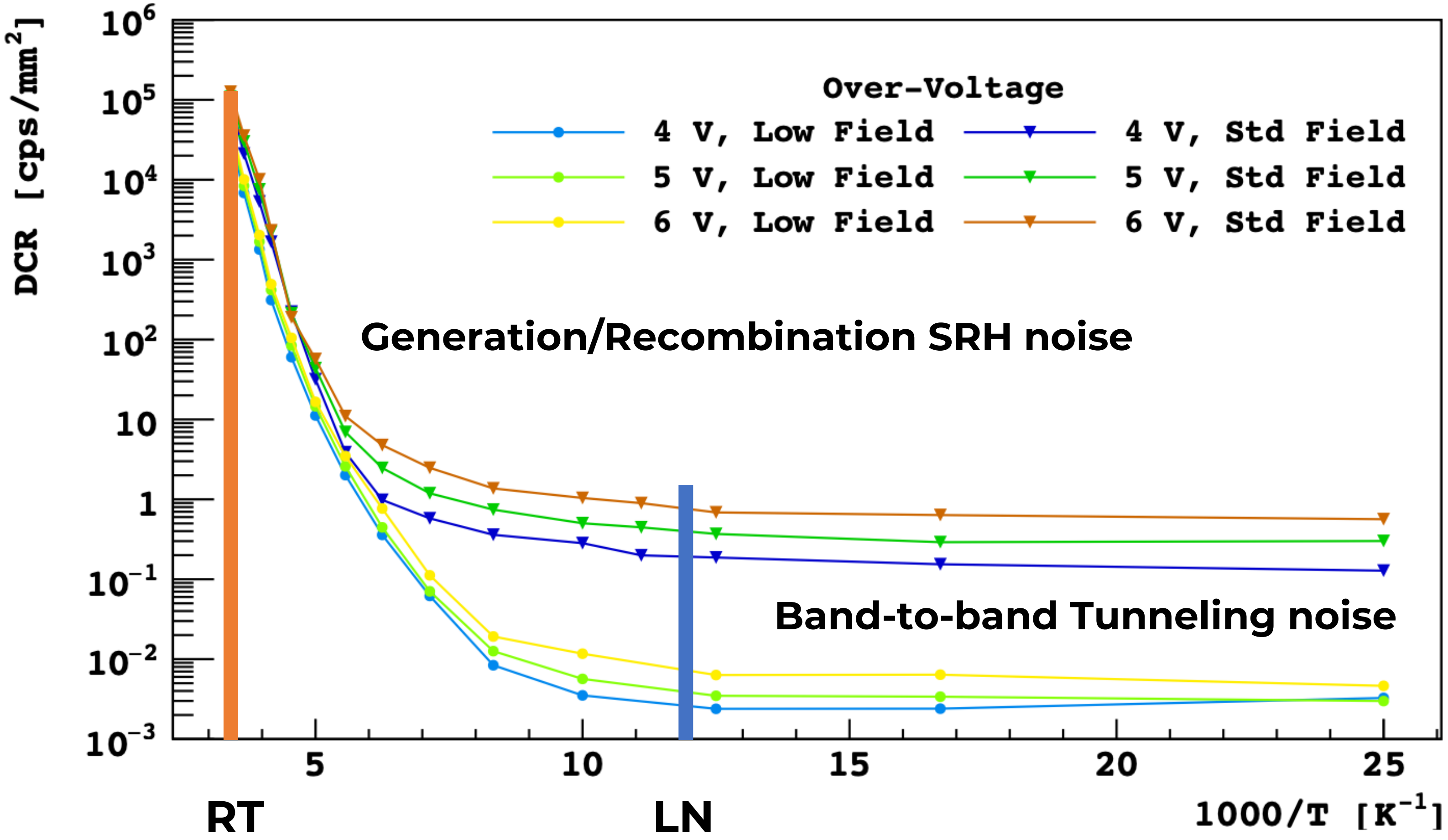

7 order of magnitude reduction (1 mm^2 - 10 m^2)

Cryogenic Characterization of FBK HD Near-UV Sensitive SiPMs

SiPM noise

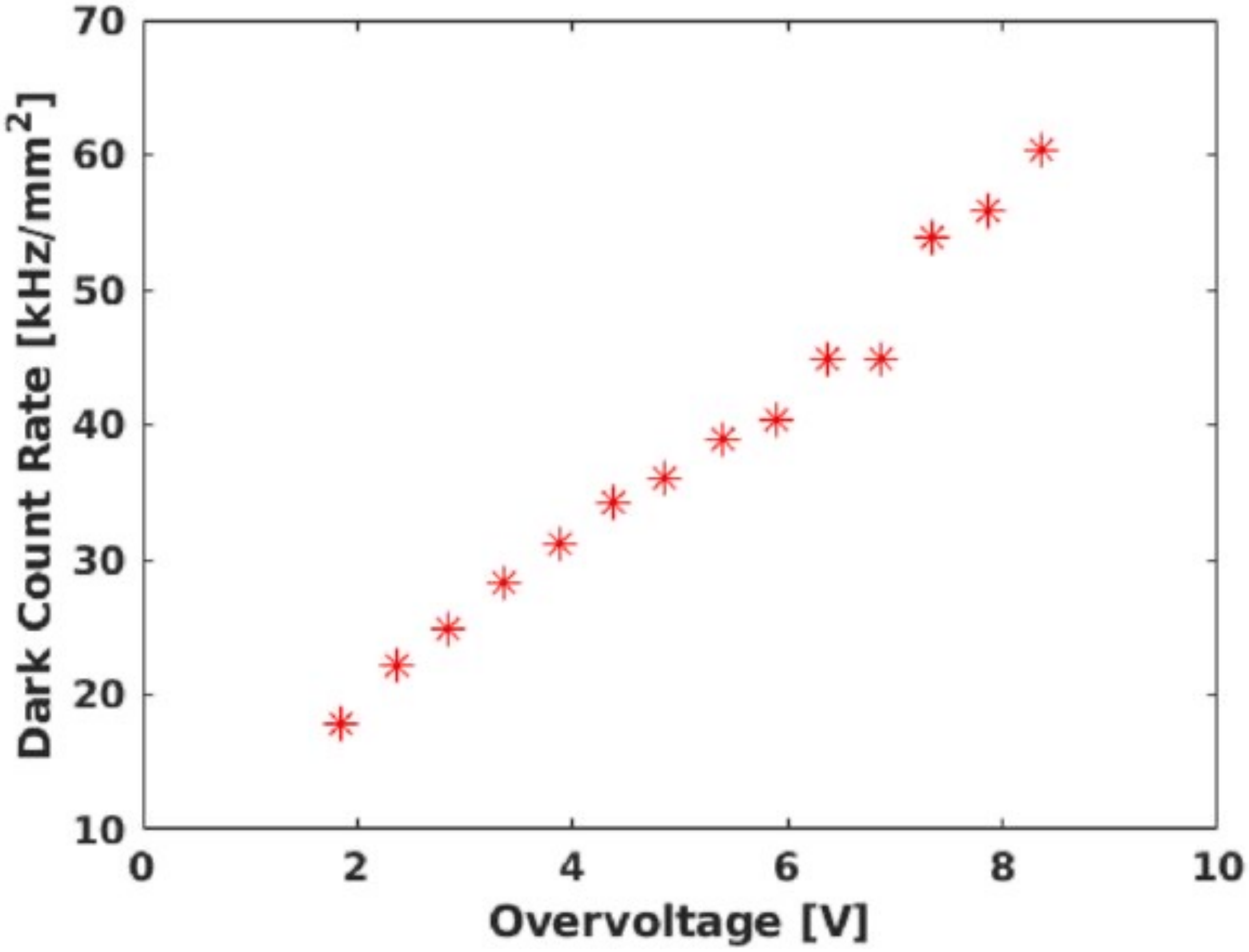

Typical values @RT

SiPM correlated noise

Caused by cells firing in correlation with a previous event. It is usually measured by the **excess charge factor** (**ECF**) or by the fraction of events manifesting a correlated event.

Afterpulse

Large amount of carriers is generated in the high-field region during the avalanche. Some of them are captured by trapping centers in the high-field region and, then, re-emitted triggering a second avalanche in the same cell. This phenomenon is called After-pulsing, or AP. O(100) ns time delay.

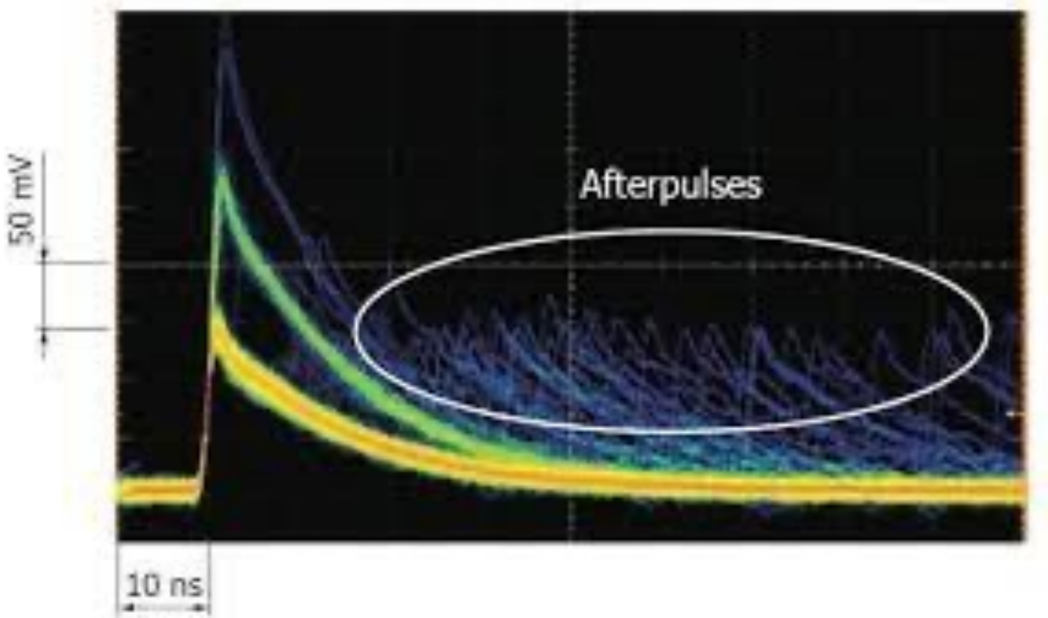

SiPM correlated noise

Crosstalk

Optical effect. When an avalanche occurs, the fast moving charges emmit photons for a superimposition of different mechanisms. These photons can be absorbed in another SPAD or in a region close to it and generate a carrier that can subsequently be collected in the high-field region and trigger a second avalanche.

External CT (external) happen when the photon is emitted towards the optical window, is reflected and reenter the SiPM and possible triggering another avalanche. (Important changes in the refractive index of the window)

Direct CT (prompt) happens when the cross-talk photon is absorbed in the active volume (depleted region) of a second close SPAD (ps time scale). The result is 2 SPADs firing at the same time (2 PE signal).

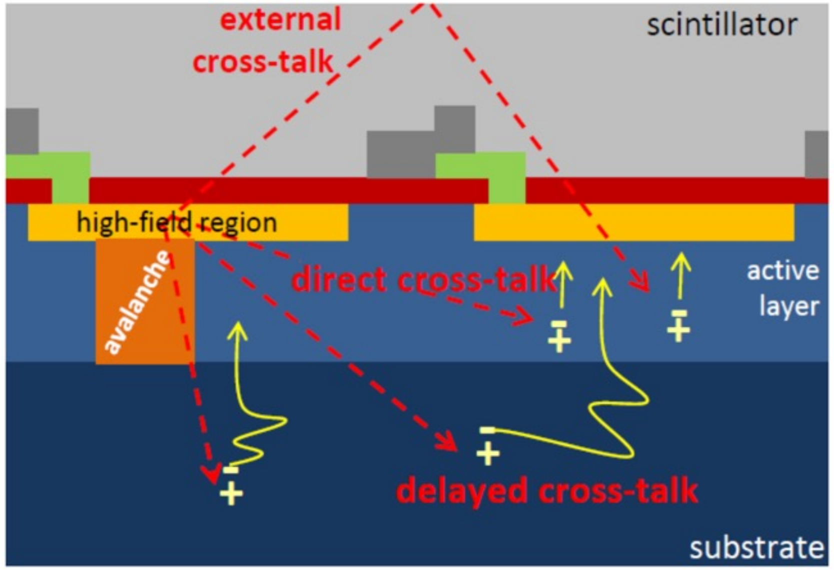

Delayed CT (delayed) happen when the cross-talk photon is absorbed in the non depleted volume of a second SPAD. The generated carriers must diffuse to the multiplication region (ns scale) resulting in a delayed correlated signal.

Direct and delayed CT and AP reduced with deep optically isolated trenches. Acerbi 2015

SiPM correlated noise

Crosstalk

Optical effect. When a[…] Infrared picture of firing cells […]ns for a uperimposition of different mechanisms. These […]AD or in a region close to it and generate a carrier that can sub[…]gion and trigger a second avalanche.

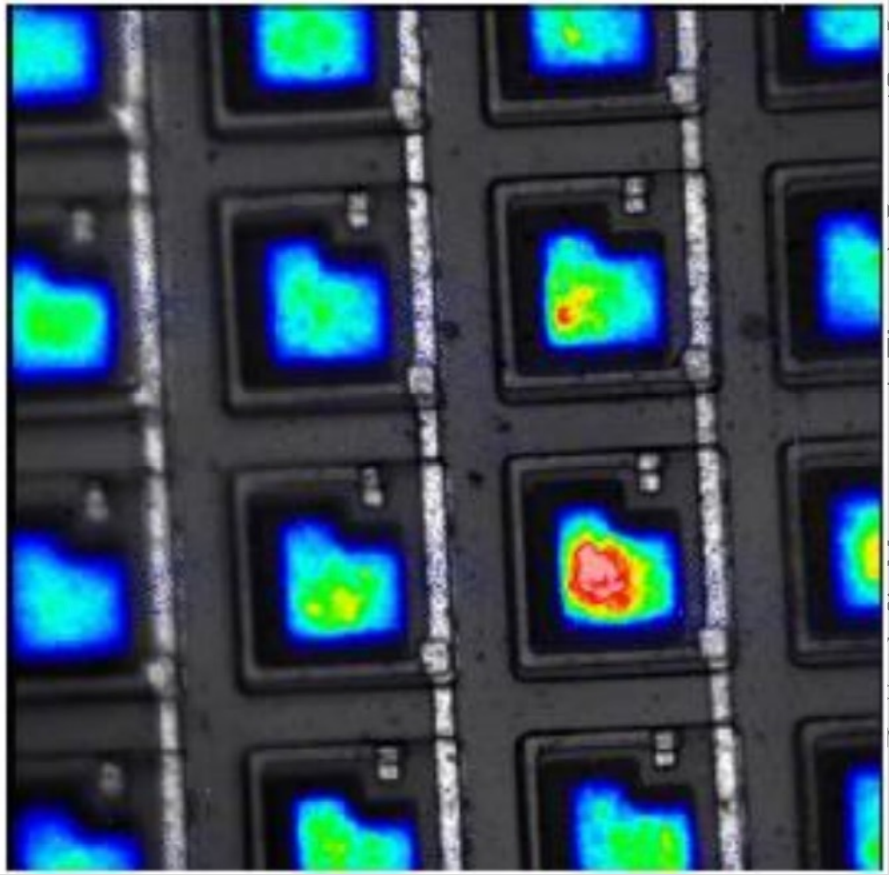

Otte 2009

[…]xternal CT (external) happen when the […]hoton is emitted towards the optical window, […]reflected and reenter the SiPM and possible […]iggering another avalanche. (Important […]hanges in the refractive index of the window)

Direct CT (prompt) happens when the cross-talk photon is absorbed in the active volume (depleted region) of a second close SPAD (ps time scale). The result is 2 SPADs firing at the same time (2 PE signal).

[…]elayed CT (delayed) happen when the cross-[…]alk photon is absorbed in the non depleted […]olume of a second SPAD. The generated […]arriers must diffuse to the multiplication region […]ns scale) resulting in a delayed correlated […]ignal.

Direct and delayed CT reduced with deep optically isolated trenches.

SiPM noise time distribution

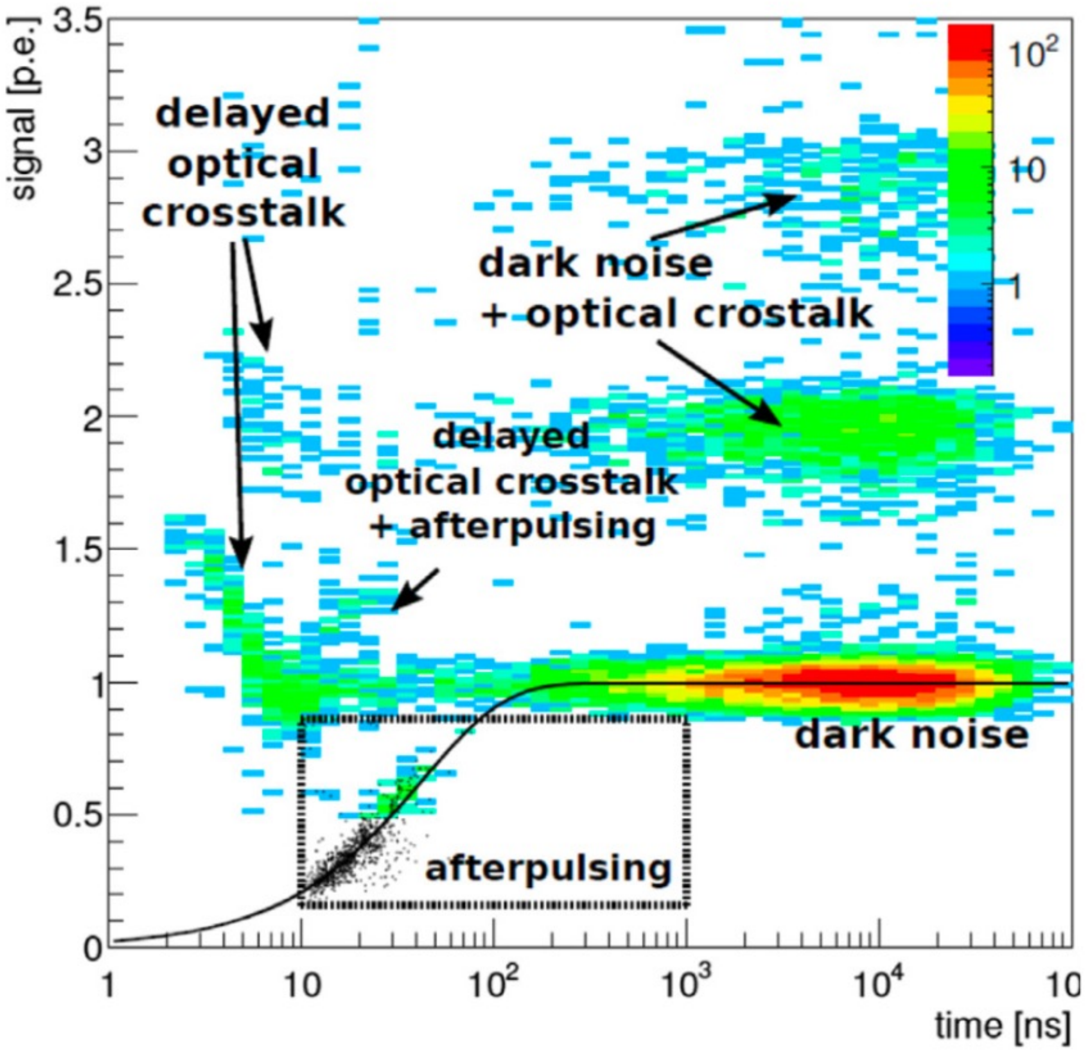

[Characterisation studies of silicon photomultipliers]

SiPM AP and CT

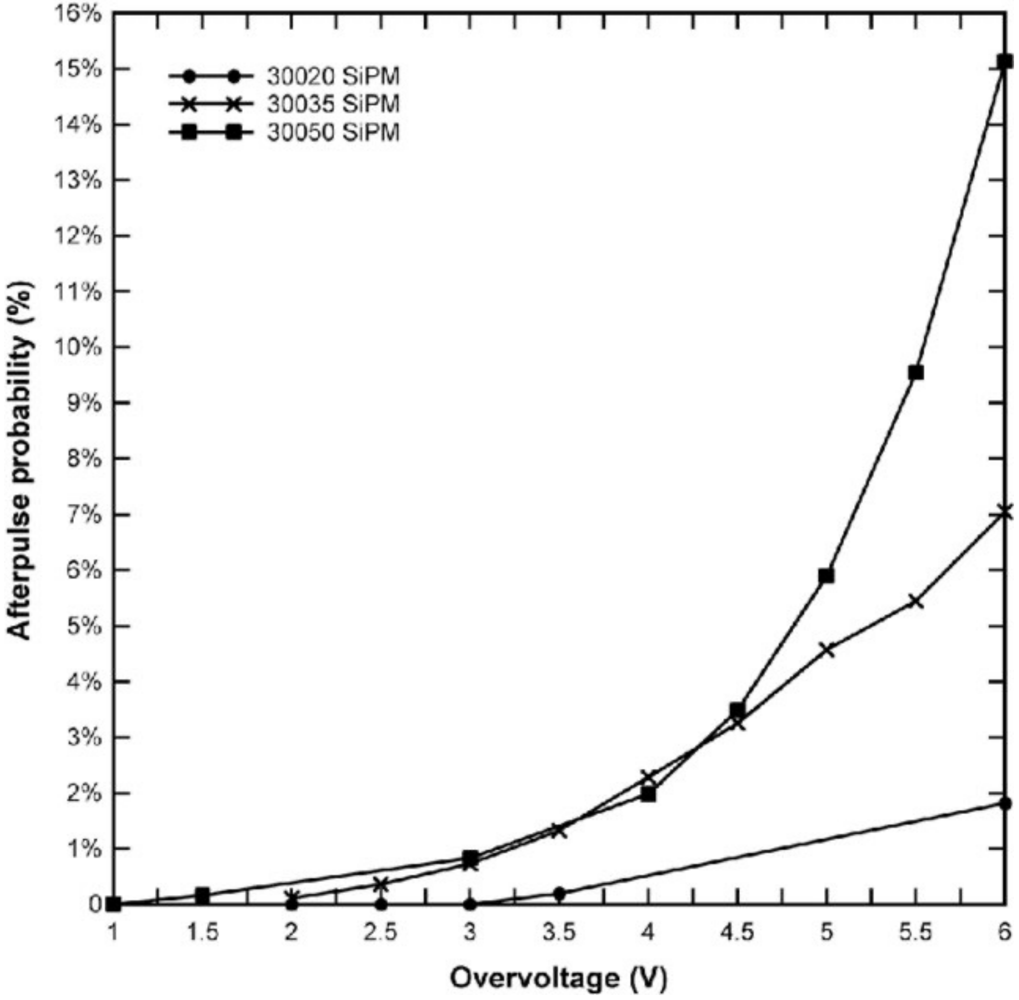

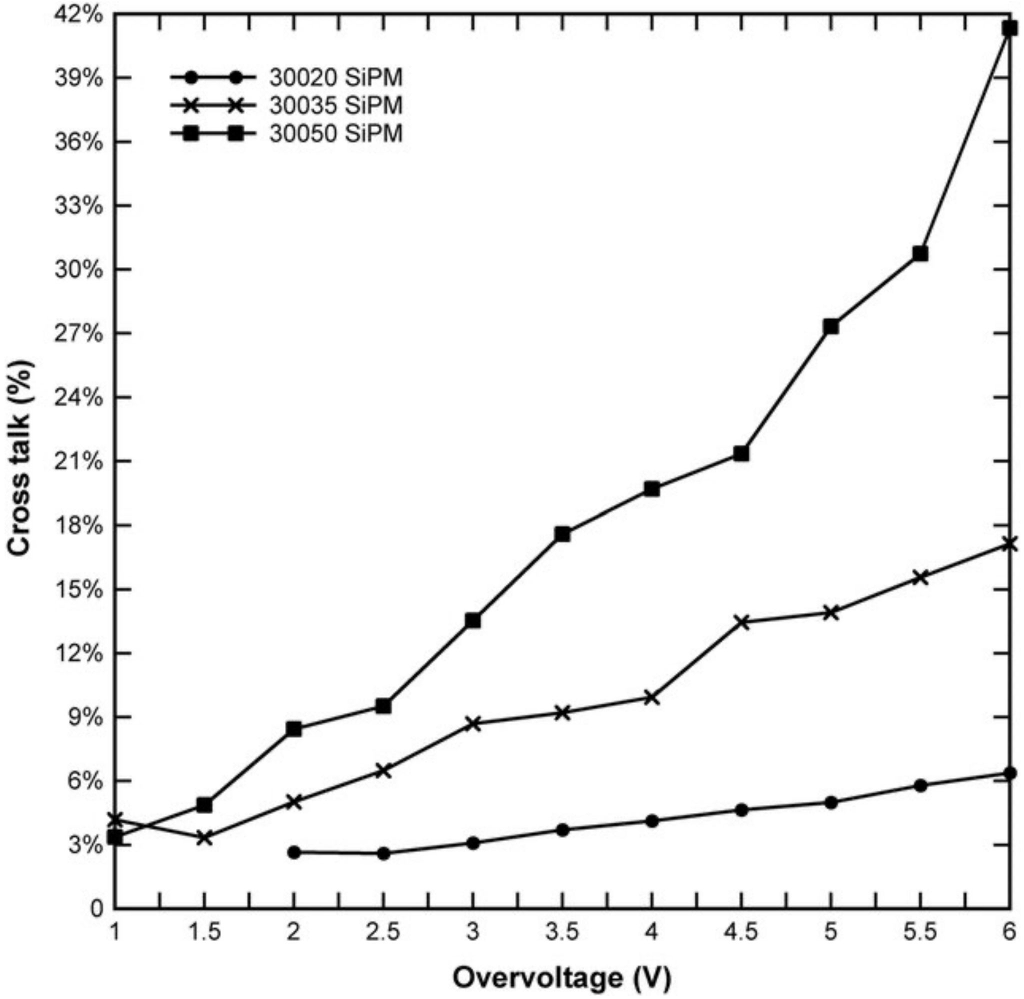

[High-volume silicon photomultiplier production, performance, and reliability]

Importance of Noise for SPDs

DCR, AP and delayed CT must be minimized because indistinguishable from SPE signal.

DCR, and correlated noise are strictly connected to the overvoltage

↕

Gain

IV - reverse bias current voltage curve

Apply a reverse voltage to the SiPM and measure the reverse current. This is usually made with a low noise high performance source meter (like **Keithley 2450** SMU 10 fA resolution)

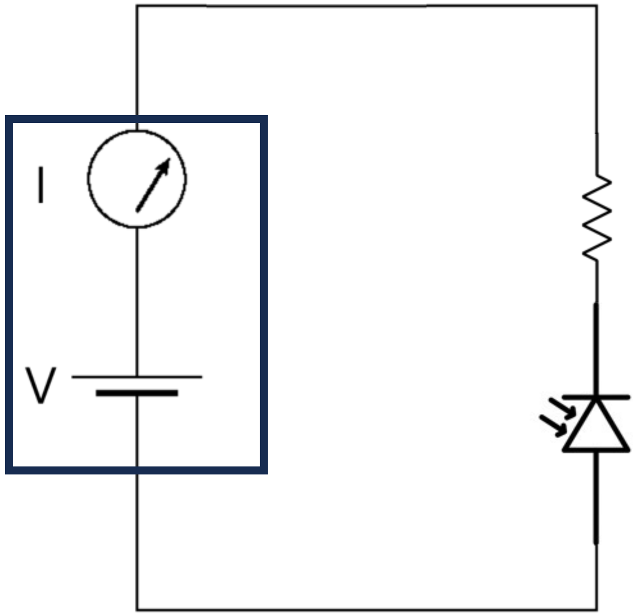

Region of interest:

- Reverse voltage (V_{BD}-5 V) – (V_{BD}+10 V)
- Direct voltage for R_q value extraction 0-3 V

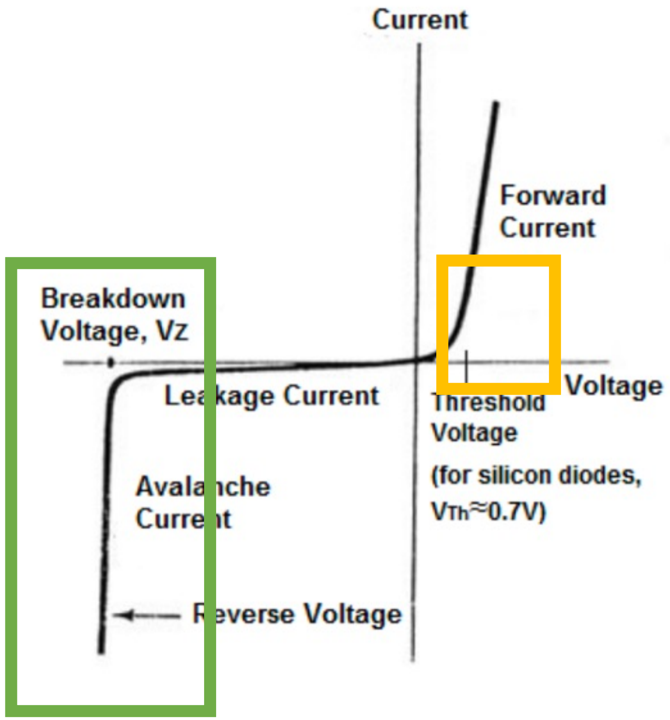

IV and Breakdown Voltage extraction

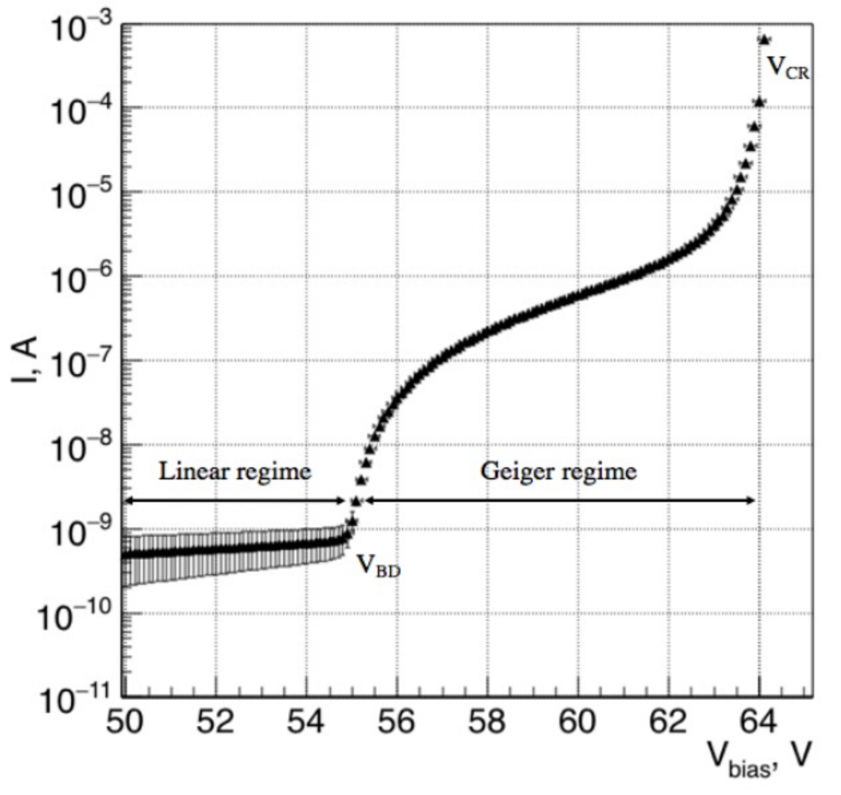

Pre BD = leakage current sum of Bulk and surface current

IV and Breakdown Voltage extraction

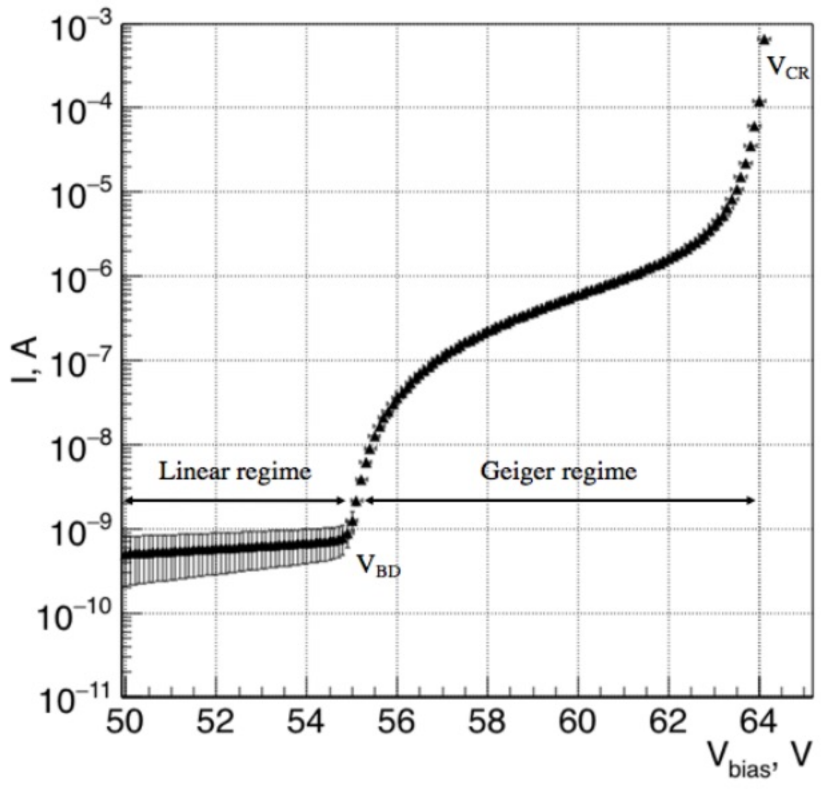

V_{BD}= Voltage that initiate the Geiger regime

Tangent	Linear fitted "baseline" and tangent drawn to $ln(I)$	Intercept of tangent and the "baseline"	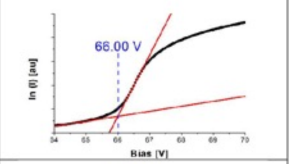
Relative derivative	$\frac{d}{dV}ln(I)$ $= I'/I$	Position of the maximum	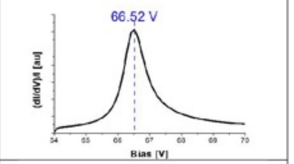
"Inverse" relative derivative	$1/\frac{d}{dV}ln(I)$ $= I/I'$	Intercept of the x-axis and the fitted line	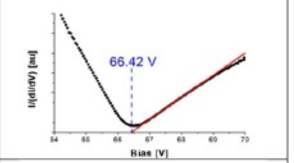
Second derivative	$\frac{d^2}{dV^2}ln(I)$	Position of the maximum	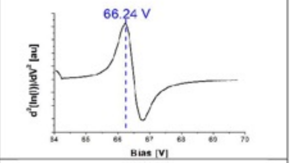
Parabolic fitting	Linear fitted "baseline" and parabola fitted to I	Intercept of the fitted parabola and the "baseline" on semi-log scale	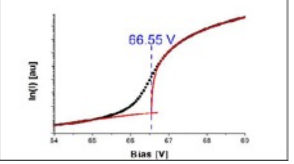

https://www.semanticscholar.org/reader/de28d2b5a71de44a9f1498d8f2ba277a447e6253

Several methods to extract the BD voltage.
Pay attention to the electronic noise of the measurement (derivate is very sensitive)
Inject some light if the measurement is taken at very low temp to increase the derivative change at the breakdown

IV and Breakdown Voltage extraction

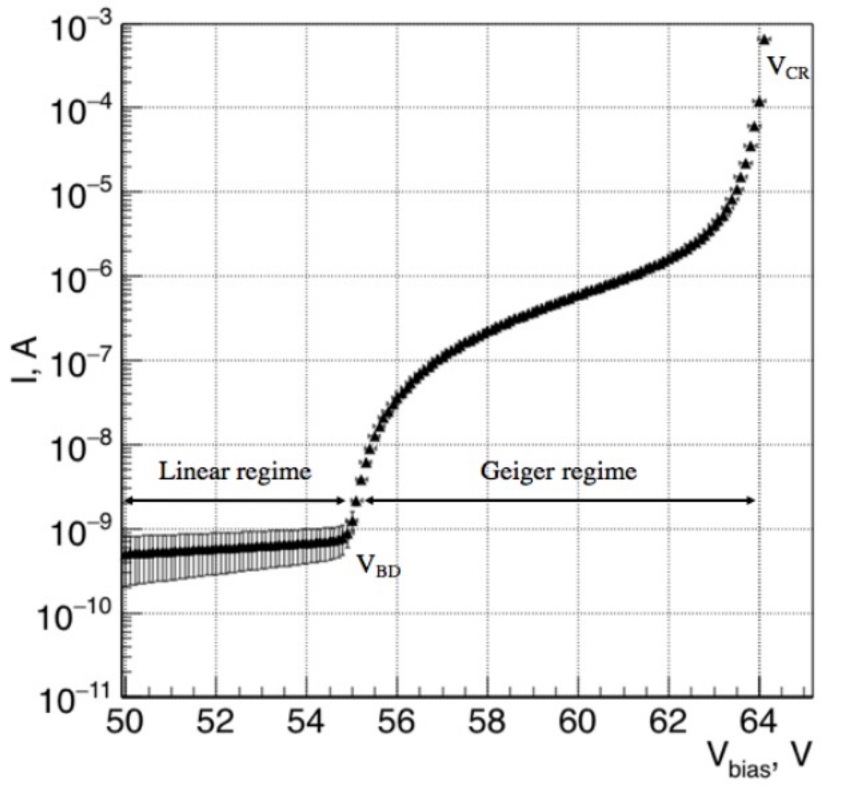

Post V_{BD} = Dark current
V_{CR}= current divergence because it is impossible to quench the avalanche

IV curve wrt temperature

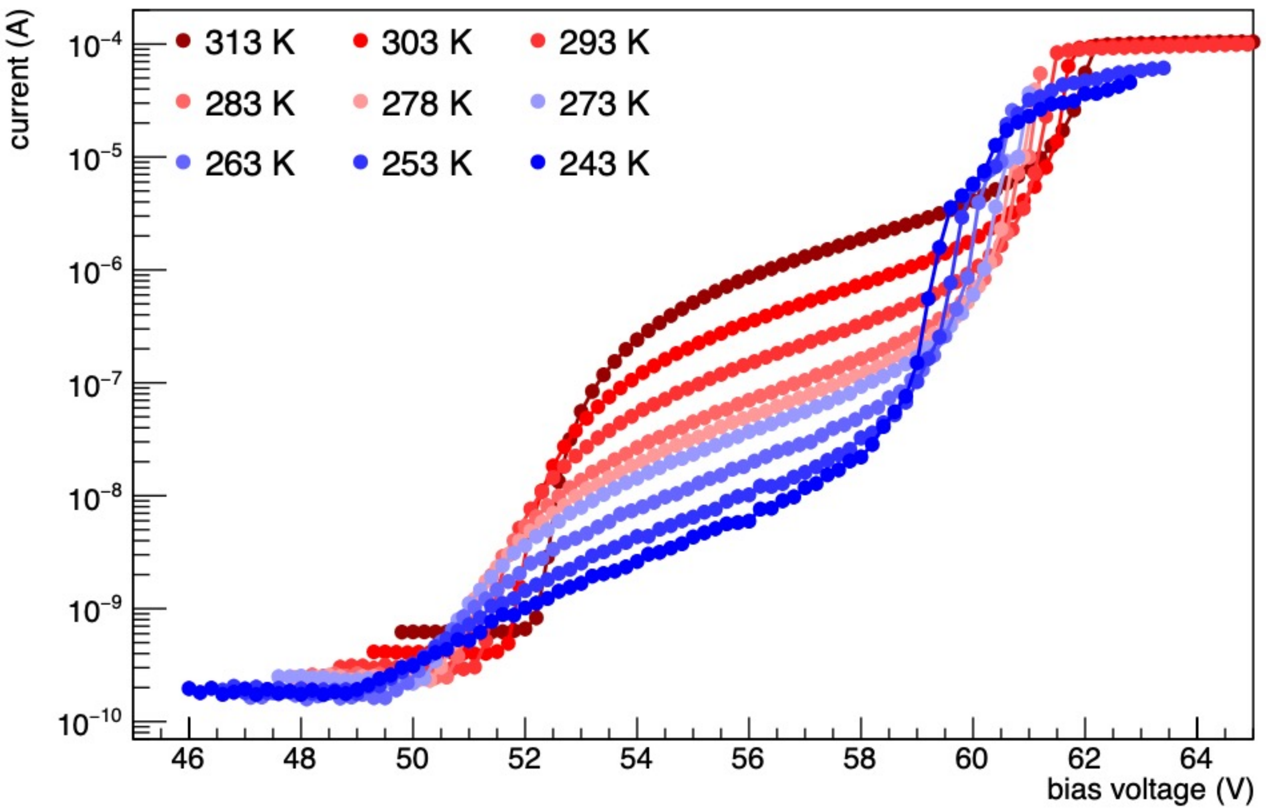

5-10 °C increase in temperature will result in **double the dark current**.

The **V_{BD} decreases** with the temperature by **30-50 mV/K**

Qualitative explanation: accelerated carriers loose energy in impacts due to thermal agitation. The higher the temperature, the higher the energy loss in this kind of collision, the lesser energy is available for start the multiplication process thus, a higher electric field is needed to start the avalanche.

$$I_{dark} = DCR(T, V_{OV}) \cdot G(V_{OV}) \cdot q \cdot ECF(V_{OV})$$

SiPM: electrical model

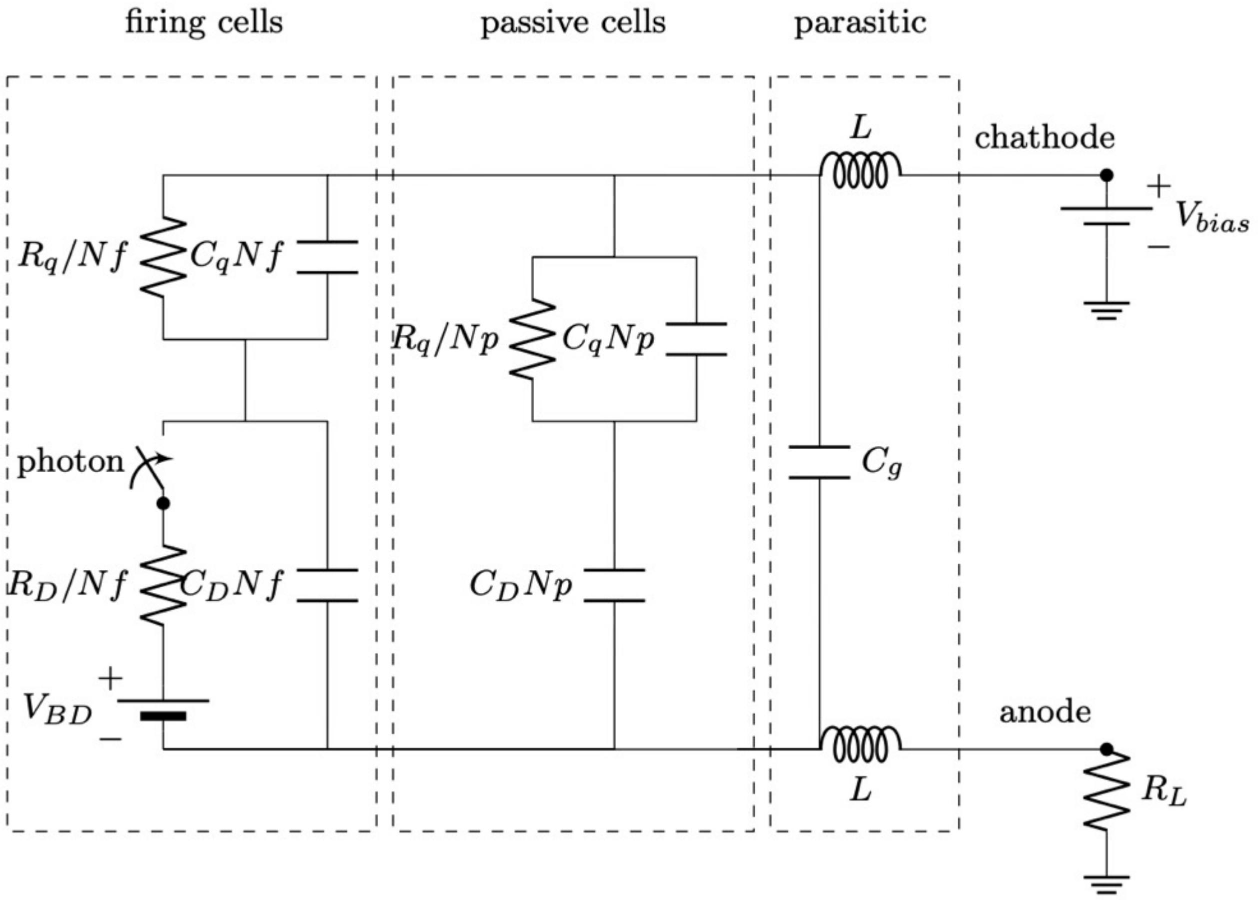

In analogy with the SPAM model, light detection is simulated by the closing switch.
The non firing cells act as a low pass filter and introduce a pole in the device response that impact both the avalanche and recharge phase leading to a multiple exponential decay signal

S.Seifert et al. IEEE TNS 56 (2009) 3726
Marano et al, IEEE TNS 61 (2014) 23
Licciulli et al, IEEE TNS 63 (2016) 2517

SiPM: signal

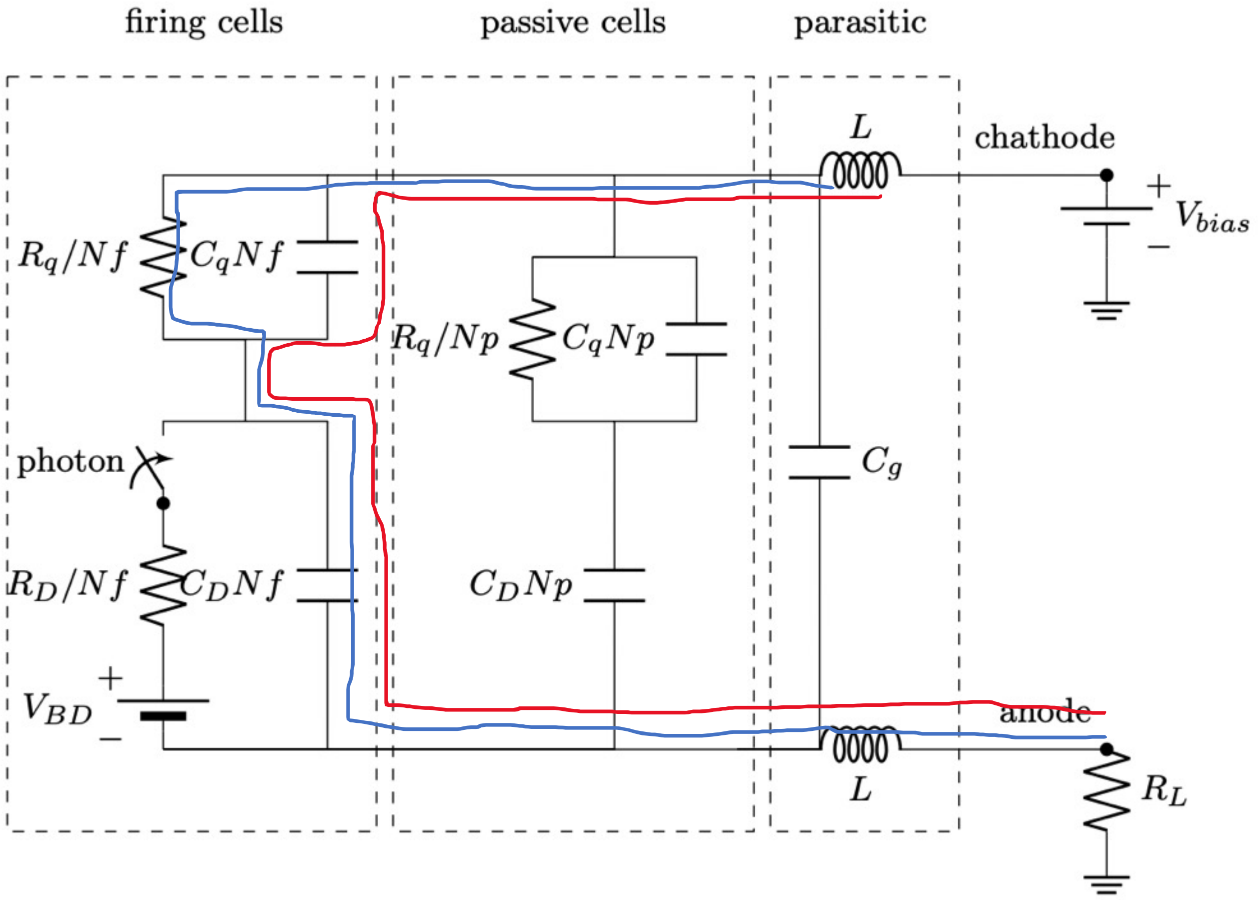

The signal is the superimposition of two pulses:

- **Slow pulse** of "external" current (R_q)
- **Fast pulse** pick up of the C_q

$$\tau_i \sim R_D(C_q + C_D) + L/R_D$$ Rise

$$\tau_{slow} \sim R_q(C_q + C_D)$$

$$\tau_{fast} \sim R_L C_{tot}$$

Decay

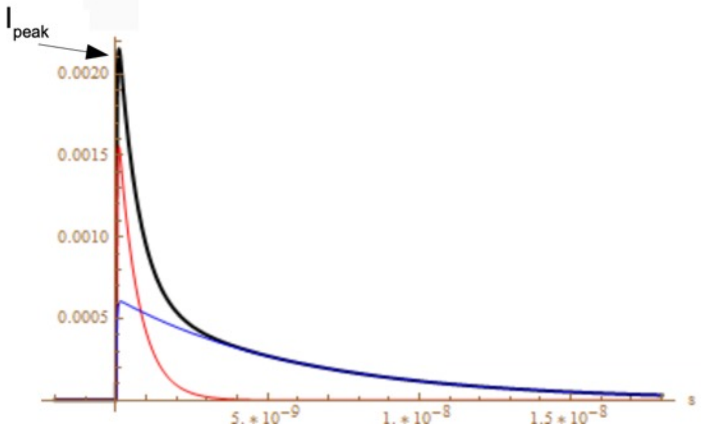

SiPM: signal

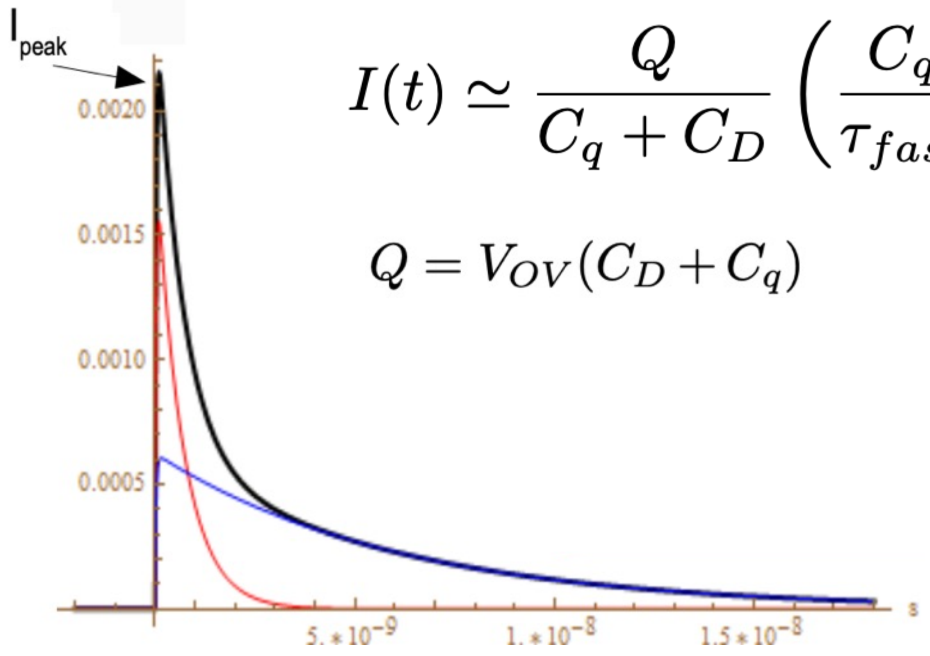

$$I(t) \simeq \frac{Q}{C_q + C_D}\left(\frac{C_q}{\tau_{fast}} e^{\frac{-t}{\tau_{fast}}} + \frac{C_D}{\tau_{slow}} e^{\frac{-t}{\tau_{slow}}}\right)$$

$$Q = V_{OV}(C_D + C_q)$$

$$I_{peak} \approx \frac{C_q}{R_L C_{tot}}$$

$$\tau_{slow} \sim R_q(C_q + C_D)$$

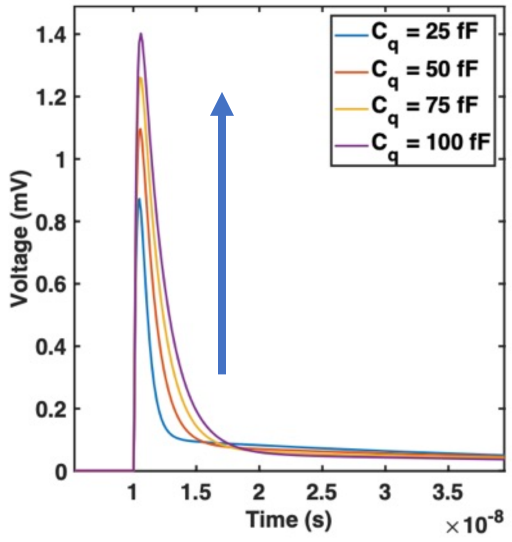

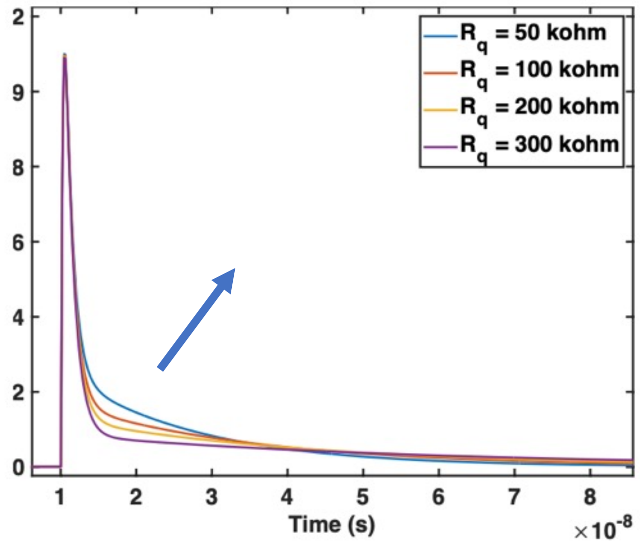

SiPM: electrical model for FE

N= number of cells 3600

$$C_{tot}(\omega) = NC_D + C_g + \frac{\omega^2 C_D^2 R_q^2 N(C_D + C_Q)}{1 + \omega^2 R_q^2 (C_D + C_q)^2} \approx NC_D$$

S1360-3050 HPK
capacity vs bias voltage

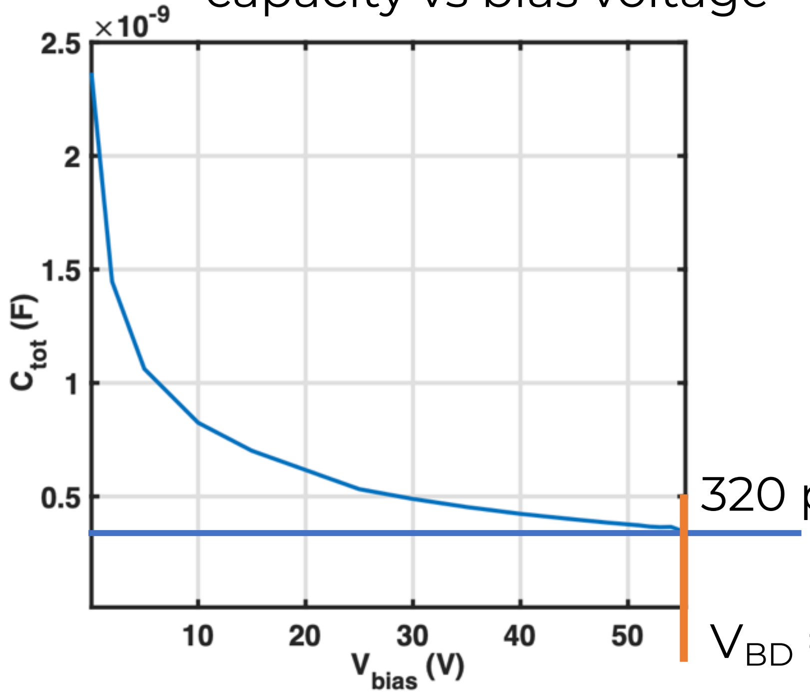

320 pF $C_D \approx$ 90 fF

V_{BD} = 55 V

Pure capacitor

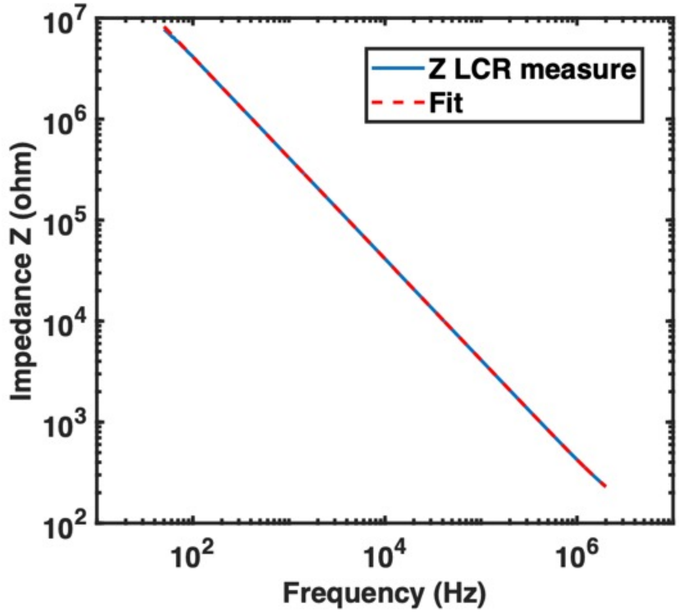

S1360-3050 HPK
impedance

SiPM: electronics

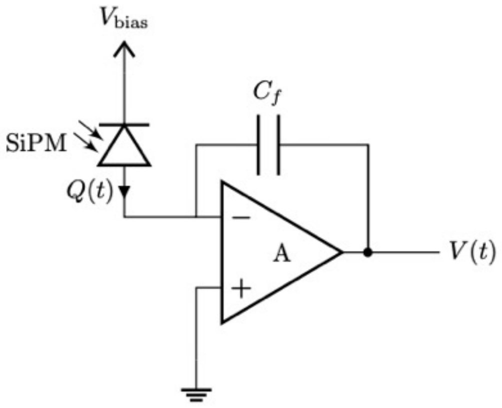

Charge amplifier: output voltage that is proportional to the integrated input current.

Good to count precisely the amount of charge generated by the SiPM. Essentially the number of detected PE.
High resistance to high frequency noise.

Usefull with **small detector capacitances**, as it offers the best performance when the feedback capacitance is significantly smaller than one of the detector. The **bandwidth** (BW) of the system is **inversely proportional** to the **detector capacitance**, it stretches the signal and is not very usable for timing and high-rate applications

SiPM: electronics

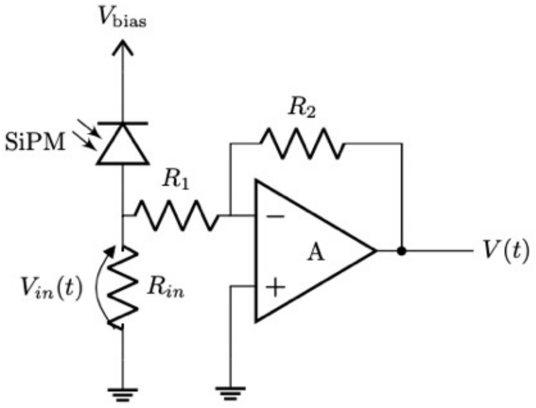

Voltage amplifier: output voltage is proportional to the input voltage.

The first stage is a load resistor (R_L) that convert the current coming from the SiPM in a voltage pulse to be amplified. R_L must be low not to spoil the fast component of the signal (and rise time) for timing applications.

All the gain is in the amplifier and **RF**, high gain high BW amplifier can be used (commercially available). **Easy** solution but **high-power consumption** and dissipation make it a viable solution for testing or **low number of channels**

SiPM: electronics

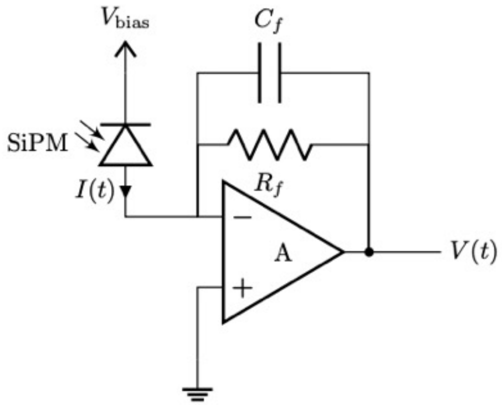

Current amplifier: output voltage is proportional to the input current (TIA).

Keeps unaltered the shape of the input current pulse.
Gain is $G = -V_{out}/I_{in} = R_f$ and has a low input impedance
$Z_{in}=R_f/A$
A=amplification

$$BW_{TIA} = \sqrt{\frac{GBW}{2\pi R_f C_D}}$$

GBW = gain bandwidth product of the opamp (> GHz)

Low power consumption and best solution for high capacitance input devices. Most used solution for large arrays of SiPM.

SiPM: electronics

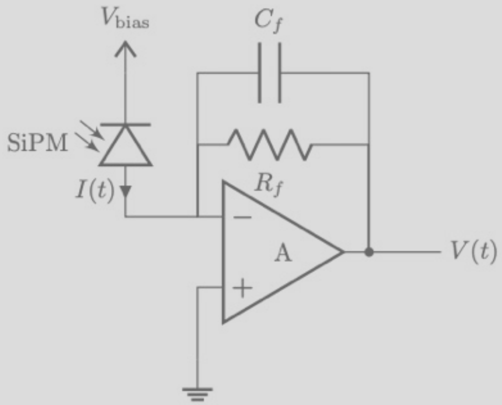

Current amplifier: output voltage is proportional to the input current (TIA).

These configurations can be implemented both with commercial off the shelf components or by specific **ASIC**

Independently from the front end used, the amplified signal must be digitized:

- Full waveform digitization (**ADC**)
- Timing extraction (**TDC**)

GBW = gain bandwidth product of the opamp (> GHz)

Low power consumption and best solution for high capacitance input devices. Most used solution for large arrays of SiPM.

SiPM: electronics example

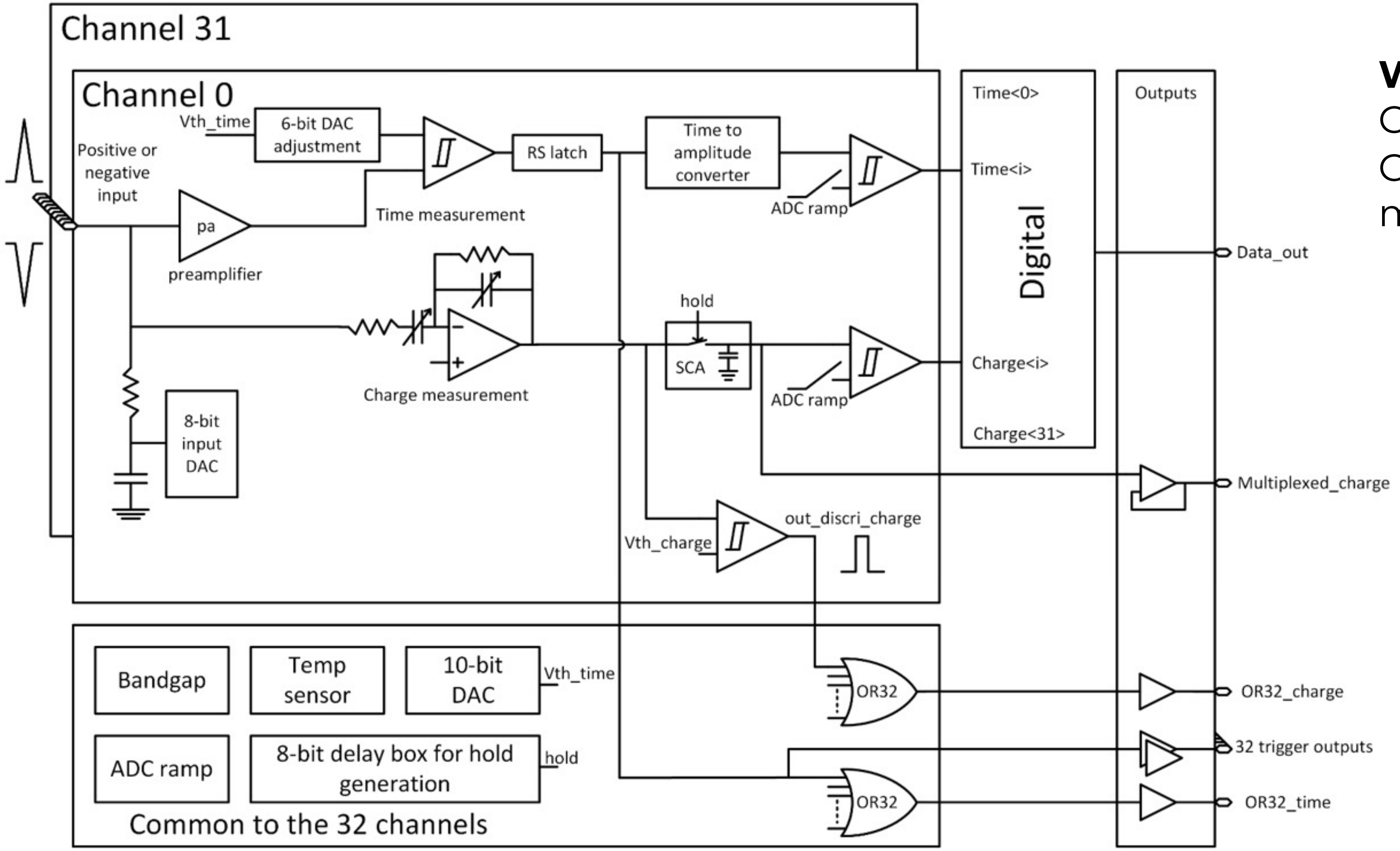

WEEROC PETIROC (ASIC)
Current amplification for timing
Charge amplification for energy measurement

SiPM: electronics example

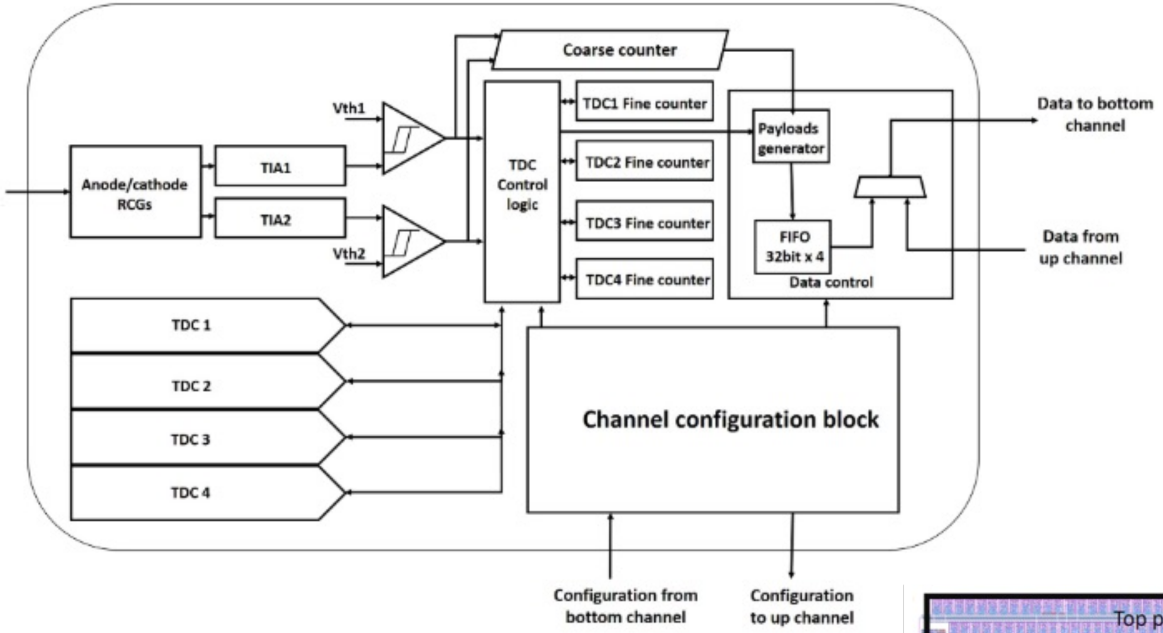

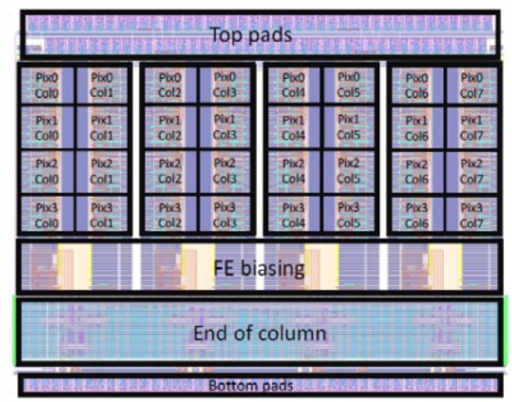

ALCOR ASIC by INFN-To

32-pixel matrix mixed signal **ASIC** developed for **SiPMs** in **cryogenics**

- Regulated common gate **amplifier** (10 Ω impedance)
- Post amp TIA for **4 gain settings**
- 2 **leading-edge discriminators** with independent
  threshold settings
- 4 **TDCs** based on analogue interpolation with **50 ps LSB** (@ 320 MHz)
- 3 **triggerless operation** modes:
  - **LET** leading edge threshold measurement, high-rate time-stamp
  - **ToT** Time-over-Threshold
  - **Slew rate** measurements for signal characterization

SiPM: electronics example

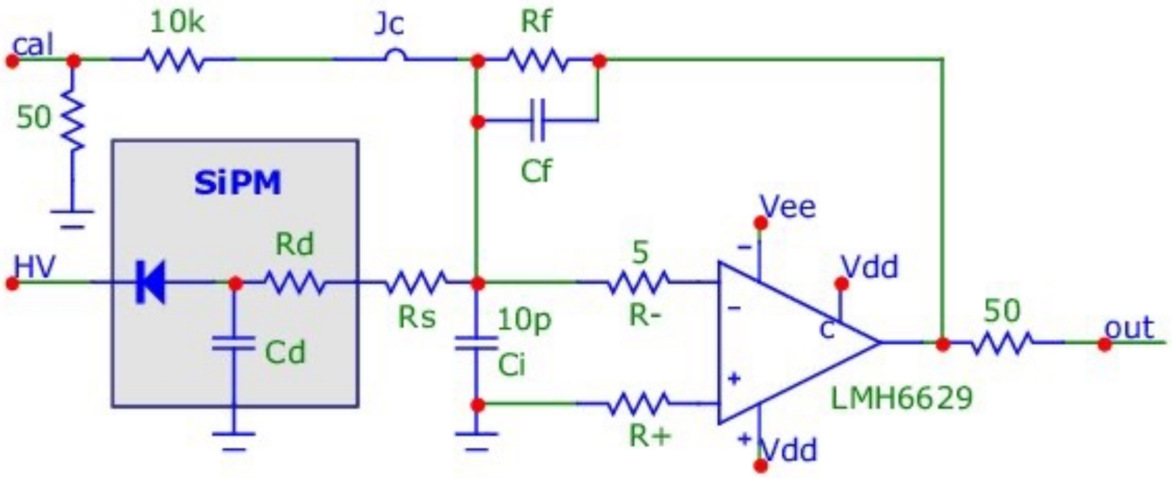

Darkside-20k cryogenic TIA
Works in LN
COTS design (few components and complexity)
1.2k transimpedance gain
18 MHz bandwidth
Very low noise **@ 77 K**
Full waveform digitized at RT

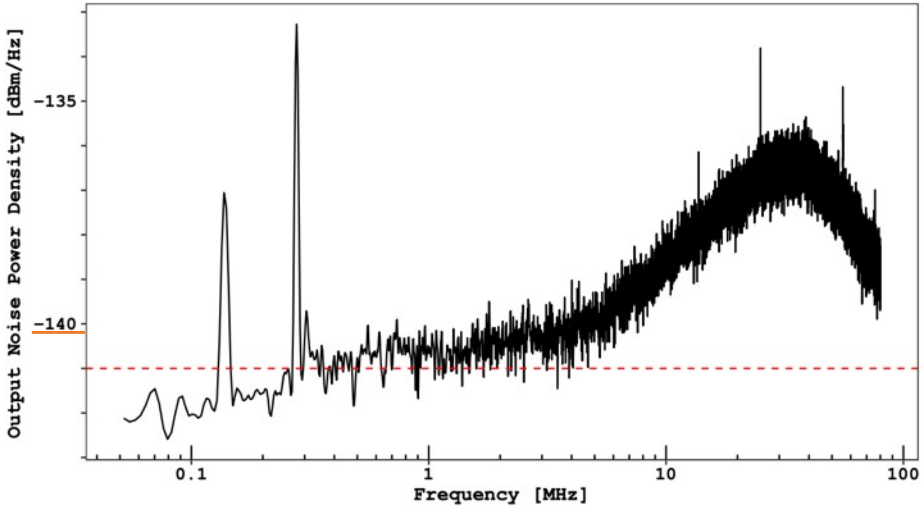

SiPM: grouping increase the area keeping the number of channels manageable. Feasible only at low temp

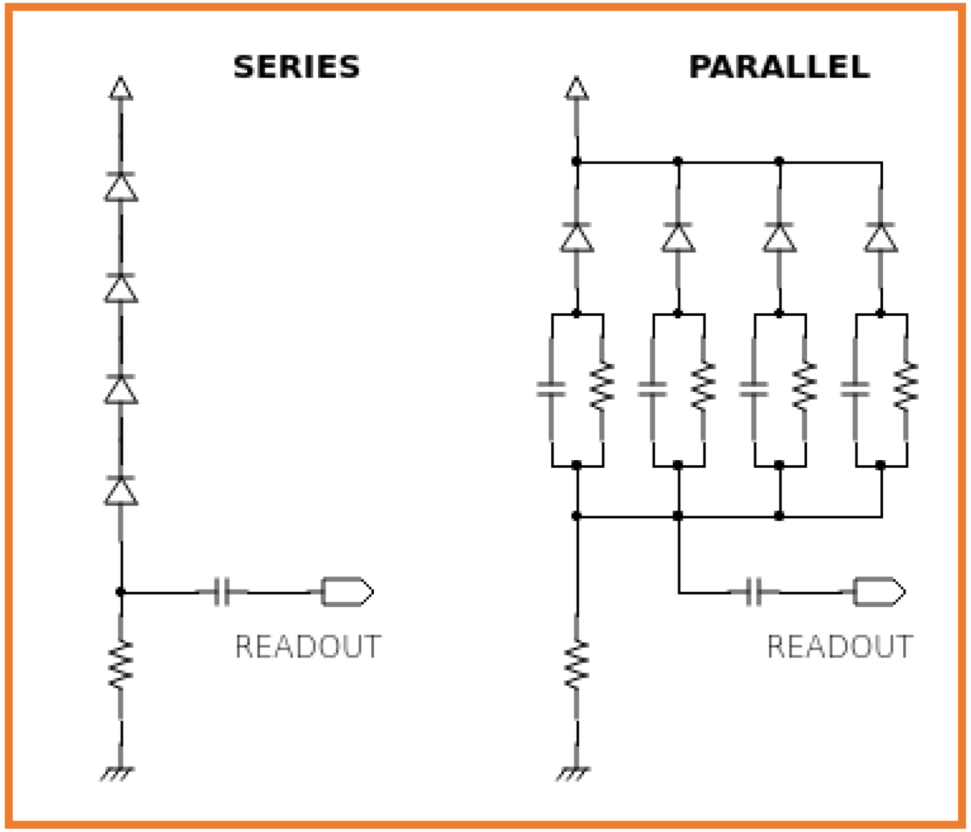

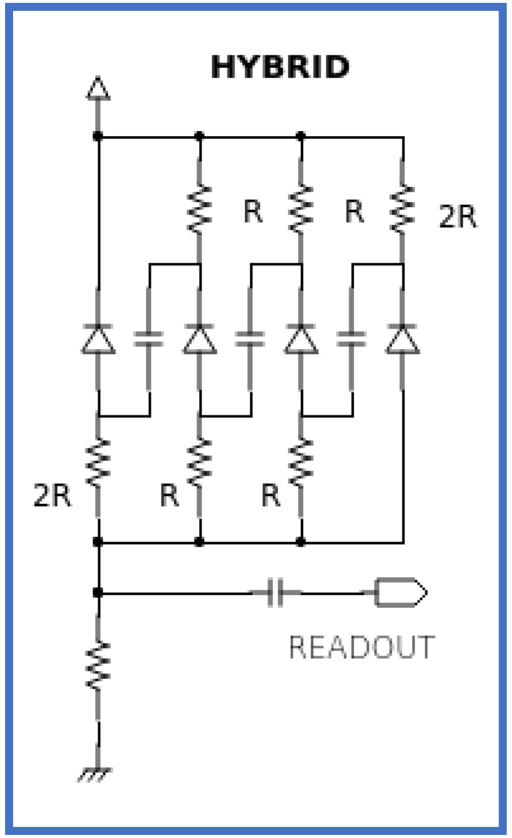

Reduced capacitance
Smaller signal
Lower noise
Higher bias voltage

Increased capacitance
Slower
Same signal
Same V_{BD}

Signal in series, bias in parallel
No V_{BD} limitations

Used in **MEG II** detector upgrade with NUV sensitive SiPM for LXe scintillation light.

https://iopscience.iop.org/article/10.1088/1748-0221/18/10/C10020/pdf

Used in combination in both Darkside-20k and DUNE for LAr scintillation laight

Improving the Time Resolution of Large-Area $LaBr_3$:Ce Detectors with SiPM Array Readout

SiPM timing

SiPM are intrinsically very fast.

Timing performance is evaluated with the **Single Photon Timing Resolution** (**SPTR**): the precision of **arrival time** estimate of a **visible photon**, impinging on a random position on the detector surface.
SPTR depends on the SiPM parameters and on the read-out chain.

The time distribution of the the arrival time shows two component:
Gaussian (<100 ps): (SPAD + SiPM) non uniformities + electronic noise
Non Gaussian tail (< few ns): carriers generated in undepleted region

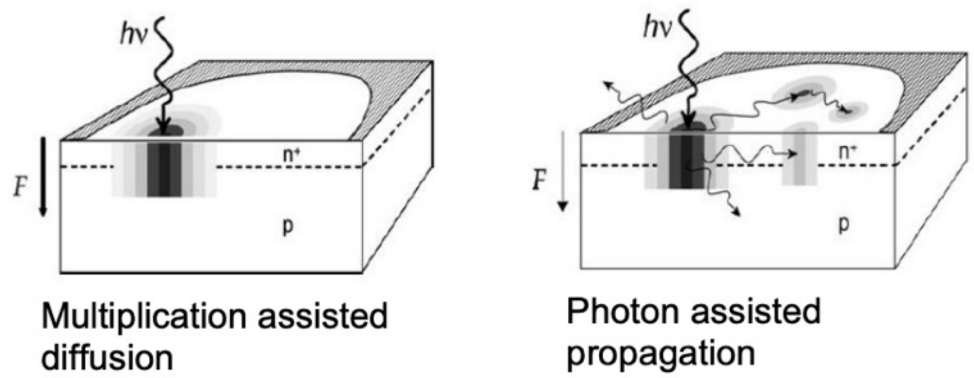

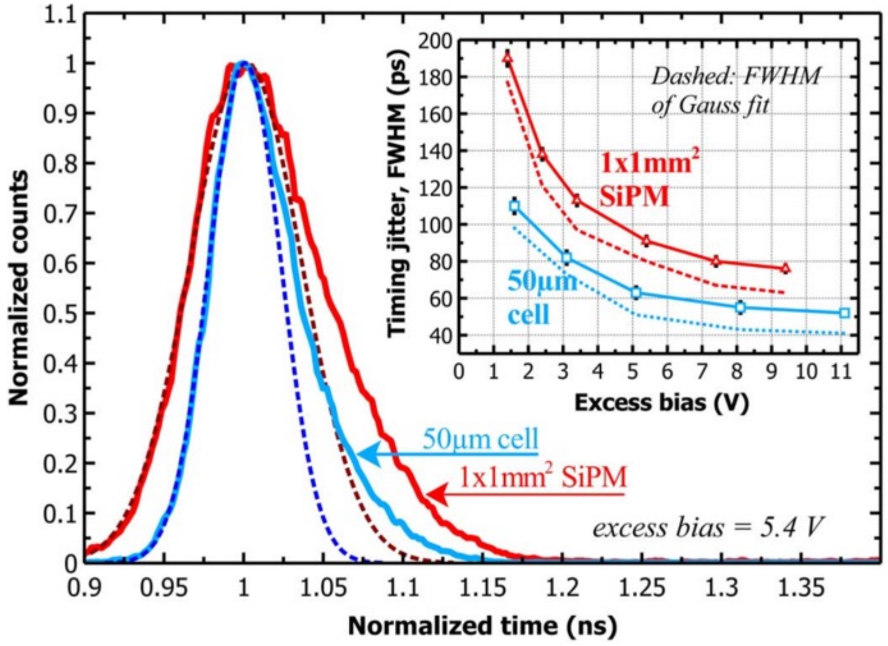

[Characterization of Single-Photon Time Resolution: From Single SPAD to Silicon Photomultiplier]

SiPM timing

SiPM are intrinsically very fast.

Timing performance is evaluated with the **Single Photon Timi** precision of **arrival time** estimate of a **visible photon**, impingin detector surface.
SPTR depends on the SiPM parameters and on the read-out ch

Time jitter decreases with the overvoltage and can reach sub 100 ps for 1 x 1 mm^2 devices

Tl

Gaussian (<100 ps): (SPAD + SiPM) non uniformities + electronic
Non Gaussian tail (< few ns): carriers generated in undepleted

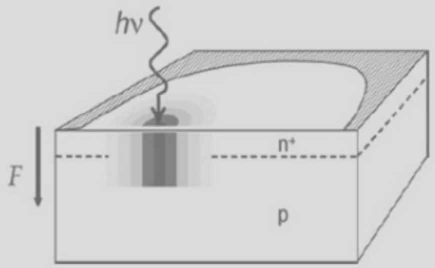

Multiplication assisted diffusion

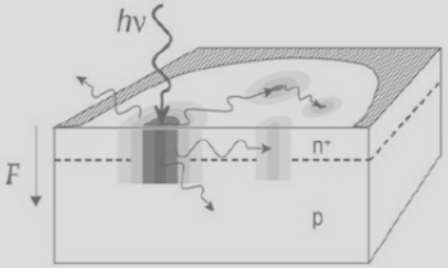

Photon assisted propagation

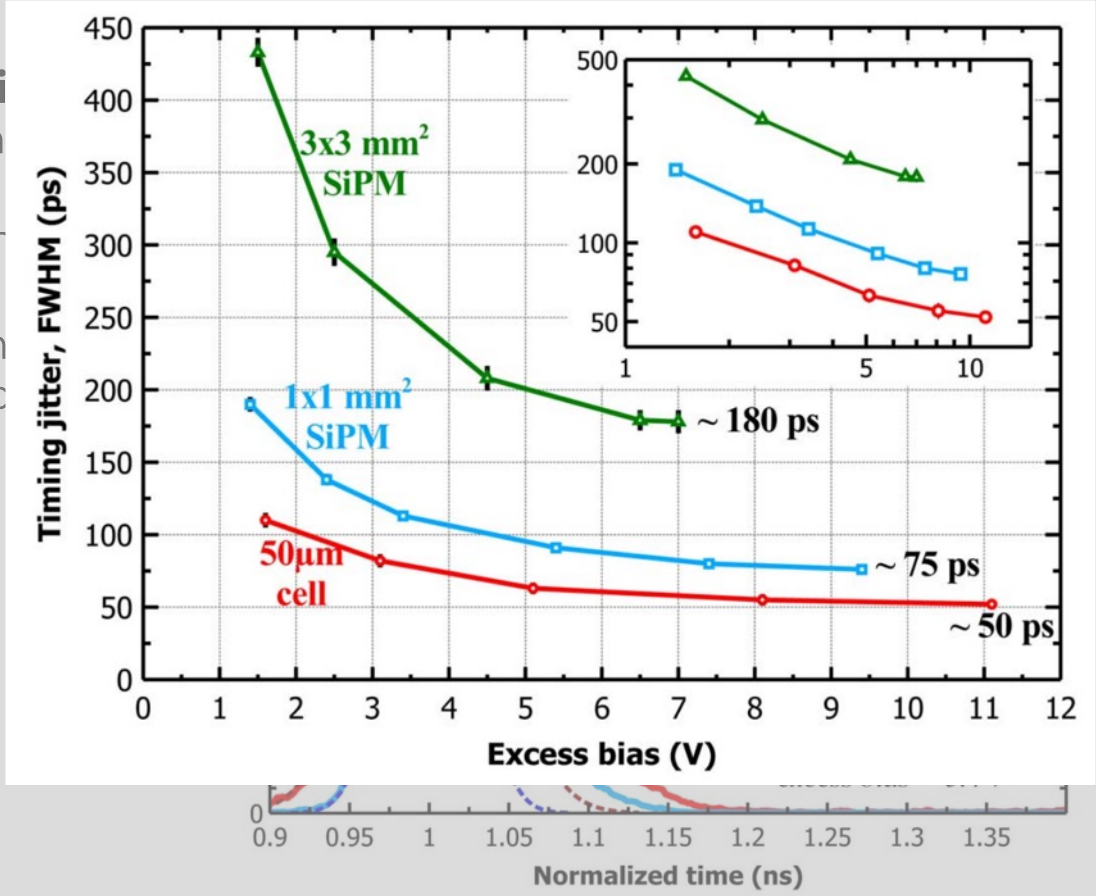

[Characterization of Single-Photon Time Resolution: From Single SPAD to Silicon Photomultiplier](#)

INFN

SiPM SPTR electronic contribution

Electronics can spoil the SPTR:

- Impact of **noise** on **leading edge triggering**
  - σ_n is the **electronic** noise (baseline oscillation) proportional to the C_{tot} of the SiPM
  - **dV/dt** is the **rising edge derivative** and is affected by C_{tot} and **BW** of the amplifier

- Impact of **time walk** (multi photon) mitigated with
  - **Time over Threshold (ToT)**
  - **Slew rate (SR)**

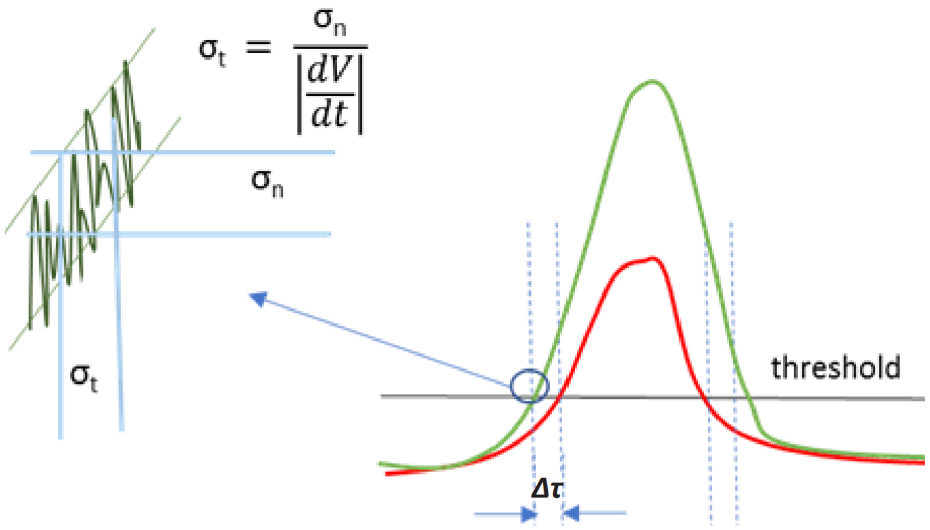

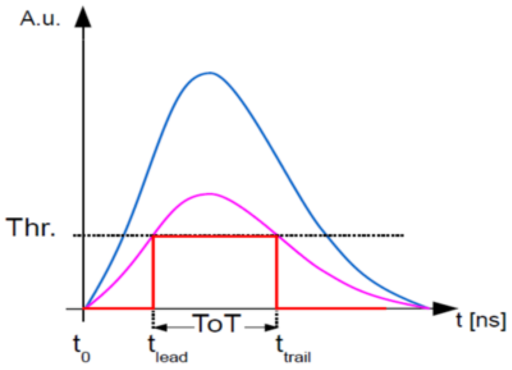

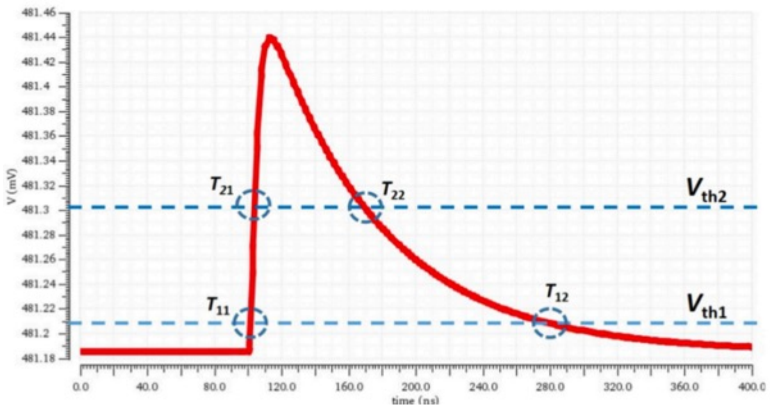

SiPM electronic contribution

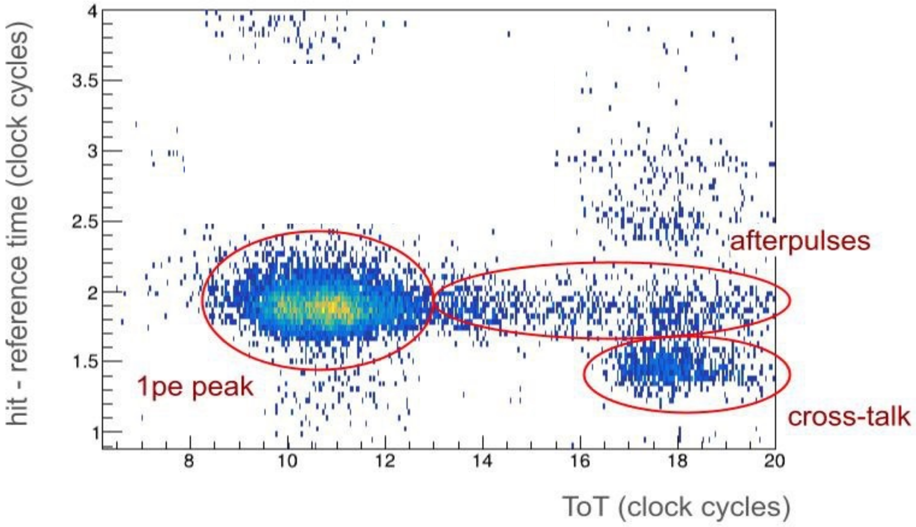

With **ToT** measurement **AP** is a problem!
(similiar problems with **CFD**)

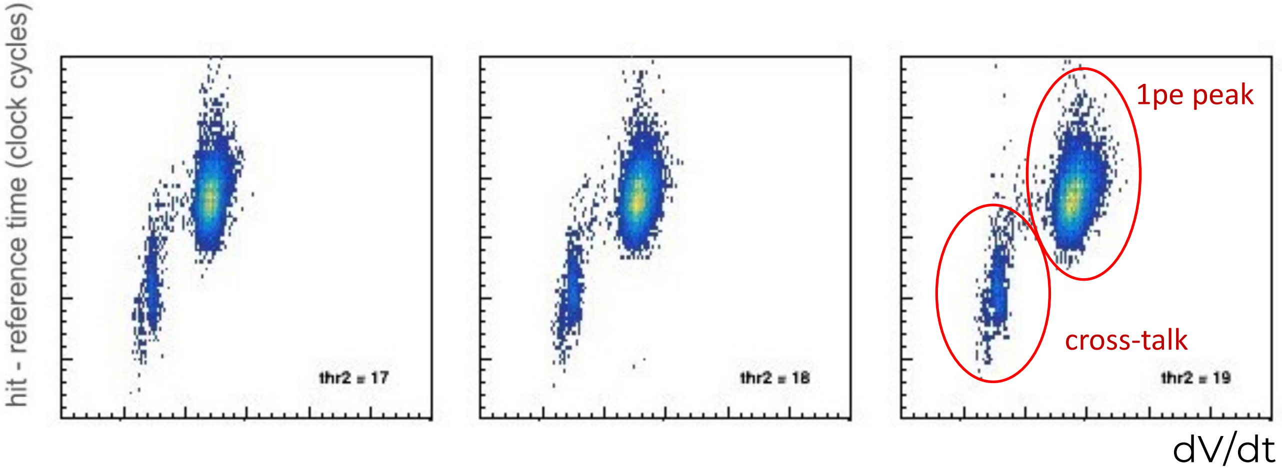

By measuring the rise time 1pe and 2pe peaks are much more separated (needs very low noise electronics)

SiPM radiation damage

SiPMs like all solid state devices are sensitive to radiation damage.
2 kind of damage:

- Non Ionizing Energy Loss (**NIEL**) **BULK** damage
- Ionizing Energy Loss (**IEL**) **SURFACE** damage

Bulk damage: **displacement** of the atoms from their original **lattice** site. Single **atoms** or **cluster** can be displaced.
Damage:

- New **generation** and **recombination** centers
- Increase **DCR**
- Increase **AP**
- Modification of the **electric field**

Surface damage: leads to the formation of **charges** in the **SiOx**
Damage:

- Increase leakeage current (**DCR**)
- Modification of the **electric field**

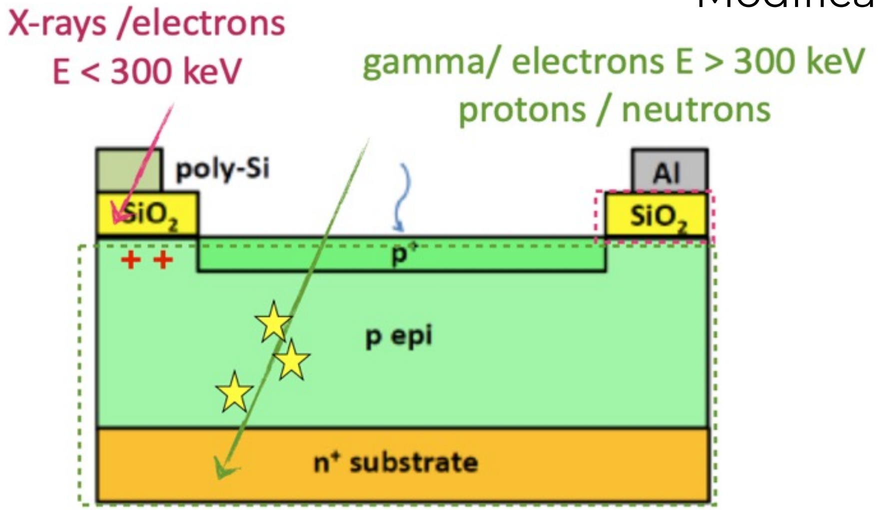

The kind of damage depends on the dose

Radiation damage of SiPMs

SiPM radiation damage

Increase in the **DCR** is the main effect even at low dose
Linear increase accordingly with the **NIEL** model
Valid only at low doses

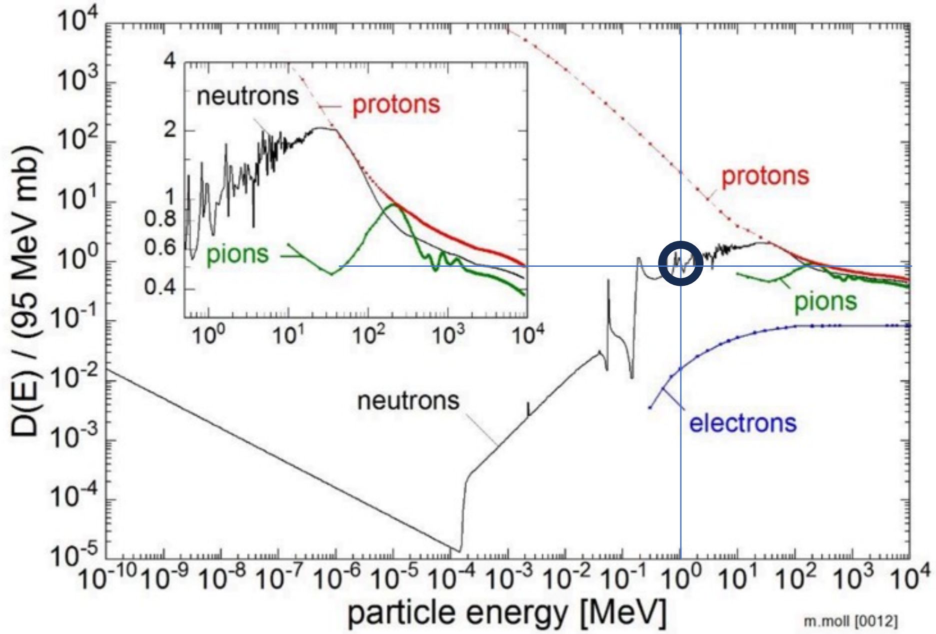

$$I(\Phi_{eq}) = I_0 + \alpha \cdot \Phi_{eq}$$

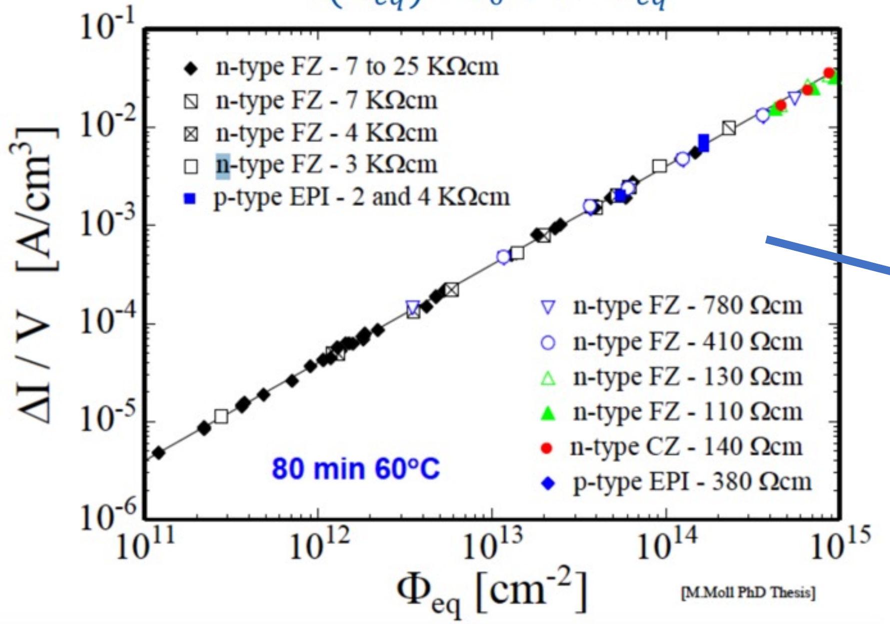

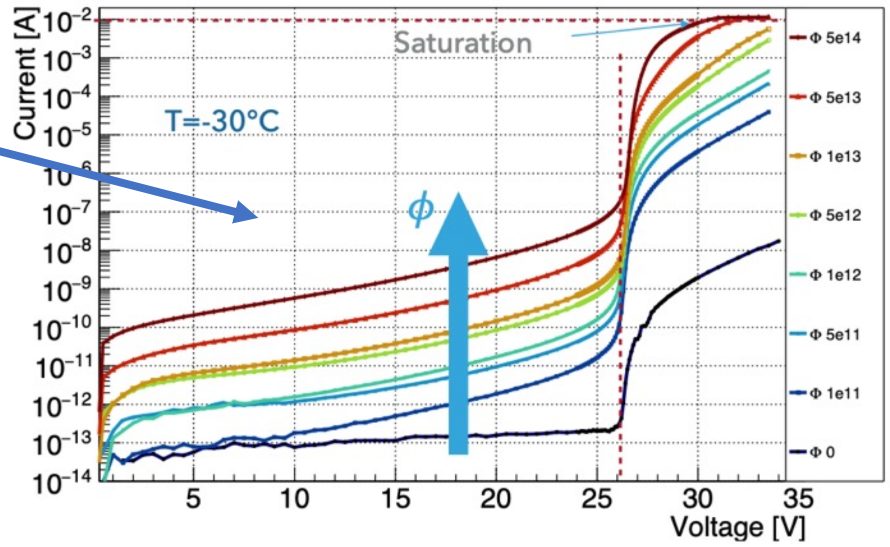

$$NIEL(E) = \frac{N_A}{A} \cdot D(E)$$

D(E): Displacement damage function

D(1 MeV neutron) = 95 MeV mb

Radiation damage of SiPMs

SiPM radiation damage

φ< 10^{13} 1MeVn_{eq}/cm$_{-2}$:
PDE unaffected

φ< 10^{12} 1MeVn_{eq}/cm^{-2}:
no changes in static parameters (C_D, Rq, V_{BD})
Small changes in G, PDE, AP (<10%)

φ> 10^{11} 1MeVn_{eq}/cm^{-2} @-30 °C:
No SPD

φ> 10^{10} 1MeVn_{eq}/cm^{-2} @-30 °C:
SPTR affected

φ> 10^{9} 1MeVn_{eq}/cm^{-2} @ RT:
No SPD

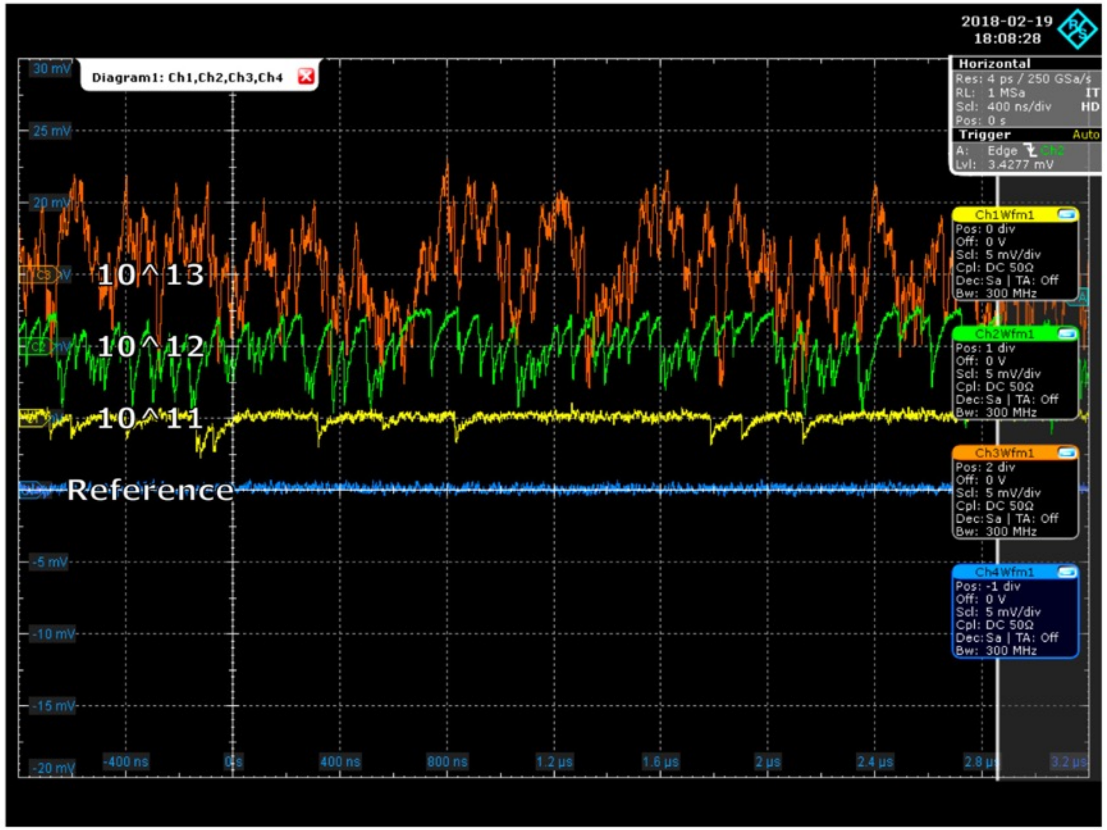

Radiation damage of SiPMs

SiPM radiation da

$\varphi < 10^{13}$ 1MeVn_{eq}/cm$_{-2}$:
PDE unaffected

$\varphi < 10^{12}$ 1MeVn_{eq}/cm^{-2}:
no changes in static parameters (C$_D$
Small changes in G, PDE, AP (<10%)

$\varphi > 10^{11}$ 1MeVn_{eq}/cm^{-2} @-30 °C:
No SPD

$\varphi > 10^{10}$ 1MeVn_{eq}/cm^{-2} @-30 °C:
SPTR affected

$\varphi > 10^{9}$ 1MeVn_{eq}/cm^{-2} @ RT:
No SPD

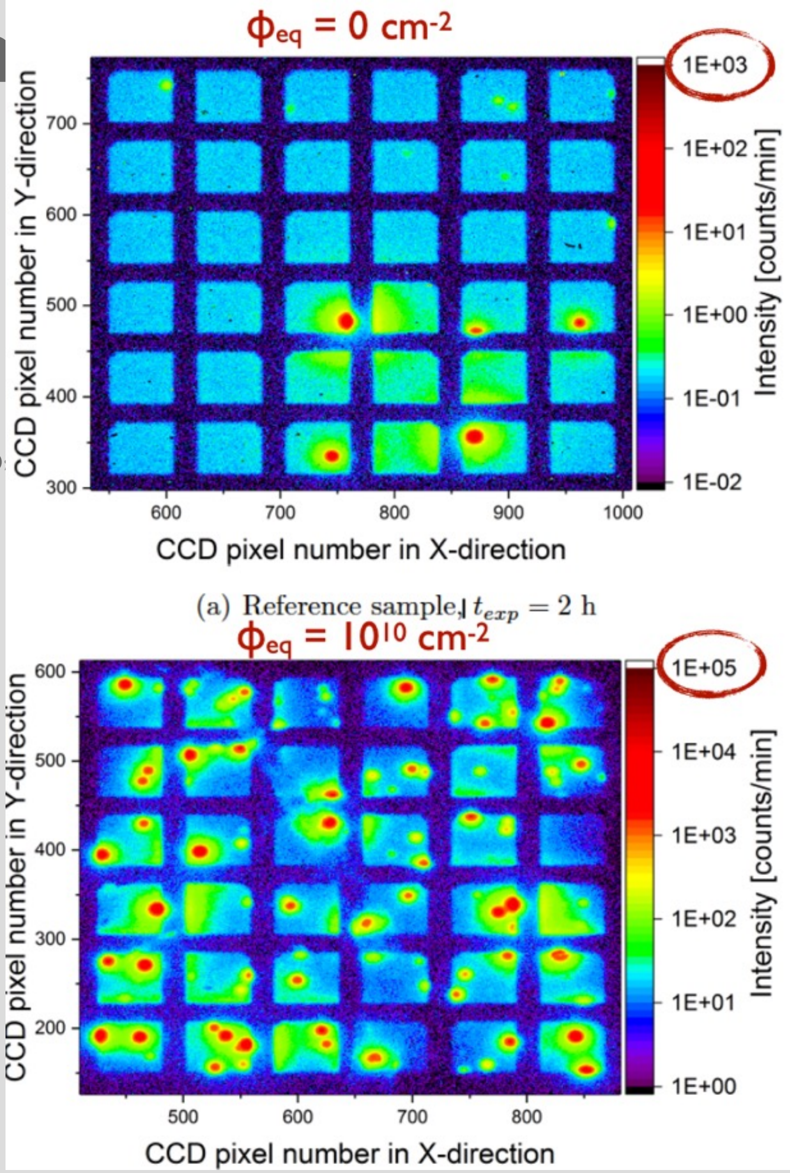

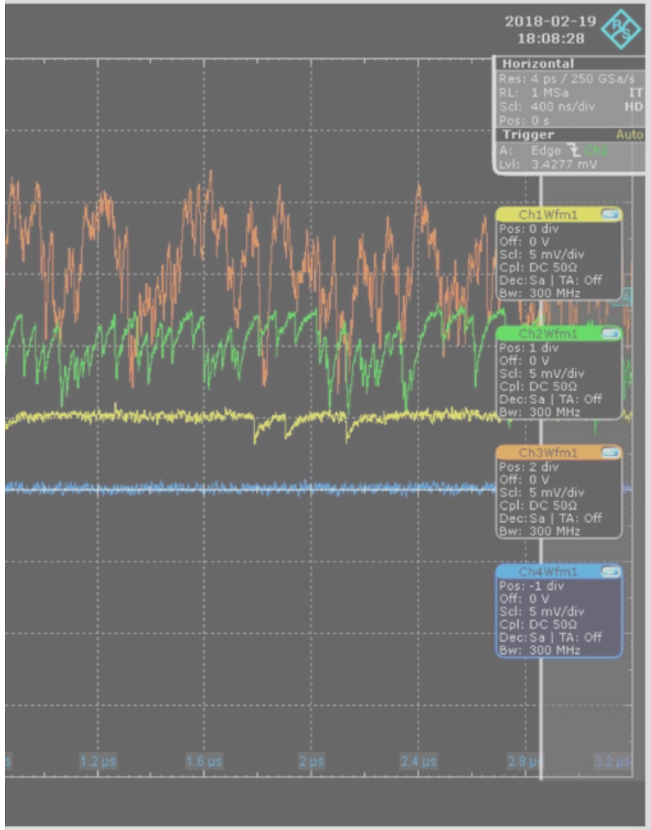

Radiation damage of SiPMs

SiPM radiation damage annealing

By putting the SiPM at high temperature (150 °C) a good portion of the damage can be healed and part of the DCR can be recovered. Permanent damage will not be cured by this procedure such that the leakage current level of the diode before irradiation cannot be fully recovered

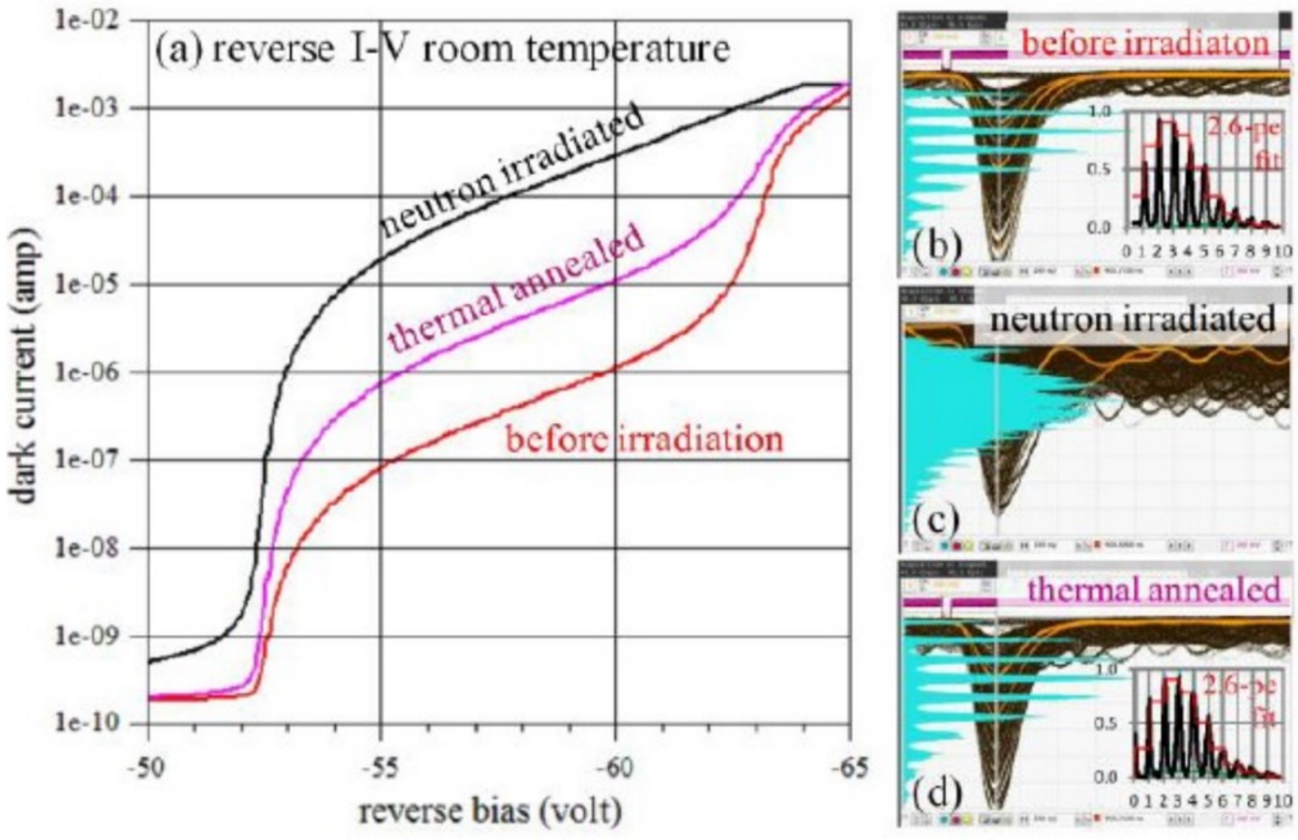

Radiation damage of SiPMs

SiPM radiation damage annealing

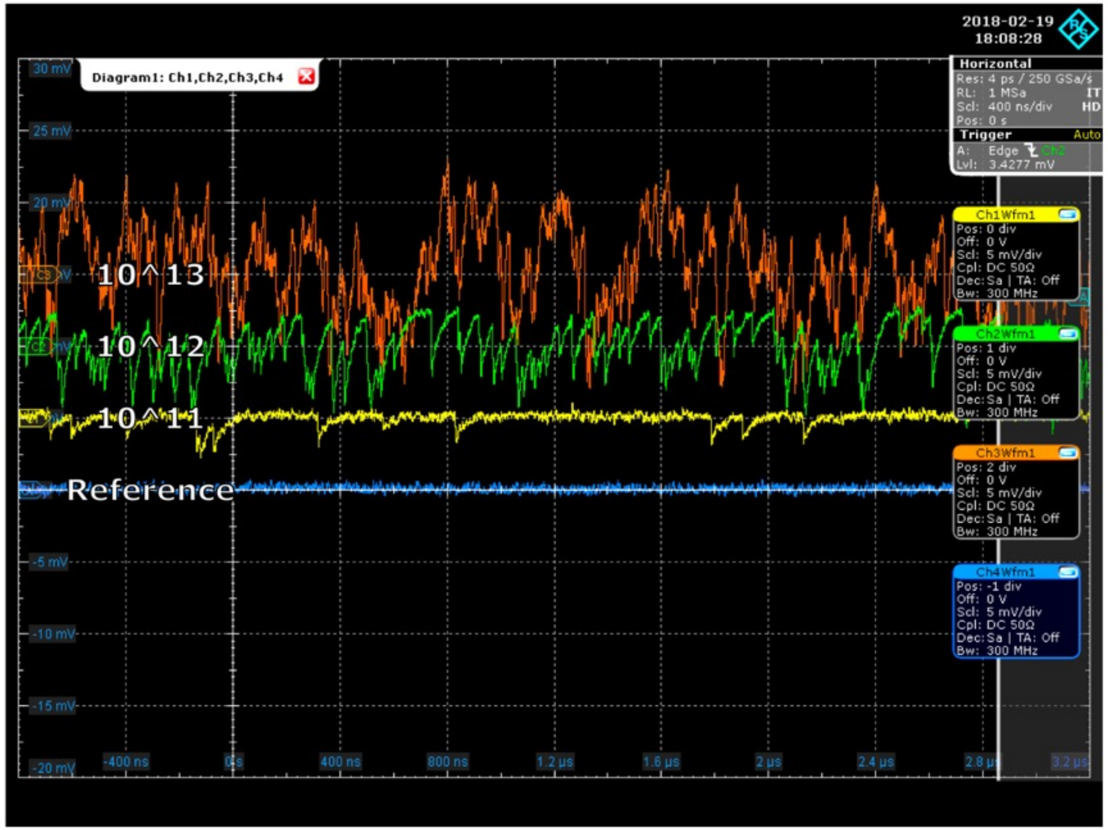

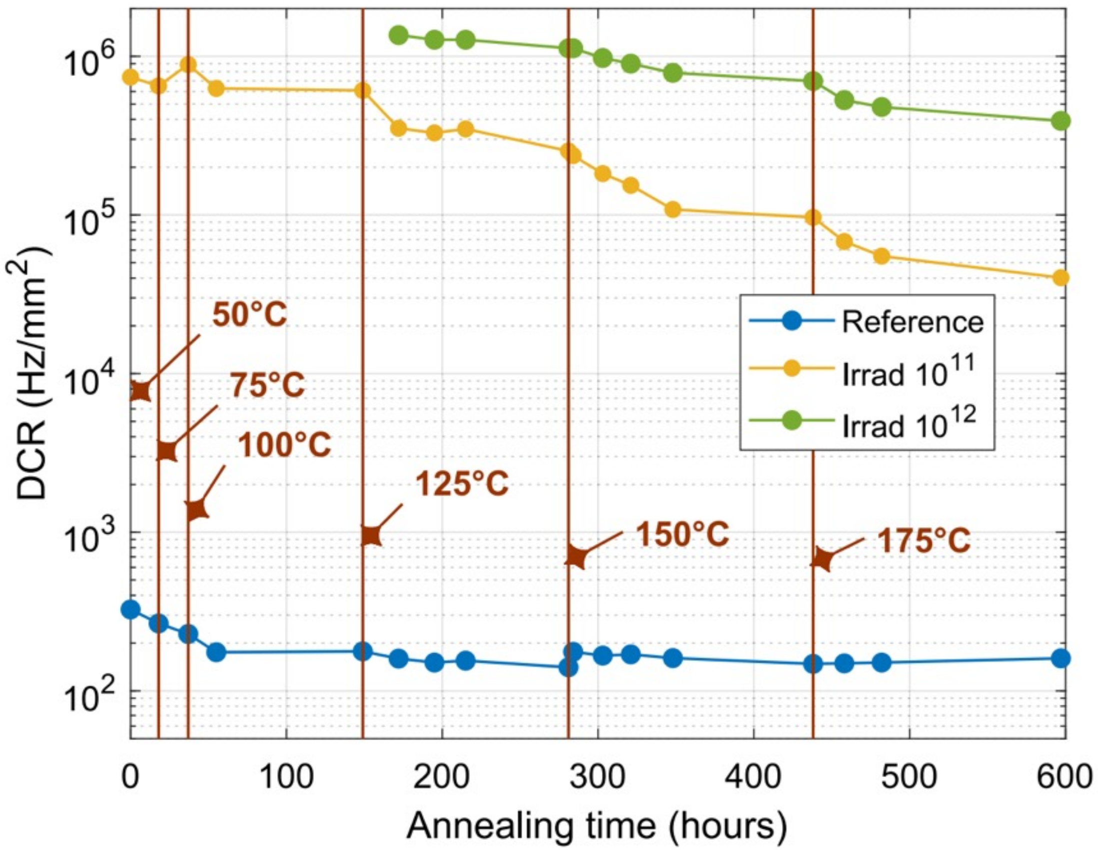

M. Calvi, et al., Nucl. Instrum. Methods A 922 (2019) 243

SiPM radiation damage annealing

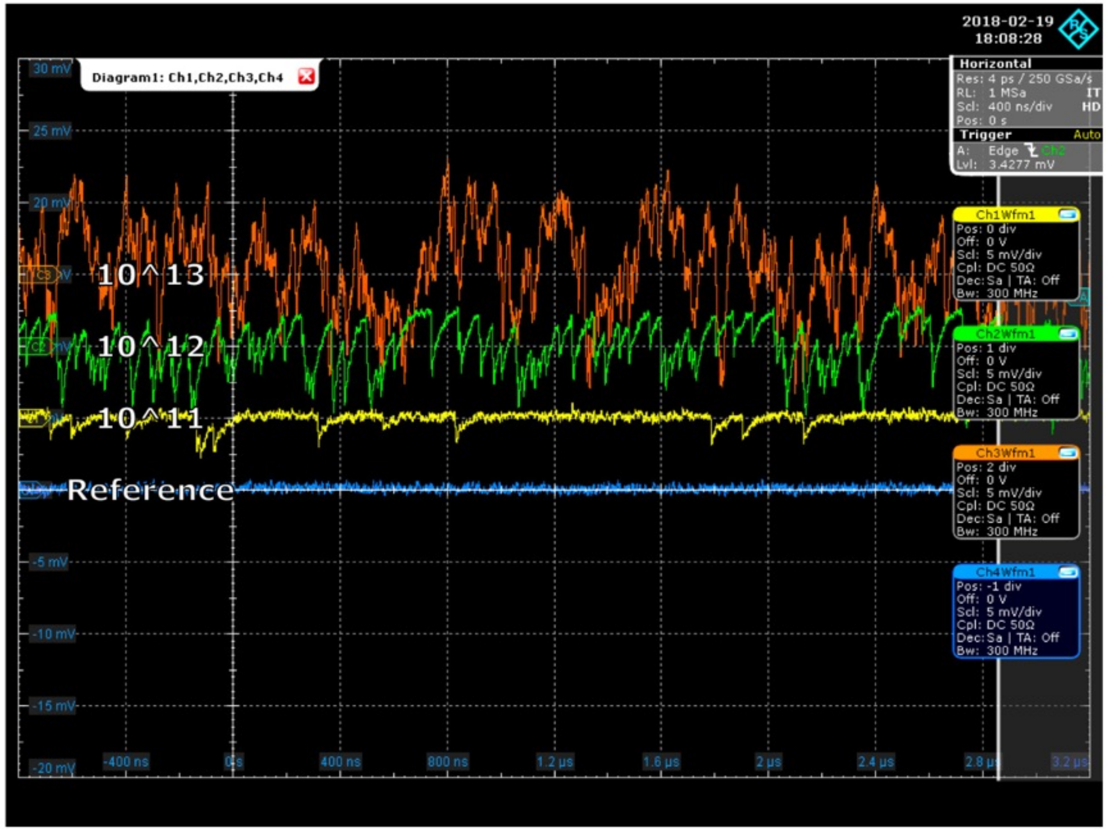

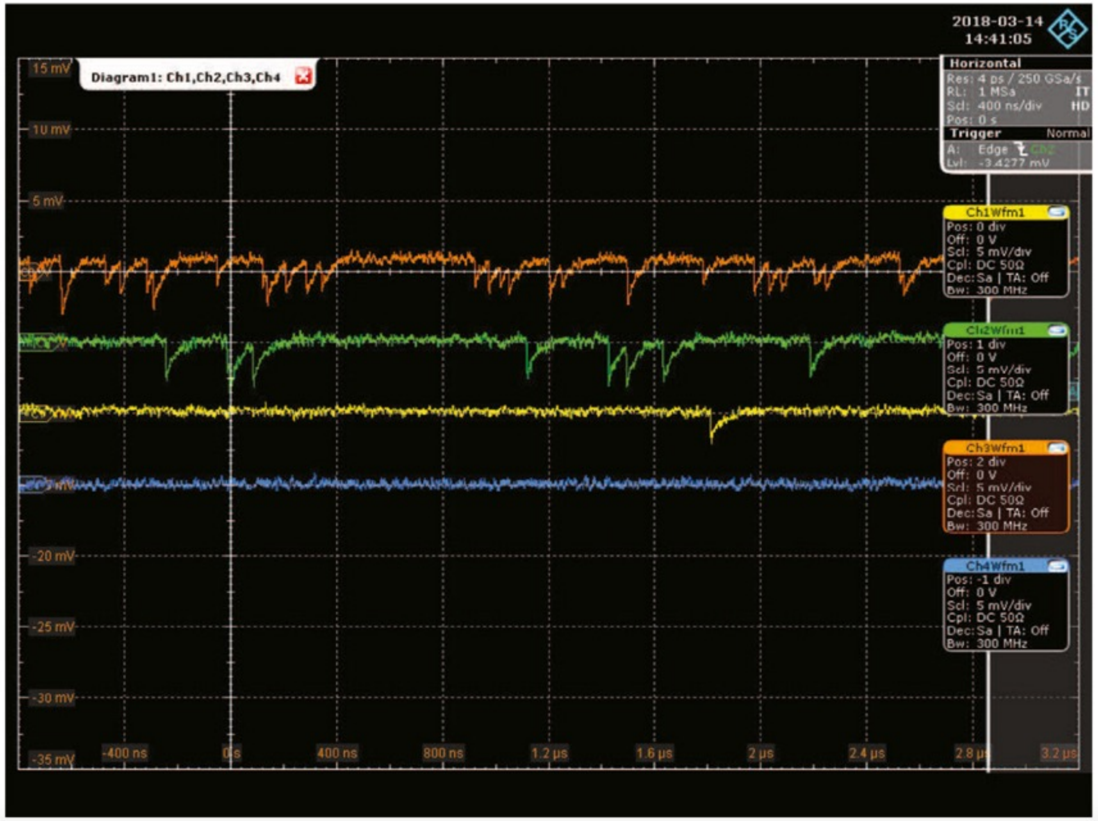

@-30 °C

M. Calvi, et al., Nucl. Instrum. Methods A 922 (2019) 243

Applications

The EIC

The **E**lectron **I**on **C**ollider (**EIC**) will be a large-scale innovative **particle accelerator** planned to be built at **Brookhaven National Laboratories** in Long Island, New York (**U.S.A**.). Constitutes the **major project** in the **nuclear physics** field.

Highly **polarized electrons** collide with **protons** and **nuclei** providing access to those regions in the nucleon and nuclei where their structure is dominated by gluons.
Polarized beams in the **EIC** will give unprecedented access to the **spatial** and **spin structure** of the **proton**, **neutron**, and **light ions**

The **EIC** covers a **center-of-mass** energy range for **e+p** collisions of **√s** of **20** to **140 GeV**
The **first beam** operations are expected to start in the **early 2030s**.

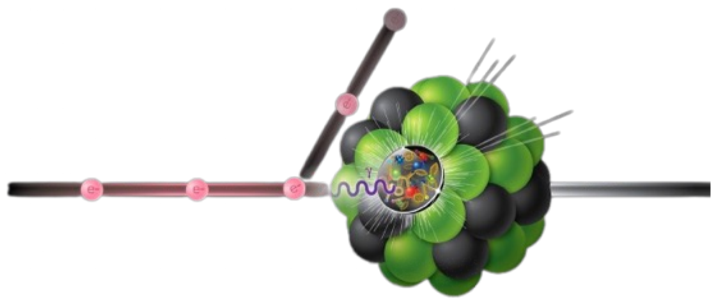

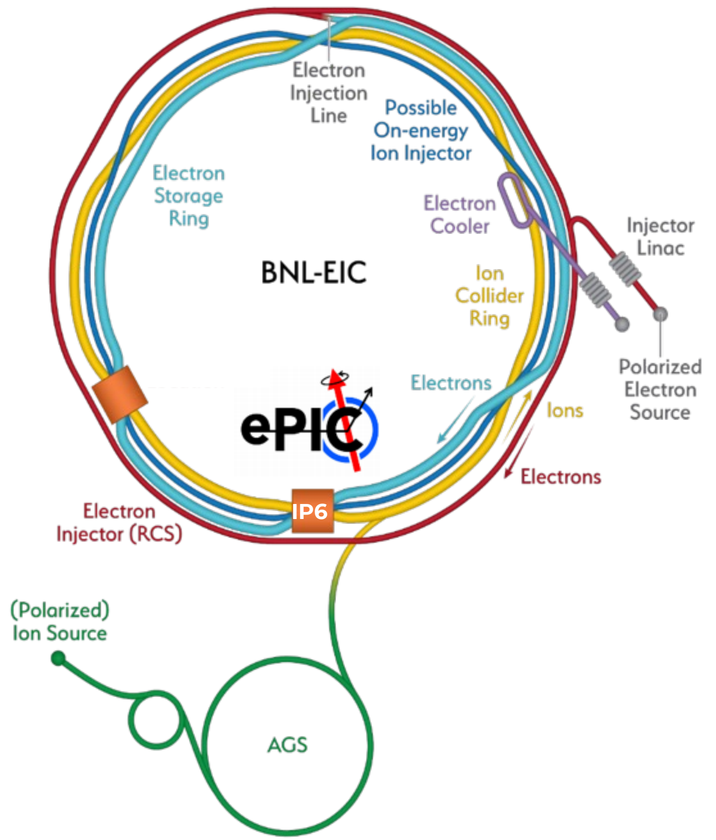

ePIC

Magnet

- New 1.7 T SC solenoid, 2.8 m bore diameter

Tracking

- Si Vertex Tracker MAPS wafer-level stitched sensors (ALICE ITS3)
- Si Tracker MAPS barrel and disks
- Gaseous tracker: MPGDs (μRWELL, MMG) cylindrical and planar

PID

- high performance DIRC (hpDIRC)
- dual RICH (aerogel + gas) (forward)
- proximity focussing RICH (backward)
- ToF using AC-LGAD (barrel+forward)

EM Calorimetry

- imaging EMCal (barrel)
- W-powder/SciFi (forward)
- $PbWO_4$ crystals (backward)

Hadron calorimetry

- FeSc (barrel, re-used from sPHENIX)
- Steel/Scint – W/Scint (backward/forward)

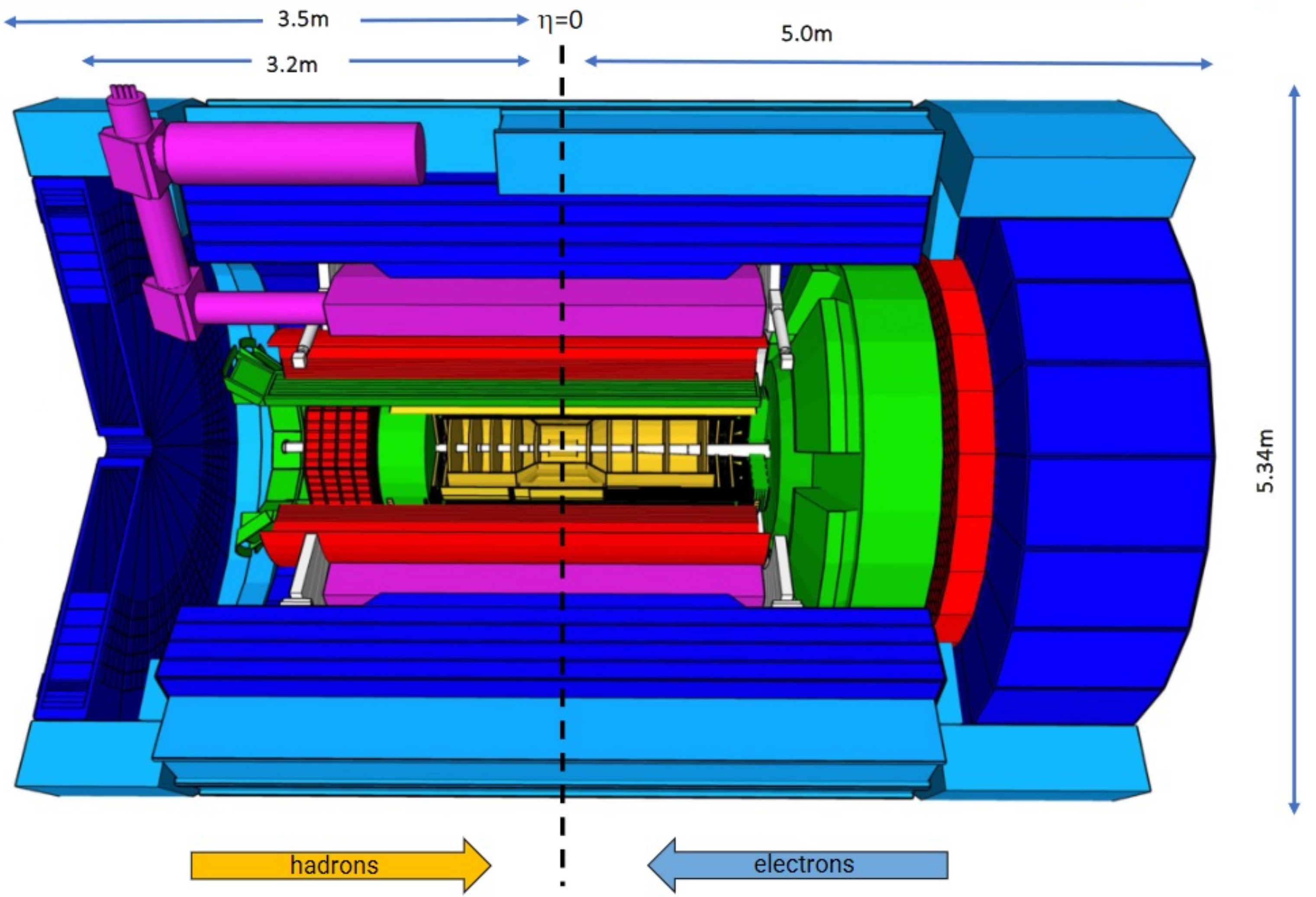

A dual-radiator (**dRICH**) is in charge for the forward **P**article **Id**entification **PID.**
It is compact and cost-effective solution for continuous momentum coverage (3-60 GeV/c)
It shows interesting capability in the elcttron-pion separation.

Radiators are made in aerogel (n ~ 1.02) and C2F6 (n ~ 1.0008) [**10-100 ph per ring**]
Mirrors: large outward-reflecting, 6 open sectors.

The Photon Detectors is made by 3x3 mm^2 Hamamatsu 50 um cell **SiPMs** arranged in **six** 0.5 m^2 / sector for a total of **3 m^2** surface (~ 300 k channels). It must withstand 1 T magnetic field, and up to 10^{10} $1MeVn_{eq}/cm^{-2}$ and operating at -30 °C.
DAQ and physics limits: **10** noise hits / sector within **500 ps** reached at 10^9 $1MeVn_{eq}/cm^{-2}$
After few months of operation annealing is needed!

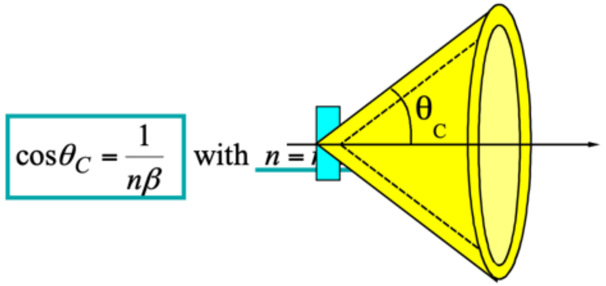

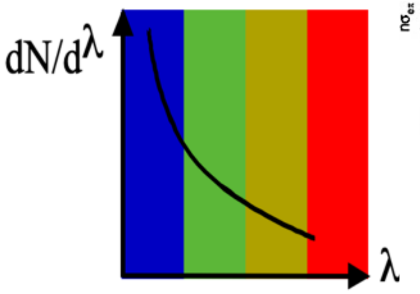

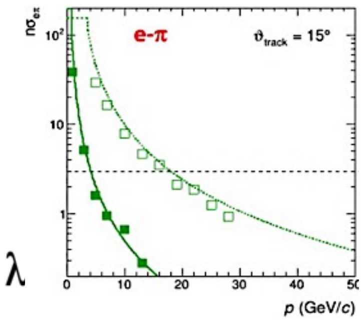

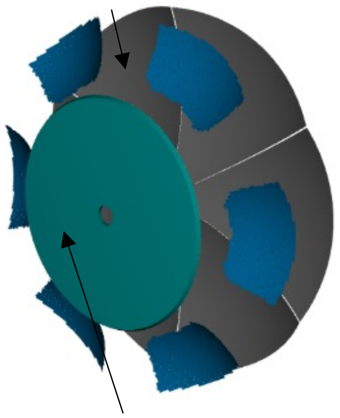

Spherical mirrors

Gas volume **120 cm**

Aerogel **4 cm**

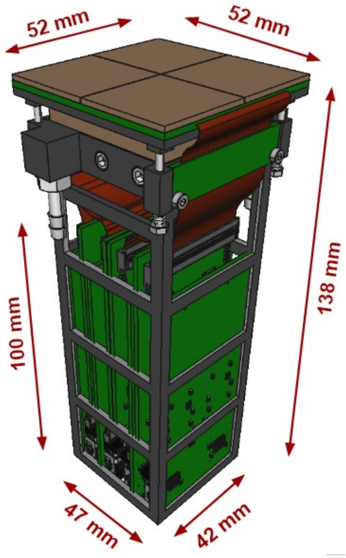

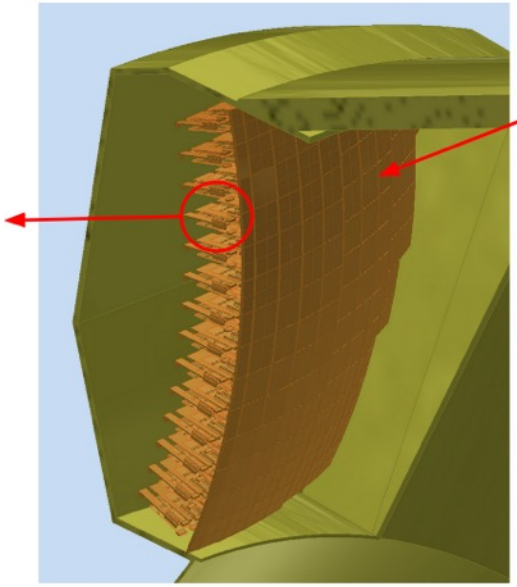

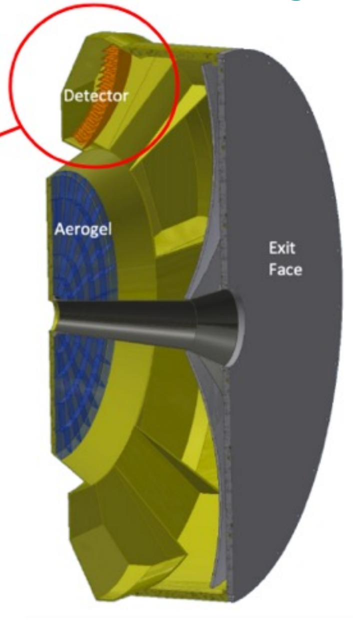

Irradiation and annealing findings

Consecutive irradiation/annealing cycles

Direct current annealing

150° C can be obtained providing 10 V and ~100 mA (**~ 1 W**) per sensor @ room temperature. **Can be done in situ** but need proper electronics

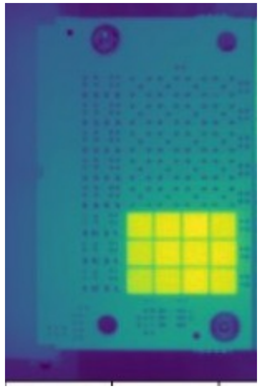

Thermal camera image of Hamamatsu S1360-3050CS on carrier board

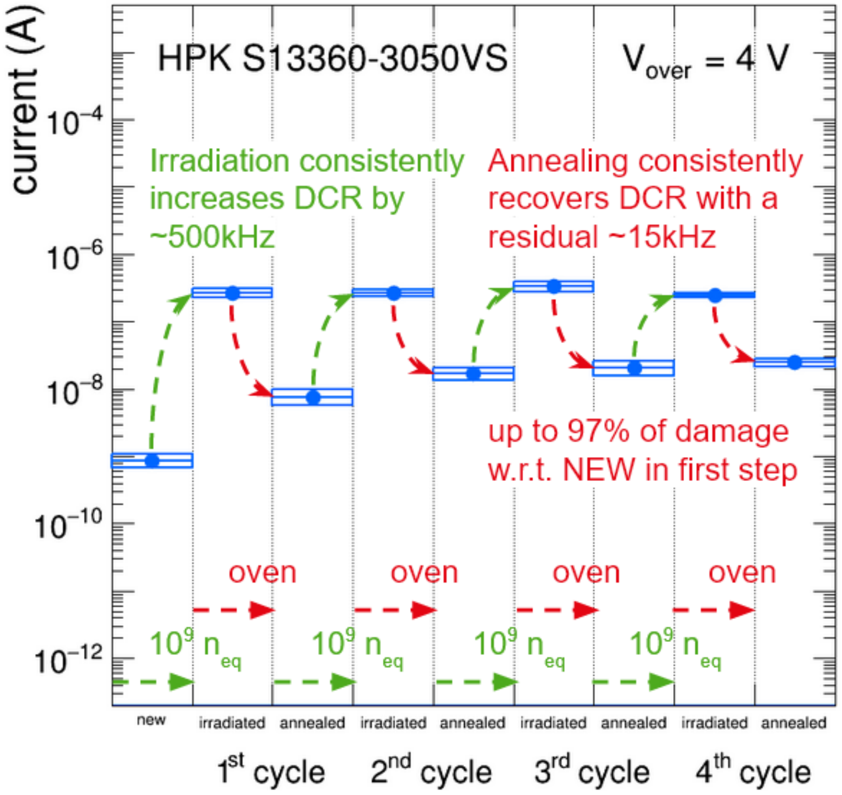

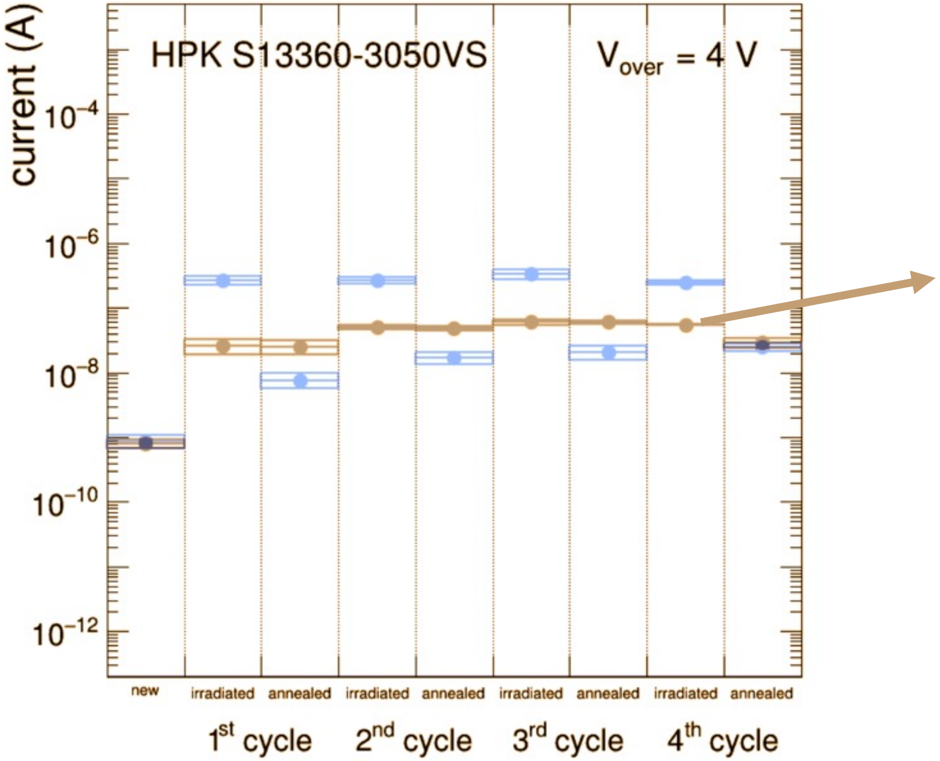

Direct current annealing
Almost same level of recovery

Irradiation and annealing findings

Consecutive irradiation/ann

Direct current annealing

150° C can be obtained prov

room temperature. **Can be**

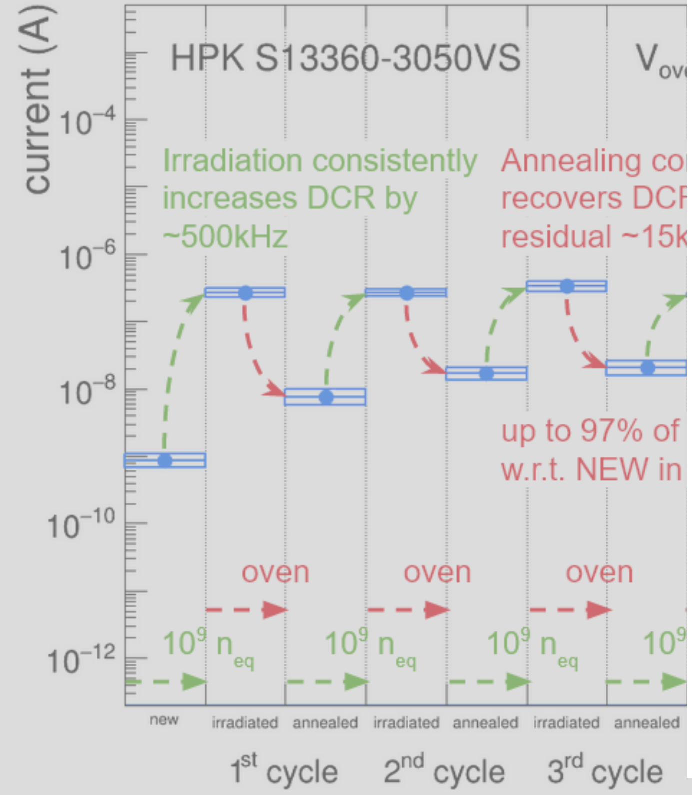

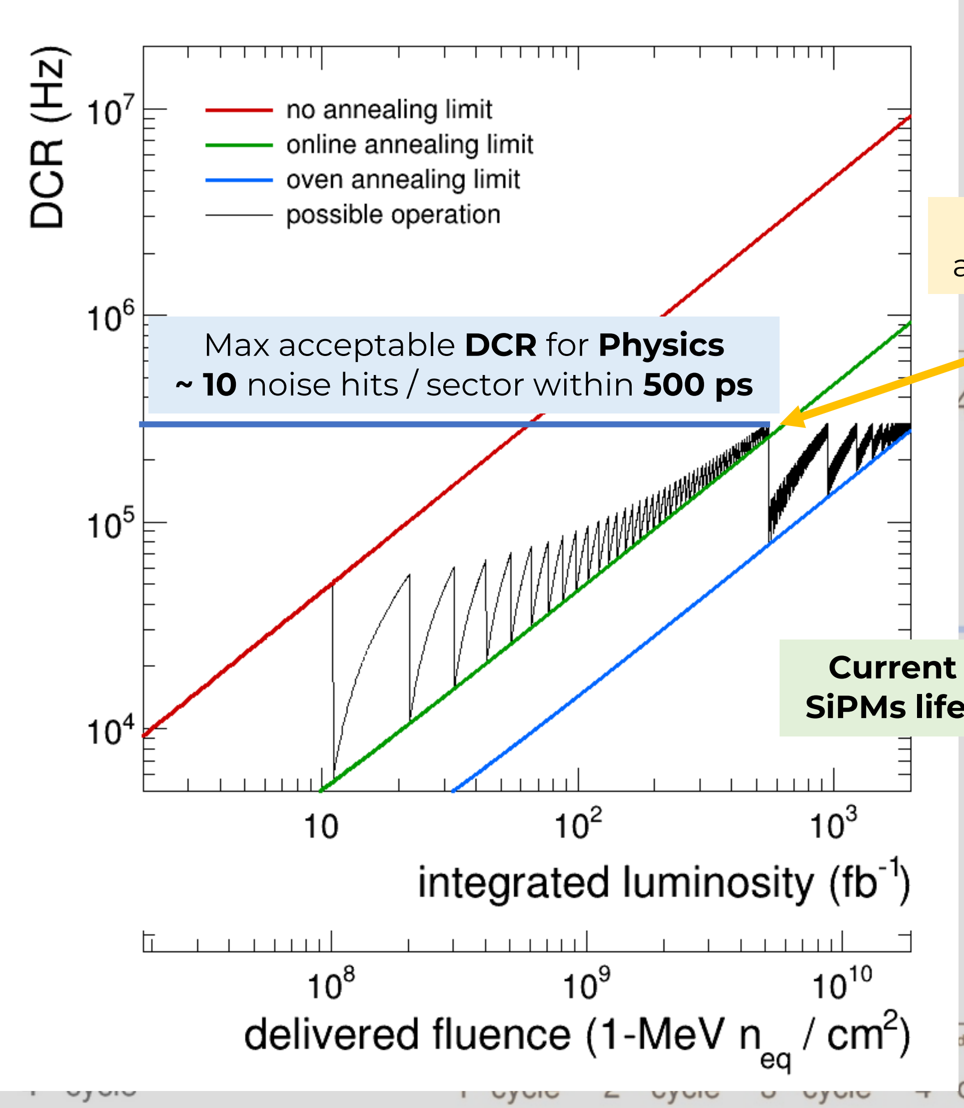

More **aggressive** annealing is needed: **oven**

Current annealing extends **SiPMs lifetime** by a factor **~ 10**

Thermal camera image of Hamamatsu S1360-3050CS on carrier board

Direct current annealing

Almost same level of

Luigi Rignanese rignanes@bo.infn.it

INFN

Prototype test with dRICH @CERN

8 PDUs with 256 HAMAMATSU S1360-3050CS read by 64 ALCOR ASICs

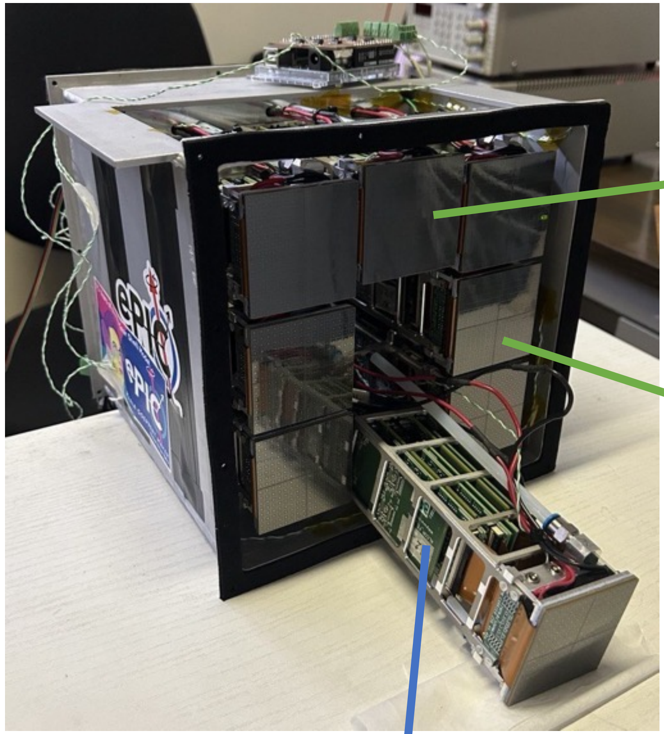

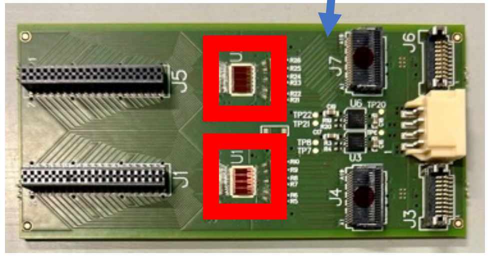

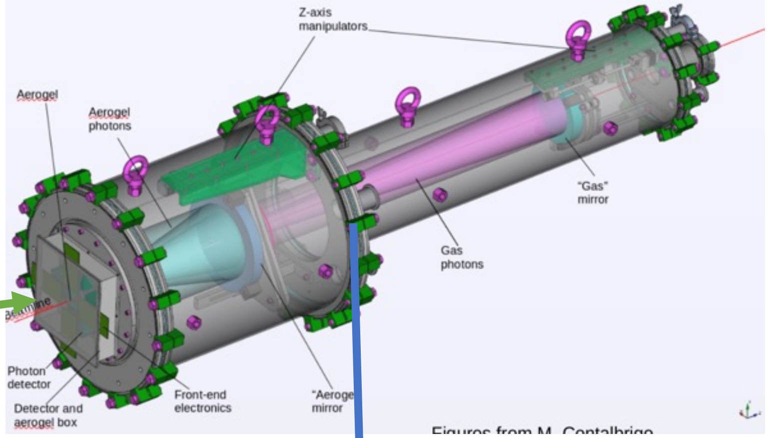

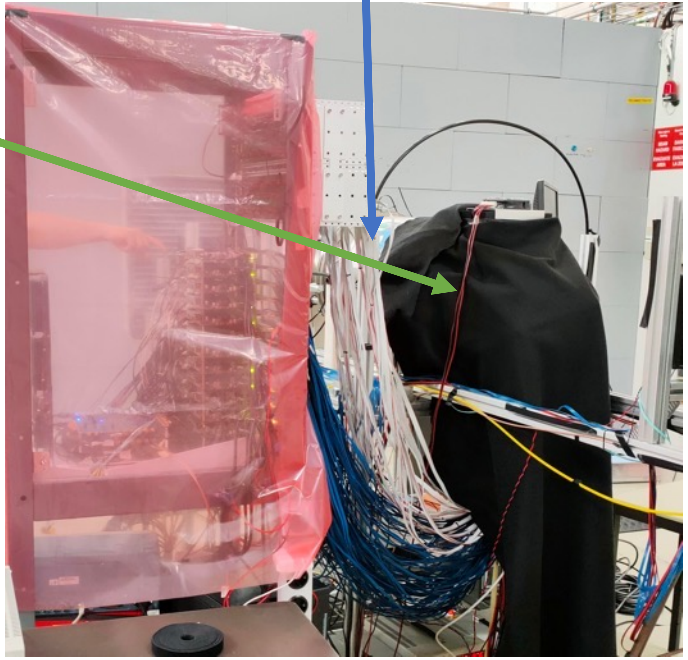

negative 11.5 GeV beam (e^-)

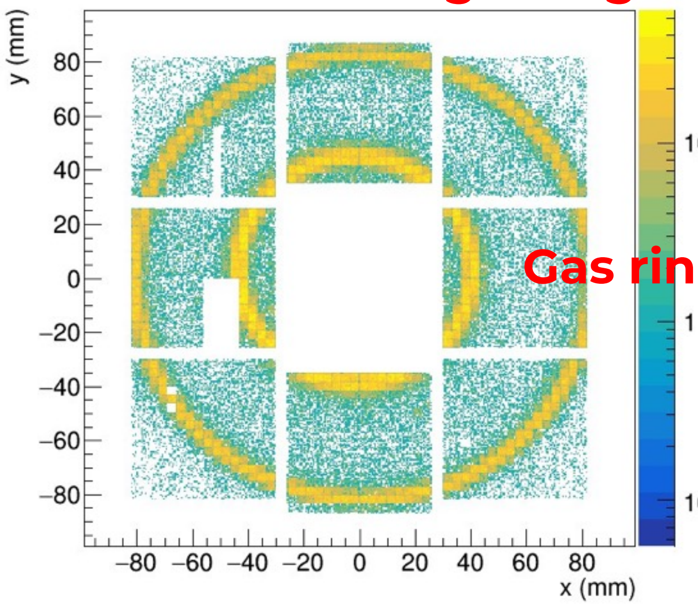

Luigi Rignanese rignanes@bo.infn.it

Future RICH with **SiPM**

- **RICH1 @ LHCB UPGRADE II**
  1 mm^2 SiPM with an accumulated dose of **10^{14}** 1MeVn$_{eq}$/cm^{-2} (new devices and -80° C cooling

- **Belle II ARICH upgraded luminosity**
  1 mm^2 SiPM (FBK) **10^{12}** 1MeVn$_{eq}$/cm^{-2} operated in LN

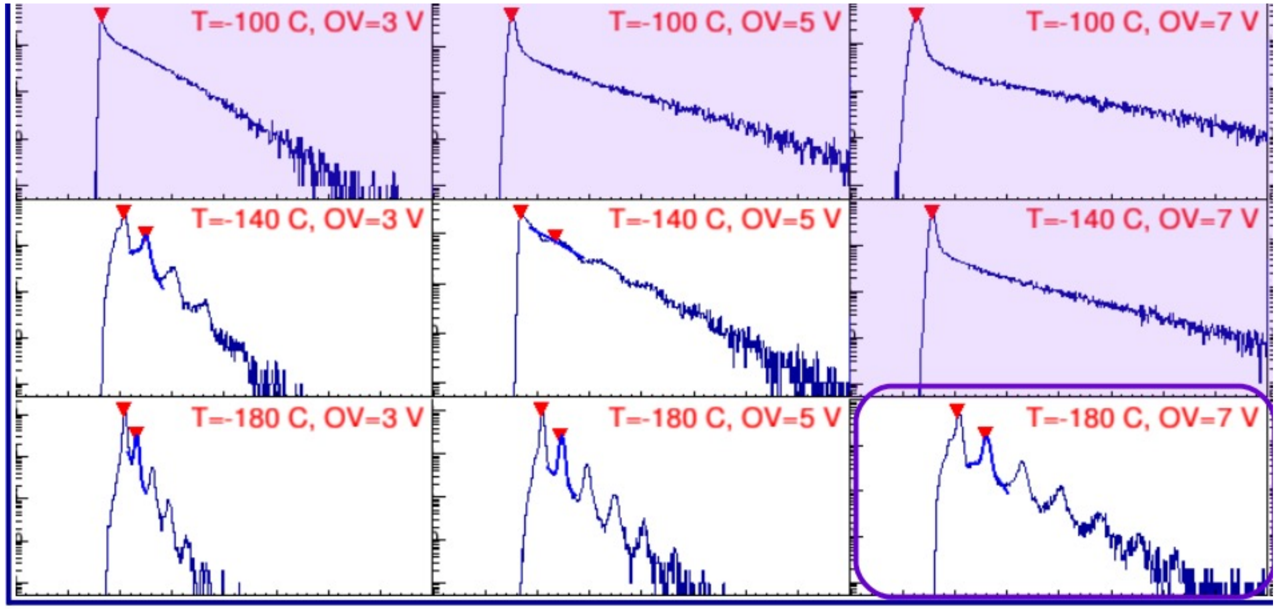

Dania Consuegra Rodríguez PHOSE2023

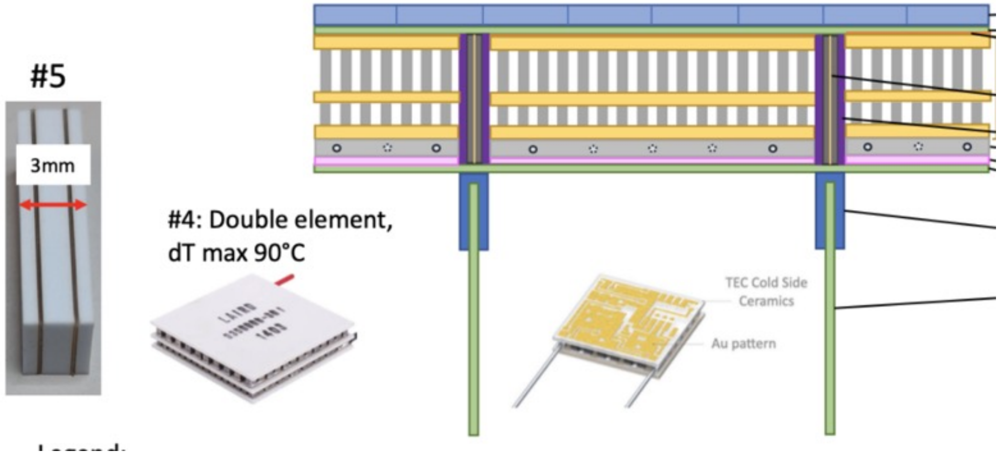

Roberta Cardinale PHOSE2023

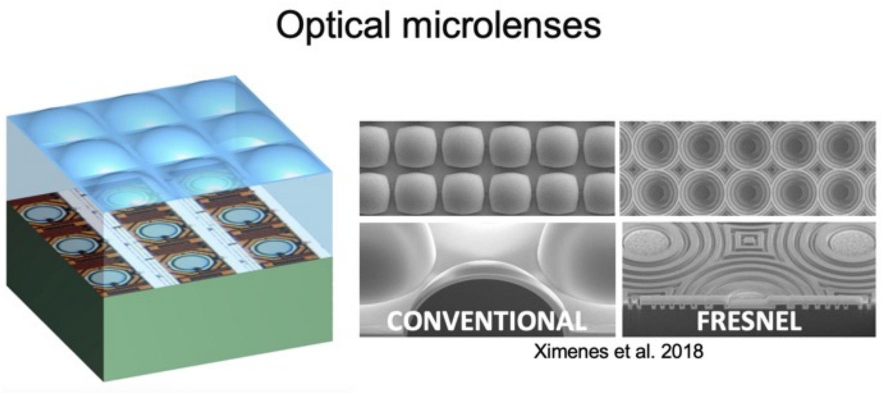

Mata Pavia et al. 2014 – Ximenes et al. 2018 – Bruschini et al. 2023

Edoardo Charbon PHOSE2023

Darkside-20K

DS-20k is a **two-phase LAr** detector with a **50 tonnes** active volume (20 t fiducial). It will operate in **LNGS Hall-C** in the next years and will either detect **WIMP** dark matter or reach a 90% exclusion sensitivity to WIMP-nucleon cross sections of $7.4 \times 10^{-48} cm^2$ at the mass of $1 TeV/c^2$.
TOP and **BOTTOM** detection planes instrumented with **528 PDUs** made by **16 tiles** of **24** $12x8\ mm^2$ **FBK NUV-HD-cryo** (**LF**) SiPMs (**200k total**!).
Mass production by **LFoundry** completed now assembled in NOA (Assergi)

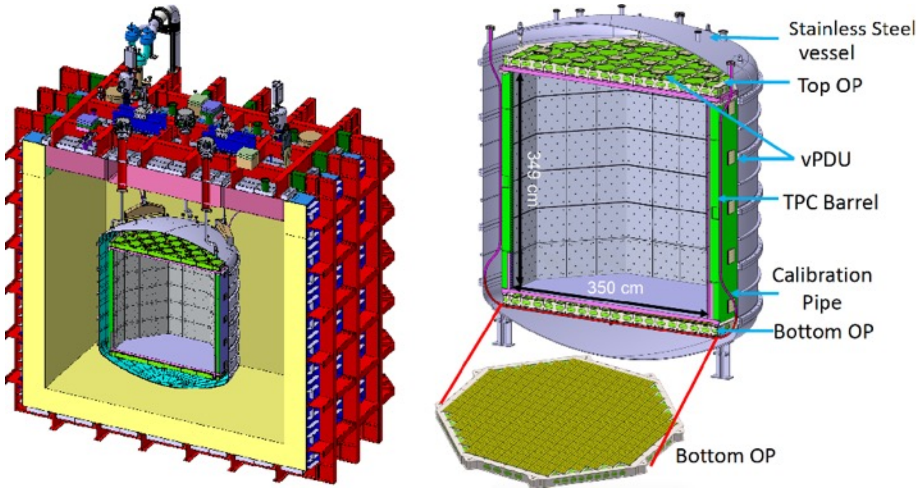

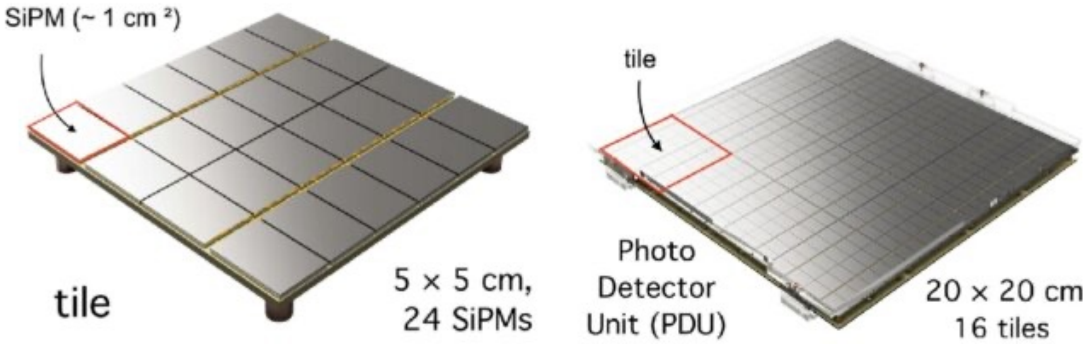

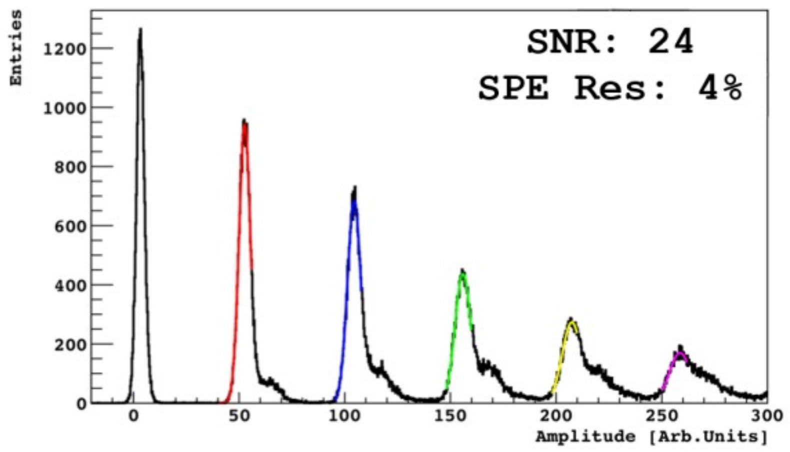

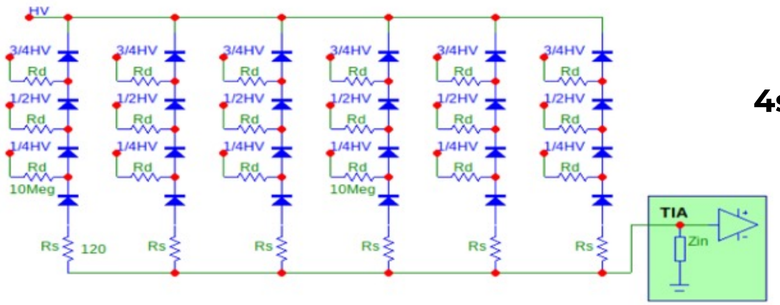

4s6p ganging

[New developments in the SiPM cryo-electronics for low background dark matter experiments](#)
[DarkSide-20k: A 20 tonne two-phase LAr TPC for direct dark matter detection at LNGS](#)

Canon has successfully developed an ultra-small (13.2mm x 9.9mm) SPAD sensor capable of capturing the world's highest resolution 3.2-megapixel color photography—a higher resolution than full HD (approximately 2.07 megapixels), even in low-light environments.

https://global.canon/en/technology/spad-sensor-2023.html